2015-2016
R&D REPORT

National Tsing Hua University

National Tsing Hua University

2015-2016 R&D REPORT

A Brief History of NTHU

National Tsing Hua University (NTHU) was established in Beijing in 1911 as "Tsing Hua Academy." The Academy was renamed as "National Tsing Hua University" in 1928. In 1956, NTHU was re-established at its present location in Hsinchu, Taiwan.

Since its relocation, NTHU has developed into a comprehensive research university offering a full range of degree programs in science, technology, engineering, humanities, social sciences, and management. NTHU has been consistently ranked as one of the premier universities in East Asia, and is widely recognized as a leading incubator for future leaders. Our outstanding alumni highlight the success of NTHU students, including Nobel Physics laureates Dr. Cheng-Ning Yang and Dr. Tsung-Dao Lee, Nobel Chemistry laureate Dr. Yuan-Tseh Lee, and Wolf Prize winner in mathematics Dr.Shiing-Shen Chern.

Contents

Message from the President

National Tsing Hua University (NTHU) is a research university with a long and proud tradition. Since the re-establishment in Hsinchu in 1956, NTHU has been known for excellent academic programs as well as outstanding alumni. Over the last sixty years, NTHU has transformed herself into a comprehensive university and is recognized in all disciplines.

NTHU provides a stimulating and nurturing environment within which our faculty can offer quality teaching and conduct innovative research. Regarded as one of the top-tier research universities, our research and development activities across the University emphasize fundamental discoveries at the forefronts of basic sciences and exploration of breakthrough technologies with a high potential for applications. These can be reflected from our publications in the world's preeminent journals, awarded international patents, and technology transfer cases. In the 2015-2016 R&D annual report, we highlight several key papers published in Scientific Breakthrough. We also provide the facts and figures related to other important R&D activities, including a coverage of the research centers jointly established with the leading corporates in Taiwan. This volume is undoubtedly too limited to give the full scope of R&D at NTHU, but a glimpse into our recent achievements. Hopefully, this can serve as a catalyst for further interactions, exchange of ideas, and establishment of collaborations.

Built on our proud heritage, NTHU will continue to promote excellent teaching and innovative research with the goal of ascending the University into the cradle of human accomplishments, important scientific discoveries and innovative technologies. I hope that you will find this R&D annual report useful and give us your precious opinions and suggestions.

President
Dr. Hong Hocheng

National Tsing Hua University
Hsinchu, Taiwan
November 2016

NTHU Today

Location

National Tsing Hua University is located in Hsinchu, a city 72 kilometers south of Taipei. The campus covers an area of over 105 hectares (260 acres) scenic land with lakes and trees. The campus has a convenient access to neighboring industrial sectors, research institutes and universities such as the Hsinchu Science Park (HSP), the Industrial Technology Research Institute (ITRI), National Synchrotron Radiation Research Center (NSRRC), National Center for High-Performance Computing (NCHC), Food Industry Research and Development Institute (FIRDI), National Chiao Tung University (NCTU), Chung Hua University (CHU), and National Hsinchu University of Education (NHCUE). These establishments have made Hsinchu known as "The Science City of Taiwan".

Academics

8 Colleges, 17 Departments and 24 Institutes

- College of Science
- College of Engineering
- College of Nuclear Science
- College of Life Science
- College of Electrical Engineering and Computer Science
- College of Humanities and Social Sciences
- College of Technology Management
- Tsing Hua College

B:Baccalaureate / M:Master / D:Doctorate

College of Science	Degree Program Offer
Department of Mathematics	B / M / D
Department of Physics	B / M / D
Department of Chemistry	B / M / D
Institute of Astronomy	M / D
Institute of Statistics	M / D
Interdisciplinary Program of Science	B
Graduate Program in Science and Technology of Synchrotron Light Source	M / D
College of Engineering	**Degree Program Offer**
Department of Chemical Engineering	B / M / D
Department of Power Mechanical Engineering	B / M / D
Department of Materials Science and Engineering	B / M / D
Department of Industrial Engineering and Engineering Management	B / M / D
Industrial Engineering and Engineering Management Professional Master's Program	M
Institute of NanoEngineering and MicroSystems	M / D
Institute of Biomedical Engineering	M
Interdisciplinary Program of Engineering	B
Molecular Engineering Program	M
Graduate Program of Advanced Energy	D
Dual Master Program for Global Operation Management	M
College of Nuclear Science	**Degree Program Offer**
Department of Engineering and System Science	B / M / D
Department of Biomedical Engineering and Environmental Sciences	B / M / D
Institute of Nuclear Engineering and Science	M / D
Interdisciplinary Program of Nuclear Science	B
Graduate Program in Science and Technology of Synchrotron Light Source	M / D
College of Humanities and Social Sciences	**Degree Program Offer**
Department of Chinese Literature	B / M / D
Department of Foreign Languages and Literature	B / M
Institute of History	M / D
Institute of Linguistics	M / D
Institute of Anthropology	M / D
Institute of Sociology	M / D
Institute of Philosophy	M
Institute of Taiwan Literature	M / D
Graduate Program on Taiwan Studies	M
Interdisciplinary Program of Humanities and Social Sciences	B
College of Life Science	**Degree Program Offer**
Department of Life Science	B
Department of Medical Science	B
Institute of Molecular and Cellular Biology	M / D
Institute of Molecular Medicine	M / D
Institute of Bioinformatics and Structural Biology	M / D
Institute of Biotechnology	M / D
Institute of Systems Neuroscience	M
Interdisciplinary Program of Life Science	B
Graduate Program of Biotechnology in Medicine	M / D
Structral Biology Program	D
College of Electrical Engineering and Computer Science	**Degree Program Offer**
Department of Computer Science	B / M / D
Department of Electrical Engineering	B / M / D
Institute of Communications Engineering	M / D
Institute of Electronics Engineering	M / D
Institute of Information Systems and Applications	M / D
Institute of Photonics Technologies	M / D
Interdisciplinary Program of Electrical Engineering and Computer Science	B
College of Technology Management	**Degree Program Offer**
Department of Quantitative Finance	B / M
Department of Economics	B / M / D
Institute of Technology Management	M / D
Institute of Law for Science and Technology	M / D
Institute of Service Science	M / D
MBA	M
EMBA	M
IMBA	M
Double Specialty Program of Management and Technology	B
Tsing Hua College	**Degree Program Offer**
Institute of Learning Sciences	M

Personnel

Year Range: 105/7/31

Faculty	Title	Total
Full-Time(630)	Professor	354
	Associate Professor	171
	Assistant Professor	94
	Instructor	4
	Military Instructor	7
Research Fellow		237
Faculty Term Appointment		25
Adjunct Professor		311

Staff	Total
Regular	197
Campus Police	20
Term Appointment	457
Research Staff (Funded by Projects)	415

Number of domestic students, as of 2016

Total: 12,466

International students, as of 2015

Total: 442

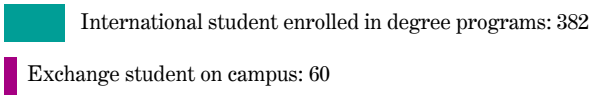

Graduates, as of 2015

Total: 3,281

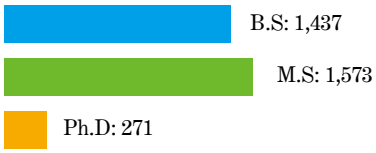

Research Funding (2003-2015)

Unit: Million NTD (30 NTD ≈ 1 USD)

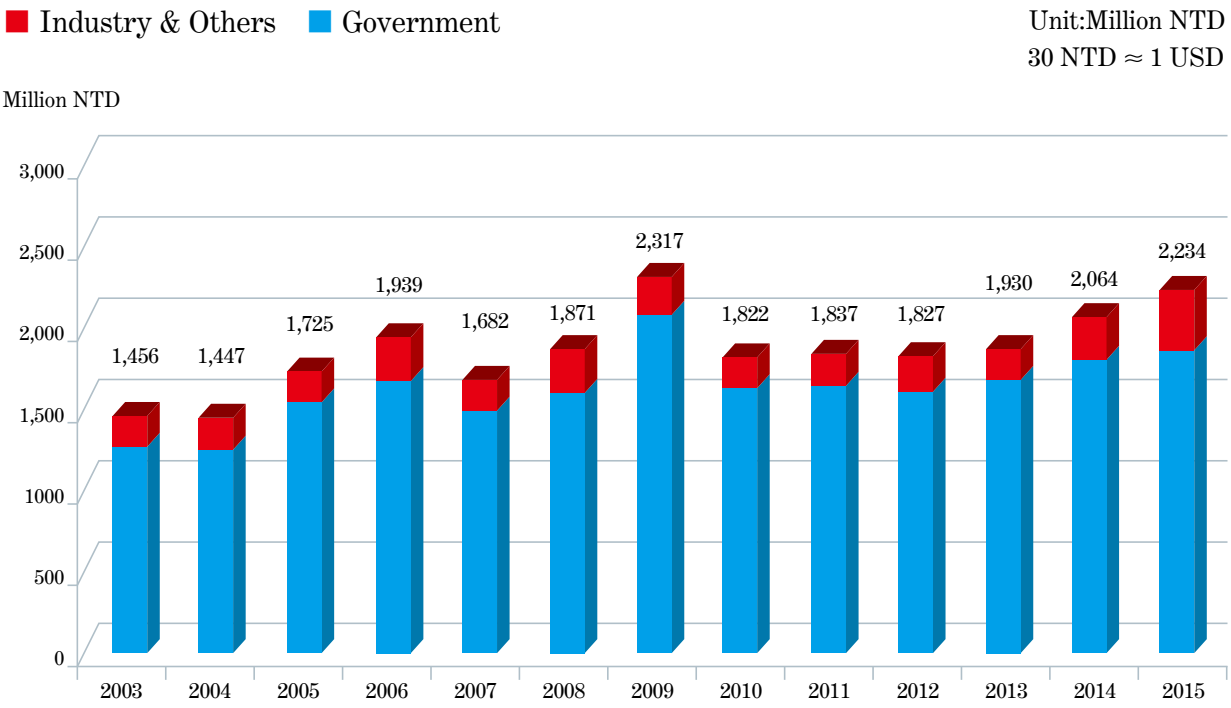

Funding Distribution by Discipline (2015)

Unit: Million NTD (30 NTD ≈ 1 USD)

Physical Sciences	577	20%
Engineering	1,291	44%
Social Sciences	140	5%
Life Sciences	219	7%
Arts & Humanities	57	2%
Clinical, Pre-Clinical & Health	642	22%

Sponsored Research Fund (2015)

Unit: Million NTD (30 NTD ≈ 1 USD)

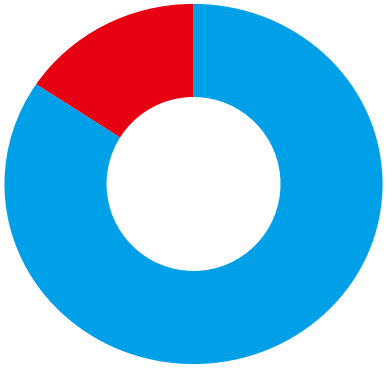

Research grant income from public sources and charities	1,978	84%
Research contract income from industry and commerce	373	16%

Government-Sponsored Research Fund (2015)

Unit: Million NTD (30 NTD ≈ 1 USD)

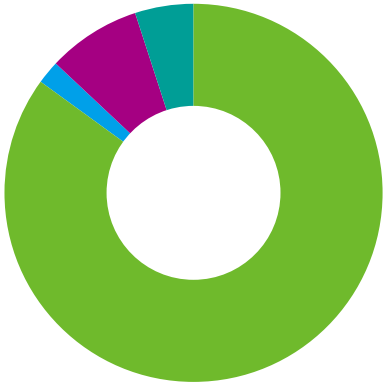

National Science Council	1,689	85%
Ministry of Economy	34	2%
Ministry of Education	148	8%
Others	107	5%

Non-Government Sponsored Research Fund (2015)

Unit: Million NTD (30 NTD ≈ 1 USD)

Non-Profit Organization	142	38%
Industry	209	56%
Overseas	22	6%

Taiwan Patent Application and Registration (2008-2015)

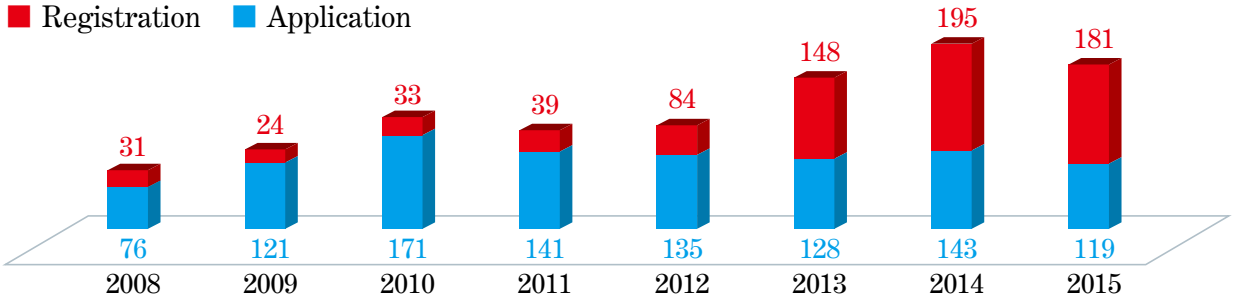

International Patent Application and Registration (2008-2015)

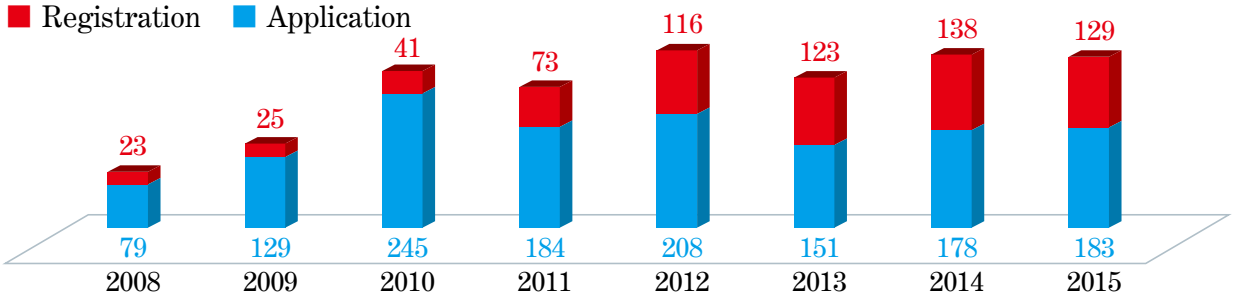

US Patent Application and Registration (2008-2015)

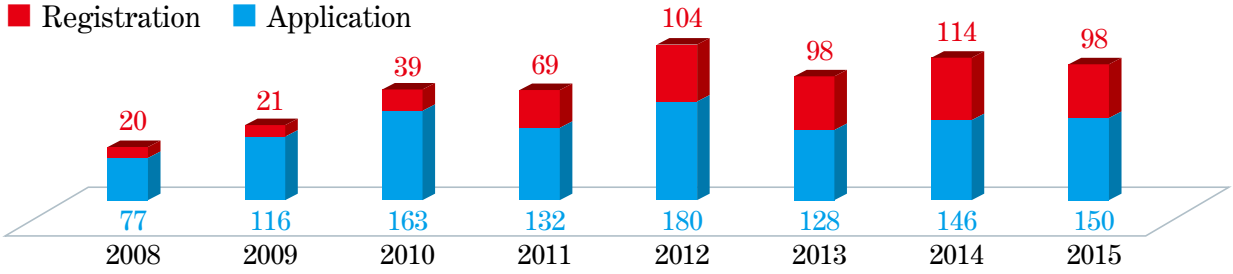

Technology Transfer Incomes (2008-2015)

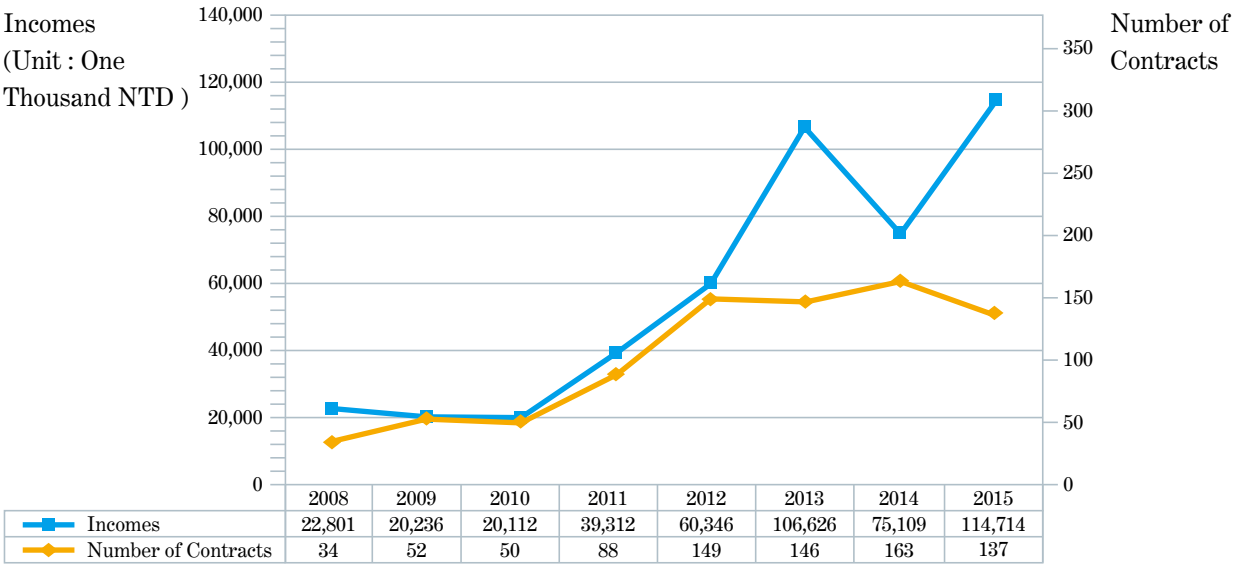

	2008	2009	2010	2011	2012	2013	2014	2015
Incomes	22,801	20,236	20,112	39,312	60,346	106,626	75,109	114,714
Number of Contracts	34	52	50	88	149	146	163	137

Number of Paper (2006-2016)

Data sorce: Essential Science Indicators[SM]: year range:2006-2016

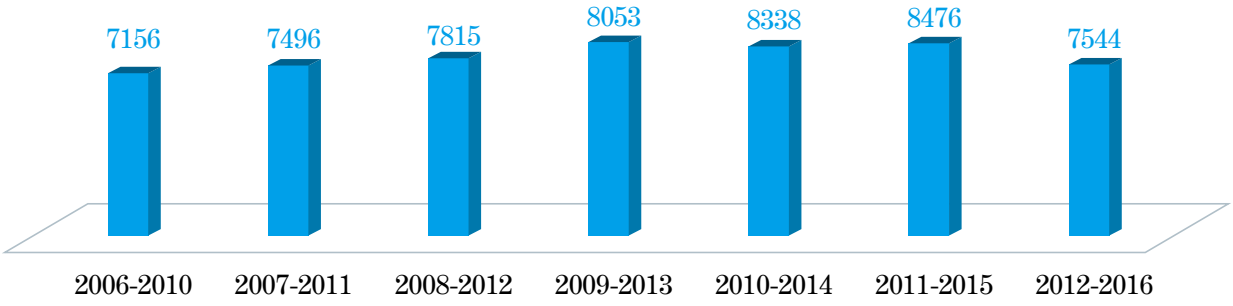

Citations Per Paper (2006-2016)

Data sorce: Essential Science Indicators[SM]: year range:2006-2016

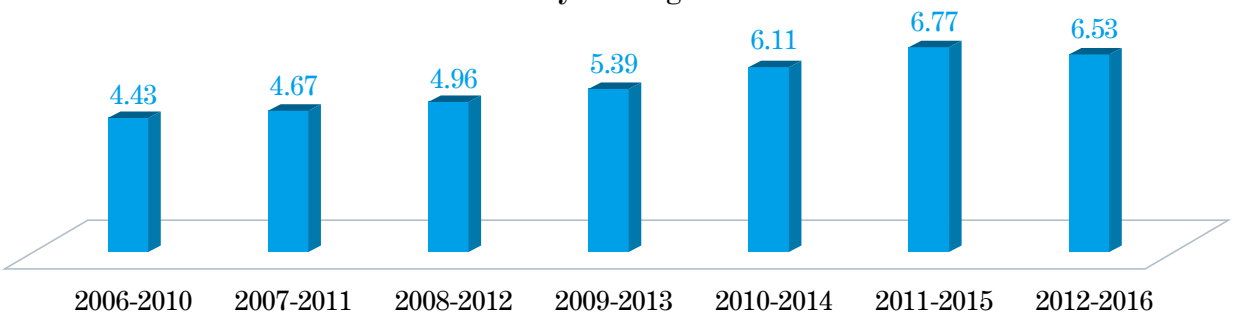

International Research Collaboration

(79 Countries / 1,368 Institutions / 36,734 Articles)

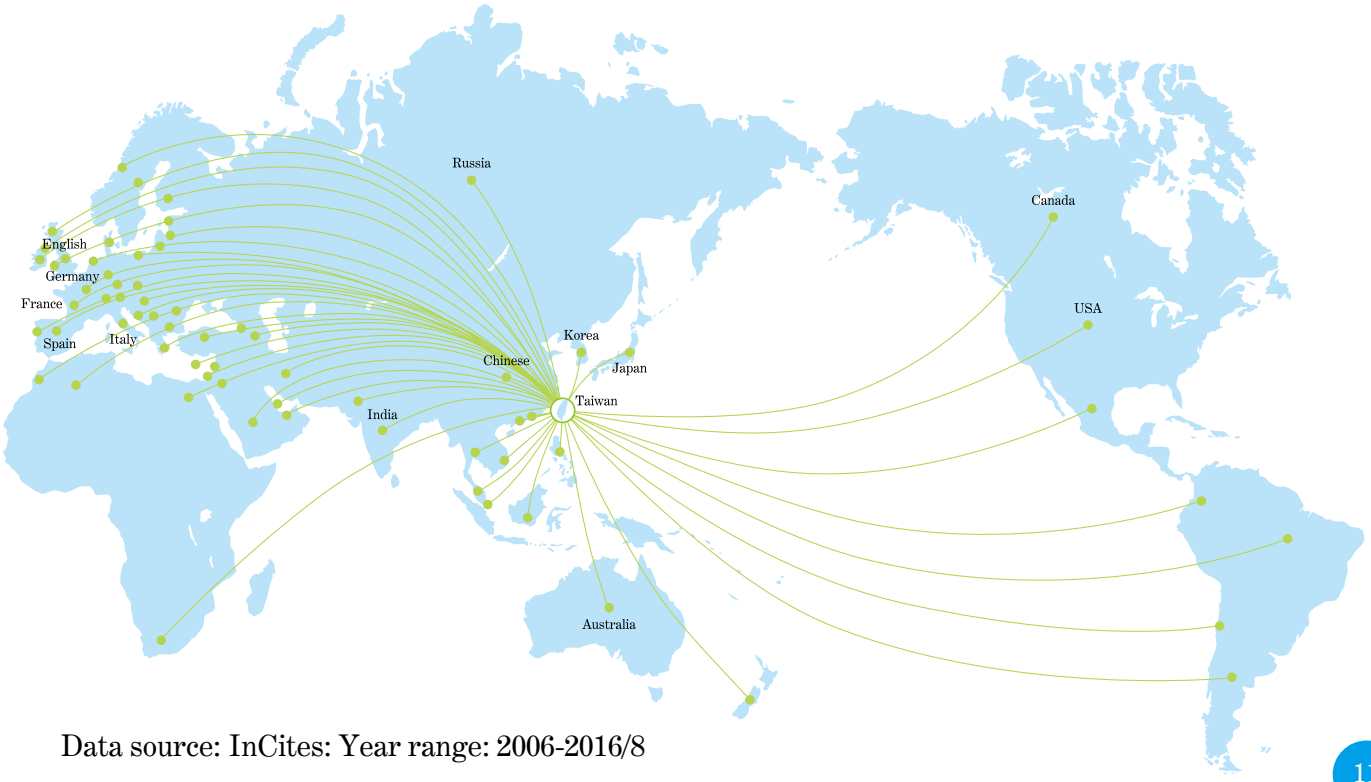

Data source: InCites: Year range: 2006-2016/8

Scientific Breakthrough

Emergence of a Fermionic Finite-Temperature Critical Point in a Kondo Lattice

Prof. Chung-Yu Mou
Department of Physics, Institute of Astronomy

Physical Review Letters 116, 177002 (2016)

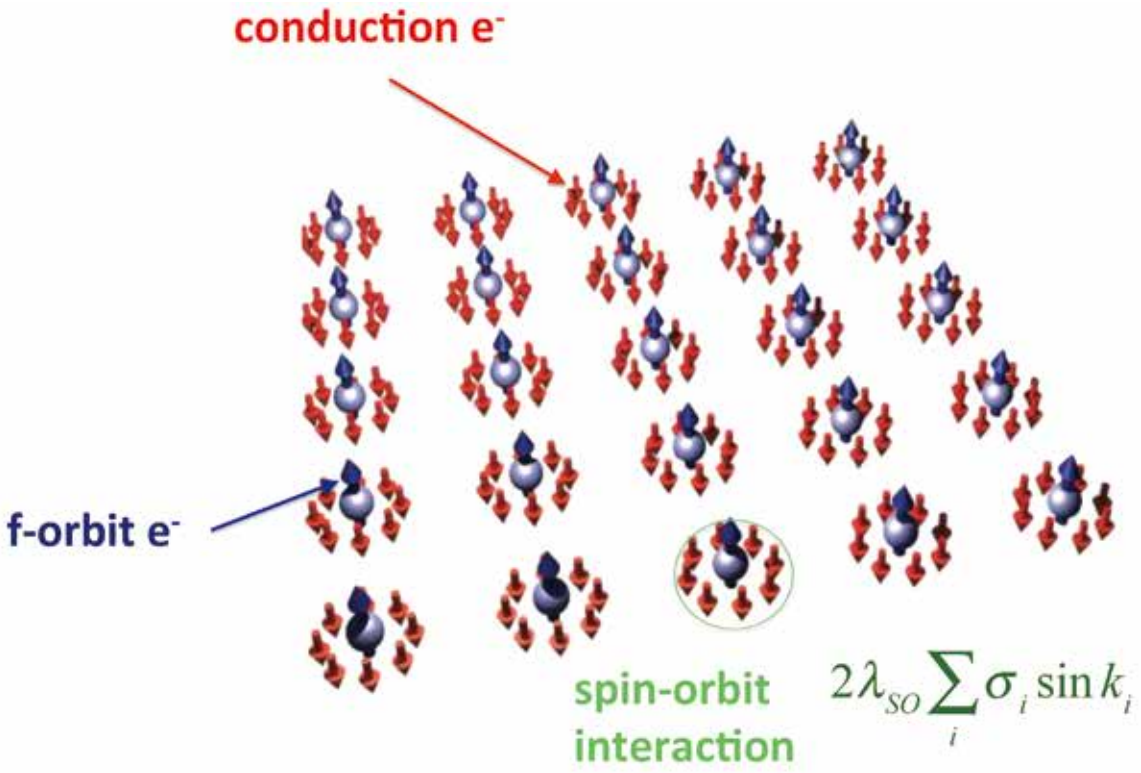

Fig. 1 Schematic plot of a Kondo lattice with spin-orbit interactions. Here the coupling between the localized electron and the conduction is characterized by λ_{SO}.

The underlying Dirac points in bulk electronic states are central to the novel properties manifested in a wide class of materials, known as Dirac materials, ranging from graphene to topological insulators. In Dirac materials, the energy gap controls the topology and the critical behavior of the quantum phase transition associated with the critical point when the gap vanishes. However, it is often difficult to drive a system across this Fermionic critical point as it requires high tunability of electronic structures without changing the underlying crystal structure. Here by exploiting the many-body screening interaction of localized spins and conduction electrons in a Kondo lattice, we demonstrate

that the electronic structures in a Kondo lattice are tunable in temperature. When spin-orbit interactions are included, we find that below the Kondo temperature, the Kondo lattice is a strong topological insulator at low temperatures and undergoes a topological transition to a weak topological insulator at a higher temperature T_D. At T_D, Dirac points emerge and the Kondo lattice becomes a Dirac semimetal. Our analysis indicates that the emergent relativistic symmetry dictates non-trivial thermal responses over large parameter and temperature regimes. In particular, it yields critical scaling behaviors both in magnetic and transport responses near T_D.

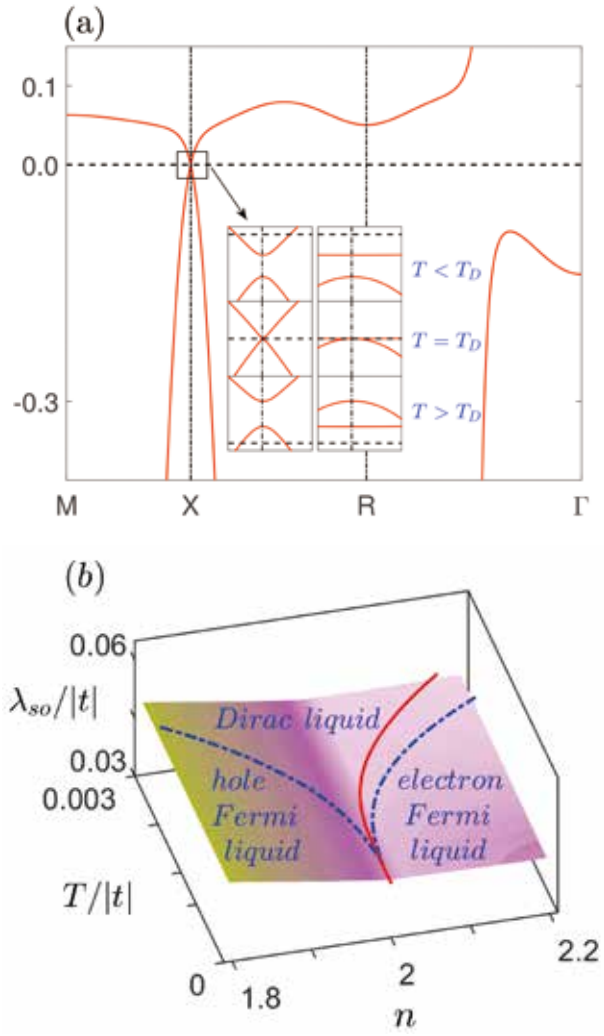

Fig. 2 (a) Emergence of a finite-temperature Dirac point at X point of a Kondo lattice with spin-orbit interactions. Inset shows relative band positions before hybridization, indicating the occurrence of a band-inversion at T_D. (b) Typical surface in the parameter space with Dirac points. Here T is temperature and n is the electron density. The red line marks critical temperatures at which the chemical potential is right at the Dirac point. The blue dash lines indicate the crossover temperature that separates the Dirac liquid regime from the Fermi liquid regime.

Authors

Po-Hao Chou, Liang-Jun Zhai, Chung-Hou Chung, Chung-Yu Mou (牟中瑜), and Ting-Kuo Lee
http://journals.aps.org/prl/abstract/10.1103/PhysRevLett.116.177002

Bis-tridentate Ir(III) Complexes with Nearly Unitary RGB Phosphorescence and Organic Light-Emitting Diodes with External Quantum Efficiency Exceeding 31%

Prof. Yun Chi
Department of Chemistry

Advanced Materials, 28, 2795-2800 (2016)

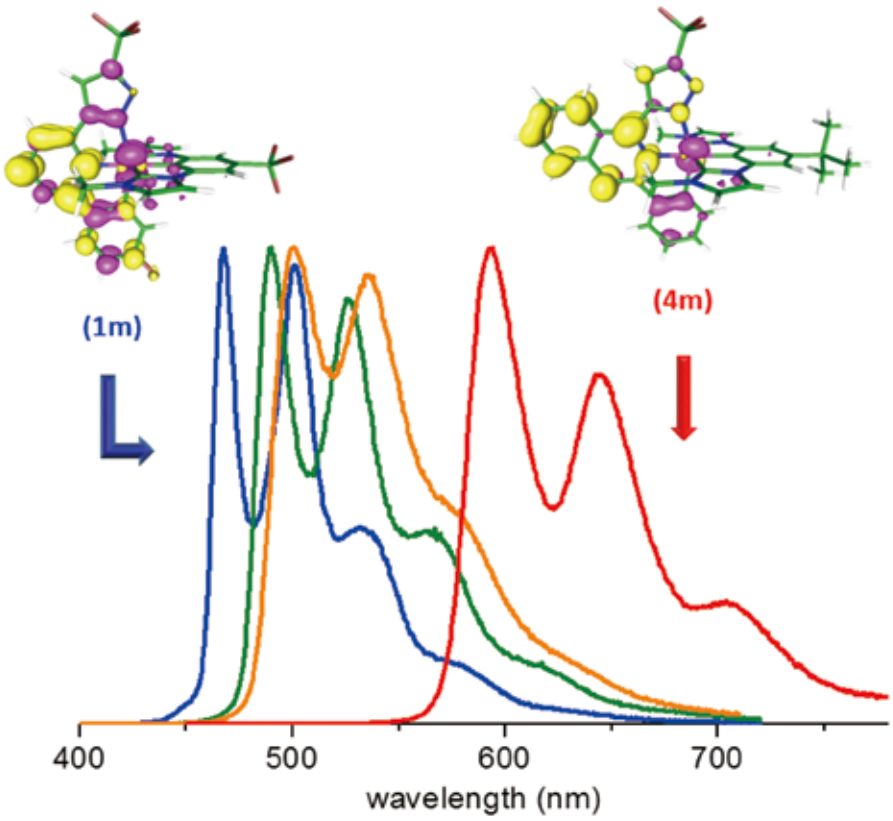

A new class of neutral bis-tridentate Ir(III) metal complexes that showed nearly unitary red, green and blue emissions in solution are prepared and employed for fabrication of both monochrome and white-emitting OLEDs, among which one green device gives the external quantum efficiency exceeding 31%.

Organic light-emitting diodes (OLEDs) have been considered as the next-generation display and lighting technologies. Thus, a great deal of effort has been focused on emitters that can effectively harvest both the singlet and triplet excitons. However, efficient phosphors, particularly those showing pure blue or broadened emission across the whole visible region, remain rare and are still in urgent demands for optoelectronic applications.

Therefore, in this work, we report a new class of neutral bis-tridentate Ir(III) metal complexes with judiciously selected bis(imidazolylidene) benzenes and functional 2-pyrazolyl-6-phenyl pyridine (or isoquinoline) chelates that showed nearly unitary red, green and blue emissions in solution. Emission color has been fine-tuned by variation of the π-conjugation and/or electronic character of chelates. Moreover, it appears that the increased rigidity and multi-dentate coordination mode of bis-tridentate architecture are the key factors that yield the excellent PL and EL efficiency. Finally, these complexes are employed for fabrication of both monochrome and white-emitting OLEDs, among which one green device gives the external quantum efficiency exceeding 31%. We believe that this relationship between structural-photophysical and device performance is expected to allow a superior design of Ir(III) metal phosphors for future OLED applications.

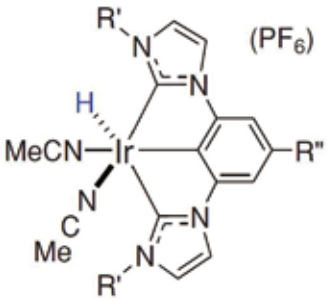

[Ir(_im_)(H)(NCCH$_3$)$_2$](PF$_6$)

R' = Me, i-Pr; R" = CF$_3$, t-Bu

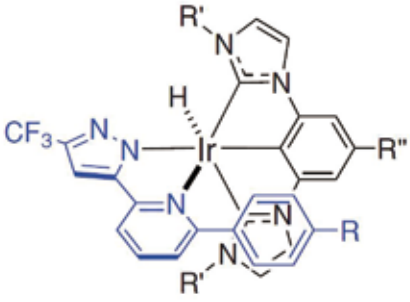

[Ir(mimf)(L2H)H]

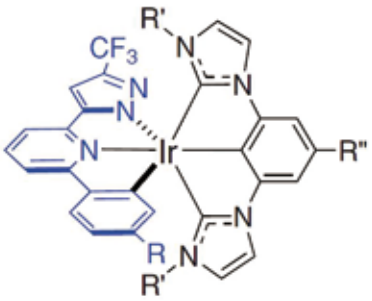

(**1m**): [Ir(mimf)(L1)]; (**1p**): [Ir(pimf)(L1)]

(**2m**): [Ir(mimf)(L2)]; (**2p**): [Ir(pimf)(L2)]

(**3m**): [Ir(mimb)(L2)]; (**3p**): [Ir(pimb)(L2)]

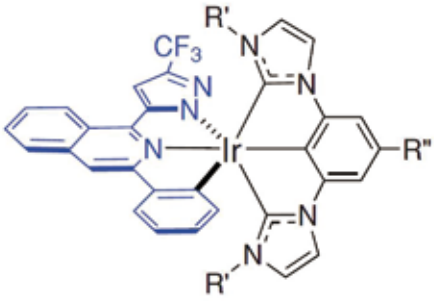

(**4m**): [Ir(mimb)(L3)]

(**4p**): [Ir(pimb)(L3)]

Authors

Chu-Yun Kuei, Wei-Lung Tsai, Bihai Tong, Min Jiao, Wei-Kai Lee, Yun Chi (季昀), Chung-Chih Wu, Shih-Hung Liu, Gene-Hsiang Lee, and Pi-Tai Chou

http://onlinelibrary.wiley.com/doi/10.1002/adma.201505790/abstract

Acoustic Emission from Breaking a Bamboo Chopstick

Prof. Tzay-Ming Hong
Department of Physics

Physical Review Letters 116, 035501 (2016)

The acoustic emission from breaking a bamboo chopstick or a bundle of spaghetti was found to exhibit similar behavior as the famous seismic laws of Gutenberg-Richter, Omori, and Bath. By use of a force-sensing detector, Professor Tzay-Ming Hong and his research group in the Physics Department established a positive correlation between the statistics of sound intensity and the magnitude of tremor. They also managed to derive these laws analytically without invoking the concept of phase transition, self-organized criticality, or fractal to which power-law behavior is often ascribed. Their theoretical model is deterministic (as opposed to being stochastic in most previous approaches) and relies on the existence of a structured cross section, either fibrous or layered. This success at explaining the power-law behavior supports the proposal that geometry is sometimes more important than mechanics.

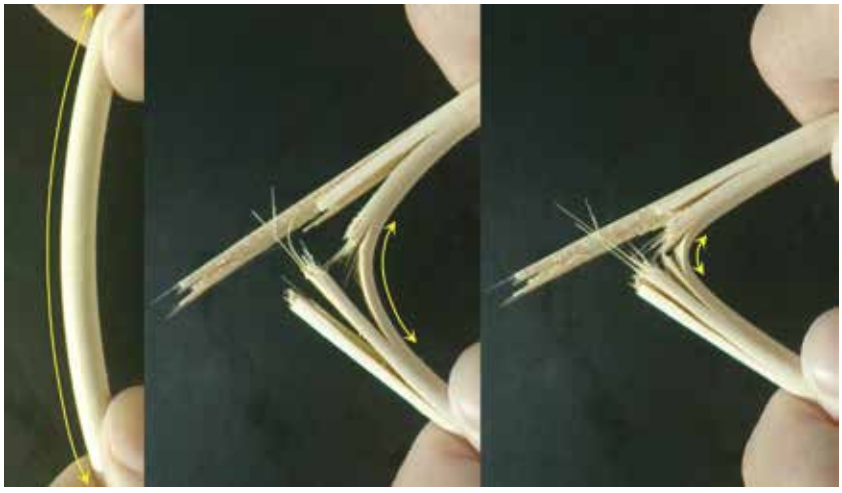

Fig. 1
Yellow double-arrowed lines highlight the progressive shortening of the effective length of the bamboo chopstick during fracture. This renders the missing of a characteristic (length) scale and causes the system to become scale-free.

Perhaps due to its wacky combination of material, this work was already featured in pop-science websites long before its publication, such as, http://thedailyorbit.com/researchers-snap-chopsticks-and-spaghetti-to-model-earthquake-fractures-102815/

Even the organization, Improbable Research, that hands out the much-publicized annual Ig Nobel Prizes highlighted this work
http://www.improbable.com/2016/01/24/the-acoustics-of-breaking-chopsticks/

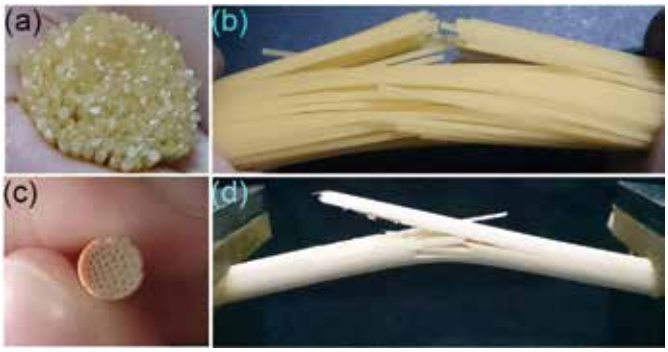

Fig. 2
Panels (a) and (c) show the similar structure in cross section between a bundle of spaghetti and a bamboo chopstick. Panels (b) and (d) are the side view during fracture.

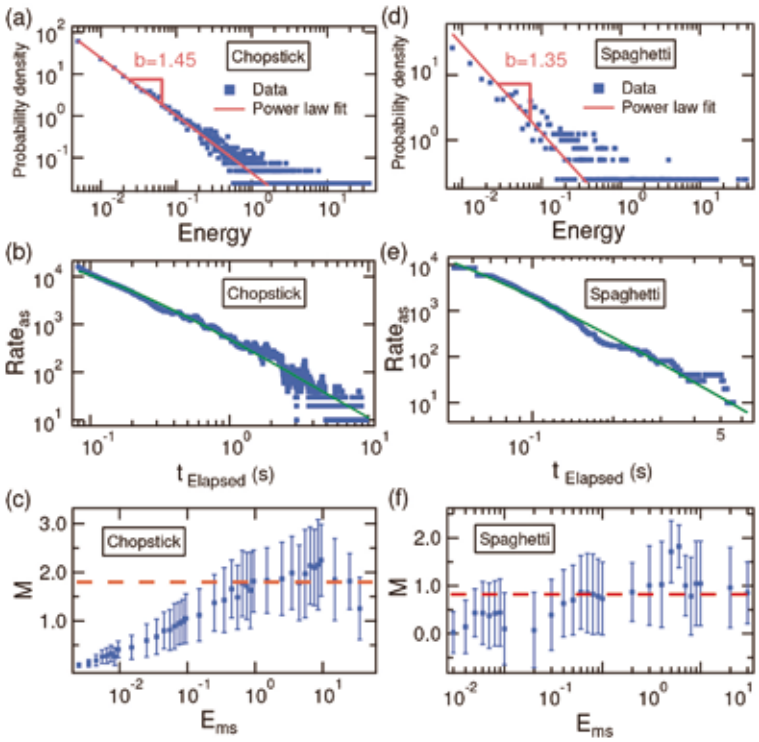

Fig. 3
(color online) Panels (a, b, c) are for crackling sound from the bamboo chopstick, while (d, e, f) from a bundle of spaghetti. They mimic the Gutenberg-Richter law, Omori's law, and Båth's law for earthquake. The power-law exponent in (a) and (d) is determined to be 1.45 and 1.35. The expo-nent and shift in (b) and (e) are (p = 1:68, c = 0:07) and (3.53, 0.027). The relative magnitude M in panels (c) and (f) is dened as the average of $\log(E_{ms}) - \log(E_{la})$ where E_{ms} and E_{la} denote respectively the energy of main shock and its largest aftershock. Error bars represent standard deviations.

Authors

Sun-Ting Tsai, Li-Min Wang, Panpan Huang, Zhengning Yang, Chin-De Chang, and Tzay-Ming Hong (洪在明)
http://journals.aps.org/prl/pdf/10.1103/PhysRevLett.116.035501

Synthesis of Ultrasmall Cu_2O Nanocubes and Octahedra with Tunable Sizes for Facet-Dependent Optical Property Examination

Prof. Michael H. Huang
Department of Chemistry

Small, 12, 3530 (2016)

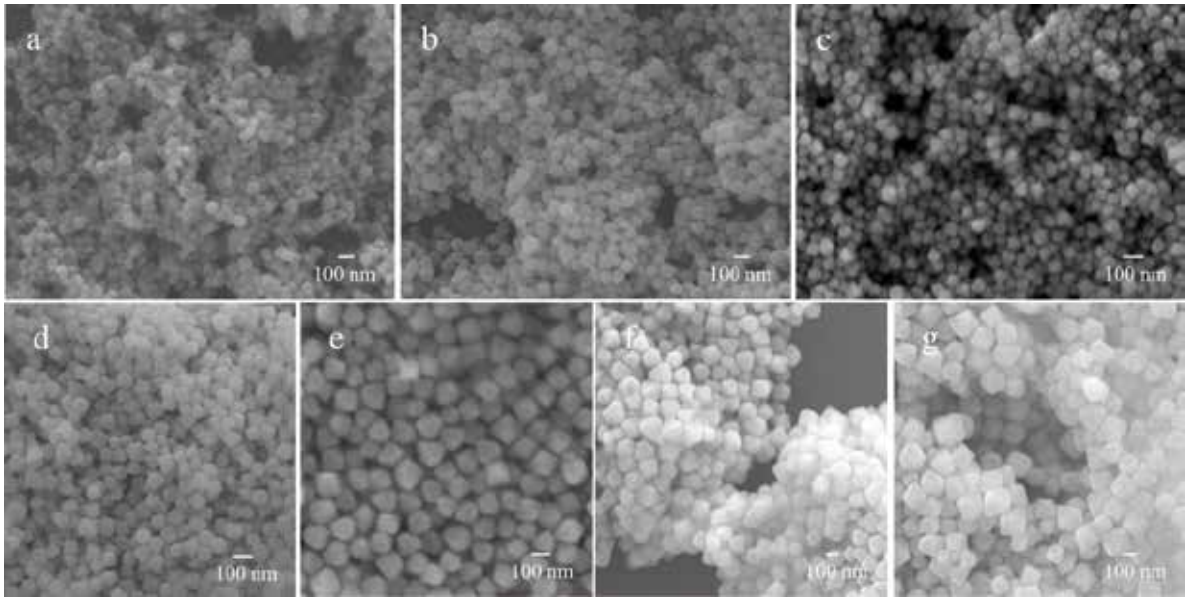

Fig. 1
SEM images of the synthesized Cu_2O a) nanocubes, b) cuboctahedra, and octahedra with average sizes of c) 52, d) 87, e) 107, f) 129, and g) 157 nm.

Through the syntheses of metal–Cu_2O core–shell polyhedra with Au, Ag, and Pd nanocrystal cores, we have demonstrated that the plasmonic bands of the metal cores are fixed in positions despite large changes in the Cu_2O shell thickness, but are tunable depending on the shape, or more correctly, exposed surface facets of Cu_2O. Since many researchers are still skeptical that optical properties of semiconductor nanocrystals are facet-dependent, believing that defects may be present somewhere in the crystals, as a result of the metal cores, leading to the observed effects, it was most desirable to make small to ultrasmall Cu_2O nanocubes and octahedra and prove clearly the existence of facet-dependent optical absorption properties of Cu_2O nanocrystals. Making ultrasmall

Cu_2O octahedra was most challenging and not achieved by others. Cu_2O octahedra with opposite corner distances of 52, 81, 107, 129, and 157 nm were synthesized at room temperature from an aqueous mixture of NaOH, N_2H_4 and copper nitrate. Cu_2O nanocubes with average edge lengths of 9, 23, 30, 44, 58, 73, and 87 nm have been synthesized at 35°C from an aqueous solution of $CuSO_4$, NaOH and ascorbic acid. They represent some of the smallest Cu_2O polyhedral nanocrystals ever known. Comparing the absorption band positions of these samples with tunable sizes, nanocubes always show a more red-shifted absorption band than that of octahedra having a similar particle volume by ~15 nm, proving convincingly the presence of facet-dependent optical properties of Cu_2O nanocrystals. This work represents the beginning of a new era changing our understanding of semiconductor optical properties.

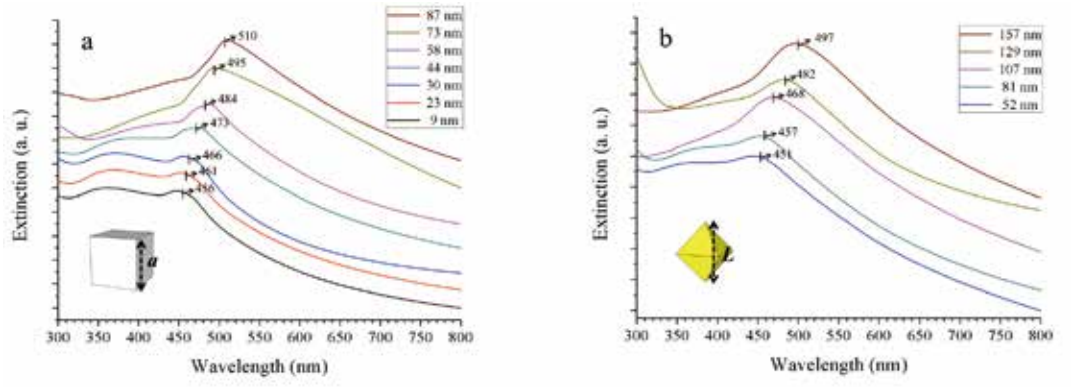

Fig. 2
UV–vis absorption spectra of small Cu_2O a) cubes and b) octahedra with tunable sizes. The measured particle sizes are indicated.

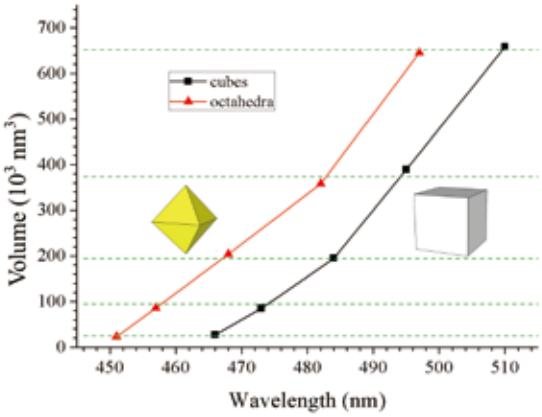

Fig.3
A plot summarizing the volume variation of Cu_2O octahedra and cubes with respect to their UV–vis absorption band positions. Red line is for octahedra and black line is for cubes. The dash lines are drawn to assist comparison of particle volumes.

Authors

Wei-Hong Ke, Chi-Fu Hsia, Ying-Jui Chen, and Michael H. Huang (黃暄益)

Controlled Release of an Anti-inflammatory Drug Using an Ultrasensitive ROS-Responsive Gas-Generating Carrier for Localized Inflammation Inhibition

Prof. Hsing-Wen Sung
Department of Chemical Engineering and Institute of Biomedical Engineering

Journal of the American Chemical Society, 137 (39), pp 12462–12465 (2015)

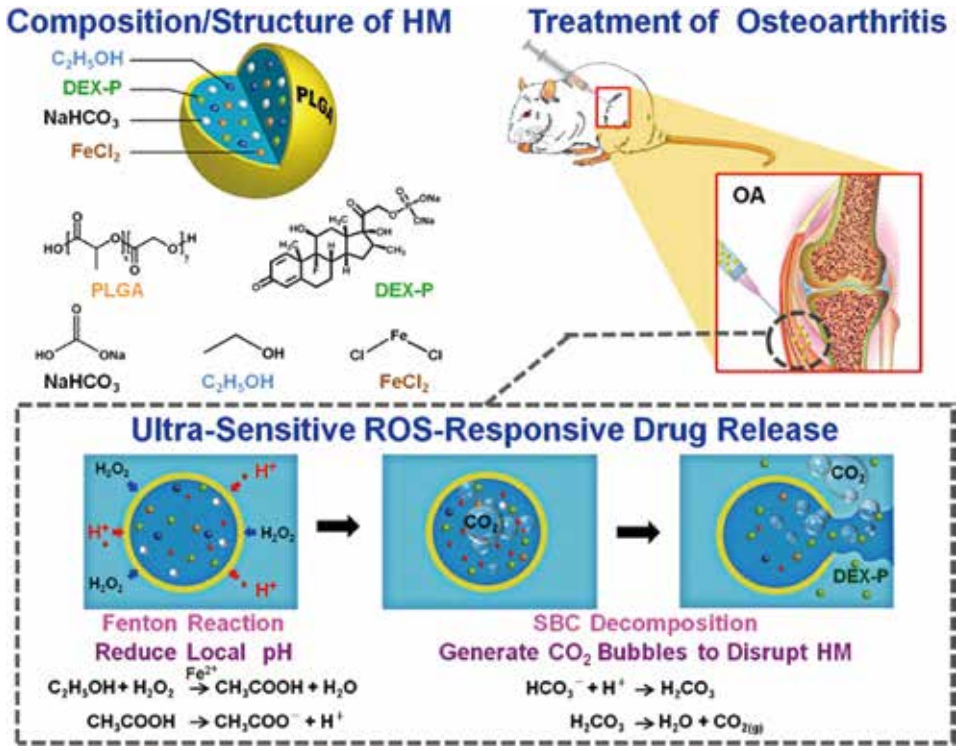

Fig. 1
Composition/structure of the ultrasensitive ROS-responsive gas-generating HM developed herein and its mechanism in the treatment of OA.

Osteoarthritis (OA) is a common joint disease that causes joint inflammation. The inflammatory responses in the OA joints depend greatly on their activated macrophages, which intracellularly generate reactive oxygen species (ROS), including H_2O_2. When formed in excess, these ROS molecules may spill out and exhibit extracellular toxicity, degrading the extracellular matrix (ECM) of the articular cartilage.

Dexamethasone sodium phosphate (DEX-P), a synthetic corticosteroid, has been widely used to treat OA, as it relieves inflammation and reduces cartilage ECM loss. However, a major challenge in the local injection of a soluble drug such as DEX-P is its rapid clearance, which requires frequent administration of the therapeutic drug (at a rate of, for example, once daily for 3–6 weeks). Therefore, the development of a controlled-release carrier that can deliver a therapeutic drug specifically to inflamed tissues is very desirable.

The release of a drug from a PLGA-based carrier is typically slow, resulting in a subeffective drug concentration. During OA inflammation, the pH in joints may reach 6.6–7.1, while the local production of ROS is enhanced. Acidification of inflamed joints is caused by the infiltration and activation of inflammatory cells that can actively pump lactic acid. Additionally, the activated inflammatory cells generate various ROS. H_2O_2 is the precursor for the production of most ROS and thus may be an important stimulus target in the design of a triggered drug release system. Currently, few, if any, polymeric carriers are sufficiently sensitive to deliver bioactive agents selectively at biologically relevant concentrations of H_2O_2 (50–100 μM). This work proposes an ultrasensitive ROS-responsive hollow microsphere (HM) carrier that can be injected and subsequently triggered upon exposure to such low concentrations of H_2O_2 (about 50 μM) to effectively deliver the encapsulated payload to inflamed tissues and protect against arthritis and joint destruction. The HMs proposed herein are fabricated using a microfluidic device in water-in-oil-in-water (W/O/W) double emulsions; each has a shell of PLGA and an aqueous core that contains the anti-inflammatory drug DEX-P, an acid precursor consisting of ethanol and an iron(II) salt ($FeCl_2$), and sodium bicarbonate (SBC) as a bubble-generating agent. Ethanol can be oxidized using Fenton's reagent, which is a system of Fe^{2+} and H_2O_2, to form an acidic (CH_3COOH) solution. Upon reaction with the acid, SBC decomposes to form bubbles of CO_2 gas, disrupting the shell wall of the HMs and releasing the anti-inflammatory drug to the problematic site, eventually protecting against joint destruction. These results reveal that the proposed HMs may uniquely exploit biologically relevant concentrations of H_2O_2 and thus be used for the site-specific delivery of therapeutics in inflamed tissues.

Authors

Ming-Fan Chung, Wei-Tso Chia, Wei-Lin Wan, Yu-Jung Lin, Hsing-Wen Sung (宋信文)
http://pubs.acs.org/doi/10.1021/jacs.5b08057

Transfer-Free Growth of Atomically Thin Transition Metal Disulfides Using a Solution Precursor by a Laser Irradiation Process and Their Application in Low-Power Photodetectors

Prof. Yu-Lun Chueh
Department of Material Science and Engineering

Nano Lett., 16 (4), pp 2463–2470 (2016)

In previous works, a research group led by Prof. Chueh Yu-Lun has demonstrated the synthesis of graphene and a few WSe_2 monolayers directly on insulators using laser irradiation as a heating source, exhibiting a good versatility to achieve 2D materials. Based on that previous acknowledge, the group has develop a novel approach for the formation of TMDs by spin coating a liquid precursor on a metal oxide layer, followed by a laser irradiation annealing process. Two kinds of TMDs, including a few WS_2 and MoS_2 monolayers confirmed by Raman, X-ray absorption spectrometer and transmission electron microscopy were demonstrated by a laser pulse with controlled power irradiation. Interestingly, the formation of the TMD monolayers was beneath the metal oxide layer instead of on the top, namely, metal oxide capped TMDs configuration to avoid the instability and degradation of the electrical measurement caused by oxygen and water absorption requiring further annealing to achieve the water desorption and measurement in vacuum.

This newly developed method allows the synthesis a few monolayers MS_2 (M=W and Mo) within a couple of minutes by combining spin coating of liquid precursors on a metal oxide layer, followed by laser irradiation annealing process. MO_3 (M=W and Mo) layer works not only as a precursor for the formation of MS_2, but also acts as a capping layer to protect against contact with air. In addition, the TiO_2 layer a barrier layer to prevent sulfur internal diffusion into Ni or Ni into the MO_3. Raman and XPS analysis support the presence of WS_2 while TEM confirmed the number of monolayers (bilayer MS_2) and the successful synthesis under the oxide protective layer. XPS results under different irradiation powers were used to support the diffusion of sulfur into the oxide layer until reaching the barrier layer prior to the formation of the MS_2. This rapid sulfur diffusion at middle temperatures explains the formation mechanism of MS_2 under the oxide layer. Besides, the precise adjustments of the laser power and irradiation time are also fundamental to the process. Furthermore, by

using standard photolithography methods to define the channel followed by the deposition of silver electrodes, a transfer-free photo sensor operated at very low power was successfully fabricated with good sensitivity and measured directly in the air. The laser-irradiation process presents several advantages such as low cost, transfer-free, fast synthesis, direct patterning, and air-stability. In addition, this approach can be also applied to other kinds of TMDs materials.

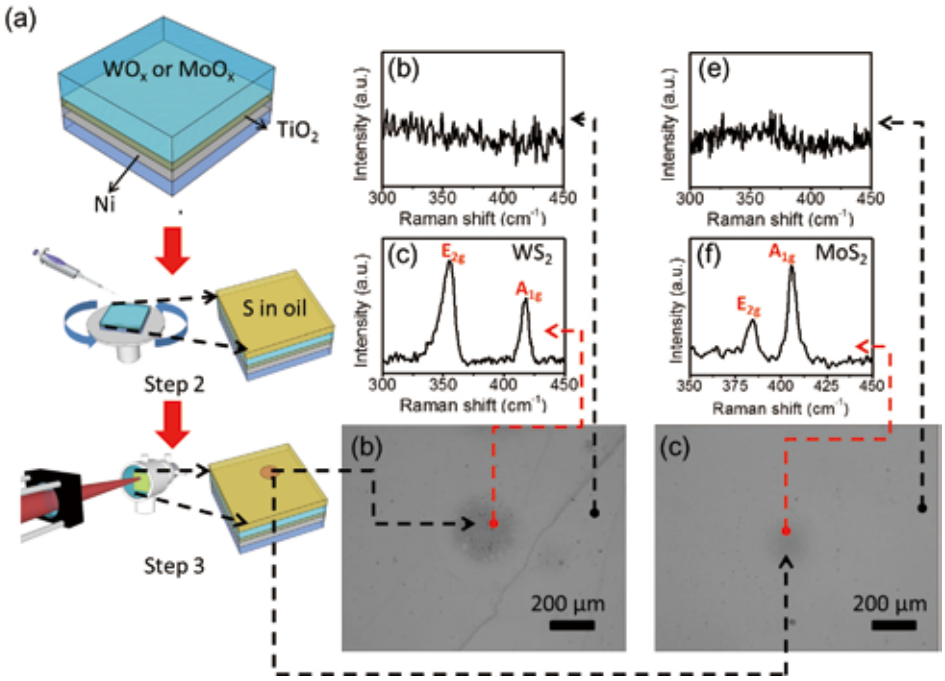

(a) Schematic illustration of the experimental steps. Optical images of WO_3 and MoO_3 samples irradiated by laser are shown in (b) and (c), respectively. (d) and (e) Raman spectra of the bright and dark areas shown in (b) corresponding to WO_3 without and with the laser irradiation. Similarly, (f) and (g) Raman spectra from the pristine and irradiated MoO_3 areas shown in (c).

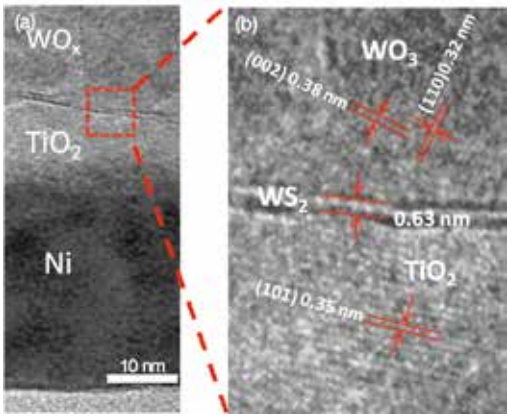

(a) Low and (b) high magnification cross sectional TEM images of WS_2 synthesized by laser irradiation irradiated MoO_3 .

Authors

Chi-Chih Huang, Henry Medina, Yu-Ze Chen, Teng-Yu Su, Jian-Guang Li, Chia-Wei Chen, Yu-Ting Yen, Zhiming M. Wang and Yu-Lun Chueh (闕郁倫)
http://pubs.acs.org/doi/abs/10.1021/acs.nanolett.6b00033

Direct Probing Se Spatial Distribution in Cu (In_xGa_{1-x}) Se_2 Solar Cells: A Key Factor to Achieve High Efficiency Performance

Prof. Chih-Huang Lai
Department of Materials Science and Engineering

Nano Energy Volume 19, January, Pages 269–278 (2016)

Control of Se content during manufacturing process has been known to determine the efficiency of $Cu(In_xGa_{1-x})Se_2$ (CIGS) solar cells. However, how Se is distributed in CIGS films and how Se distribution in hundred-nanometer scale affects the cell performance have not been realized due to limited spatial resolution of composition mapping technique. In this study, a promising nondestructive analysis by using field-emission electron probe microanalysis (FE-EPMA) is first demonstrated to directly probe the Se distribution within the depletion region of CIGS absorbers. We observe that Se-deficient-related defects are still exist in CIGS films even with high Se concentration but non-uniform distribution, leading to relatively low efficiency (~7%). By correlating photoluminescence spectra and conductivity mapping with composition distribution, we clarify that the uniform Se distribution is the key factor to suppress the defect formation and to enhance the p–n inversion at grain boundaries, resulting in significant efficiency boost to 12%.

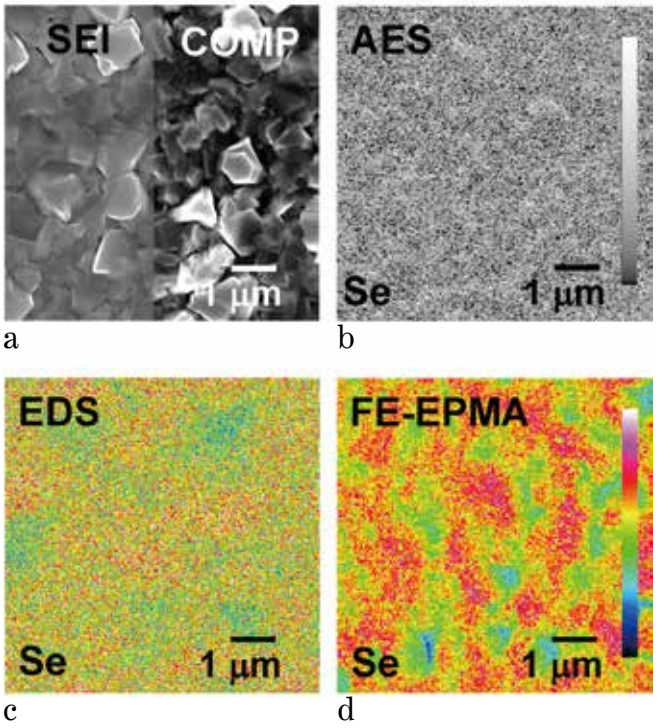

Fig. 1
(a) SEIimage,andcompositionalimage(COMP),Se-mappingfrom(b)AES,(c)EDS,and(d)FE-EPMAoftheCIGS film(sample B)byco-sputteringCu$_2$Se andCIGStargets.

a **Sample A(pristine)**

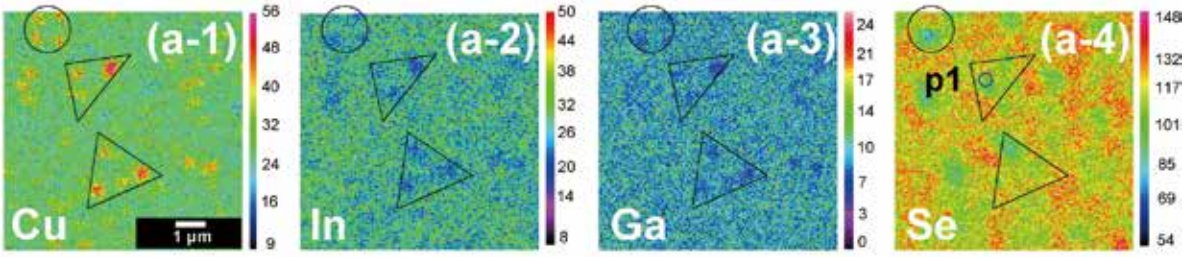

b **Sample C(pristine with KCN)**

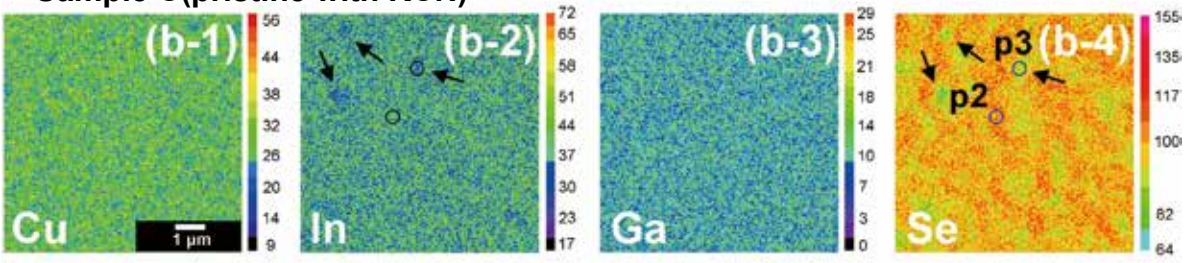

c **Sample D(post-selenization at 300ºC)**

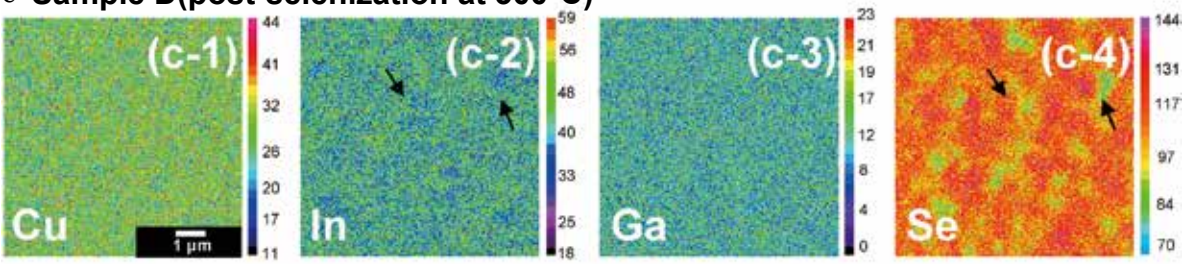

d **Sample E(post-selenization at 400ºC)**

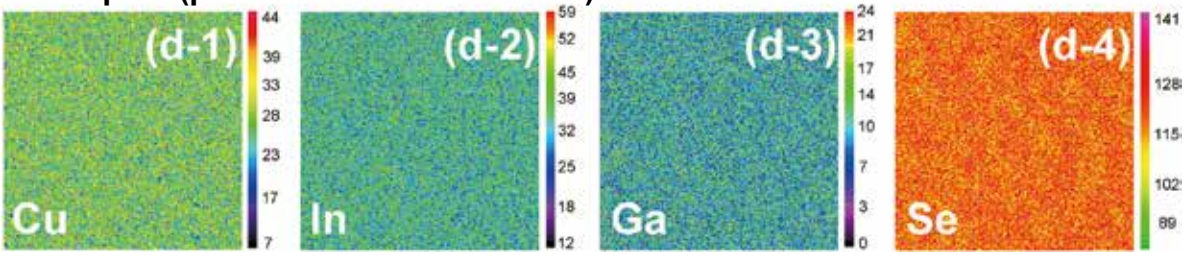

Authors

Tzu-YingLin,Chia-HsiangChen,Wei-ChihHuang,Wei-HaoHo, Yan-HuieWu,
Chih-Huang Lai (賴志煌)
http://www.sciencedirect.com/science/article/pii/S2211285515004218

Robust Fuzzy $H\infty$ Estimator-Based Stabilization Design for Nonlinear Parabolic Partial Differential Systems With Different Boundary Conditions

Prof. Bor-Sen Chen
Department of Electrical Engineering, Institute of Communications Engineering

IEEE Trans on Fuzzy Systems 24, 208-222 (2016)

In this paper, a new robust fuzzy H∞ estimator- based stabilization design for a class of N -dimensional nonlinear parabolic partial differential systems (PDSs) with either the Dirichlet or Neumann boundary conditions is proposed. First, an N -dimensional parabolic Takagi–Sugeno (T–S) fuzzy PDS is used to approximate the N -dimensional nonlinear parabolic PDS via the knowledge-based T–S fuzzy system technique. Second, based on the N -dimensional parabolic T–S fuzzy PDS, a robust fuzzy estimator-based controller is employed not only to stabilize the PDS, but also to attenuate the effects of external and measurement noises on the PDS in the spatiotemporal domain below a prescribed attenuation level. The robust fuzzy H∞ estimator-based stabilization design problem can be formulated as a diffusion matrix inequality (DMI) problem. To solve DMIs via the traditional algebraic matrix techniques, we utilize the divergence theorem and the Poincare´ inequality to transform the DMIs into bilinear matrix inequalities with a Poincare´ constant defined according to the spatial domain of the corresponding PDS. Finally, the robust fuzzy H∞ estimator-based stabilization design problem can be effectively solved by a set of linear matrix inequalities instead of the BMIs with the help of the proposed decoupled method. optimal robust fuzzy H∞ estimator-based stabilization design can be realized via minimizing the noise attenuation level. A simulation example is provided to illustrate the design procedure and verify the performance of the proposed optimal design.

We consider a class of N -dimensional nonlinear parabolic PDSs in the bounded domain Ω as follows:

$$\frac{\partial y(x,t)}{\partial t} = D\Delta y(x,t) + f(y(x,t)) + Bu(x,t) + E_d d(x,t) \quad (1)$$

$$z(x,t) = h(y(x,t)) + E_n n(x,t) \quad (2)$$

where $x = [x_1, x_2, ..., x_N]^T \in \Omega \subset \mathbb{R}^N$; f (·) and h(·) are smooth functions, $y(x,t) \in [y_1(x,t), y_2(x,t), ..., y_{n_y}(x,t)]^T \in \mathbb{R}^{n_y}$ is the state variable; $u(x,t) \in [u_1(x,t), u_2(x,t), ..., u_{n_u}(x,t)]^T \in \mathbb{R}^{n_u}$ is the control force to be designed; $d(x,t) \in [d_1(x,t), d_2(x,t), ..., d_{n_d}(x,t)]^T \in L_2(\Omega \times \mathbb{R}_+; \mathbb{R}^{n_d})$ represents external noise influence matrix $E_d \in \mathbb{R}^{n_y \times n_d}$. $z(x,t) \in [z_1(x,t), z_2(x,t), ..., z_{n_z}(x,t)]^T \in \mathbb{R}^{n_z}$ represents the measurement output measurement noise $n(x,t) \in [n_1(x,t), n_2(x,t), ..., n_{n_n}(x,t)]^T \in L_2(\Omega \times \mathbb{R}_+; \mathbb{R}^{n_n})$, $\Delta = \nabla^2$ represents the effect of diffusion on the system,

Additionally, an

$$D\Delta y(x,t)=[d_{ij}]_{n_y\times n_y}$$

$$\begin{bmatrix} \frac{\partial^2 y_1(x,t)}{\partial x_1^2}+\frac{\partial^2 y_1(x,t)}{\partial x_2^2}+\cdots+\frac{\partial^2 y_1(x,t)}{\partial x_N^2} \\ \frac{\partial^2 y_2(x,t)}{\partial x_1^2}+\frac{\partial^2 y_2(x,t)}{\partial x_2^2}+\cdots+\frac{\partial^2 y_2(x,t)}{\partial x_N^2} \\ \vdots \\ \frac{\partial^2 y_{n_y}(x,t)}{\partial x_1^2}+\frac{\partial^2 y_{n_y}(x,t)}{\partial x_2^2}+\cdots+\frac{\partial^2 y_{n_y}(x,t)}{\partial x_N^2} \end{bmatrix} \quad (3)$$

The boundary conditions are

(D) Dirichlet boundary condition : $y(x,t)=0,\ \forall x\in\partial\Omega,$

(N) Neumann boundary condition : $\frac{\partial y(x,t)}{\partial \vec{n}}=0,\ \forall x\in\partial\Omega$ (4)

we have designed the following robust fuzzy estimator-based controller:

$$\frac{\partial\hat{y}(x,t)}{\partial t}=\sum_{i=1}^{L}\mu_i(\zeta)[D\Delta\hat{y}(x,t)+A_i\hat{y}(x,t)+Bu(x,t) +L_i(z(x,t)-\hat{z}(x,t))] \quad (5)$$

$$\hat{z}(x,t)=\sum_{j=1}^{L}\mu_j(\zeta)C_j\hat{y}(x,t) \quad (6)$$

$$u(x,t)=\sum_{i=1}^{L}\mu_i(\zeta)K_i\hat{y}(x,t) \quad (7)$$

on the spatiotemporal domain Ω × [0, T] with boundary conditions similar to (4); such that the fuzzy estimation error $e(x,t)=y(x,t)-\hat{y}(x,t)$ is as small as possible and the following robust H_∞ estimation and stabilization is achieved for a prescribed ρ.

$$\int_0^T\int_\Omega[e^TP_ee+y^TP_yy]dx\le\rho^2\int_0^T\int_\Omega v^Tvdxdt \quad (8)$$

In order to realize the optimal robust fuzzy H_∞ estimator-based stabilization design for a reaction diffusion system, we utilize the Belousov–Zhabotinsky (BZ) reaction system, as an illustration example. The estimation errors and stabilization results are given in Fig.1 ~Fig.4.

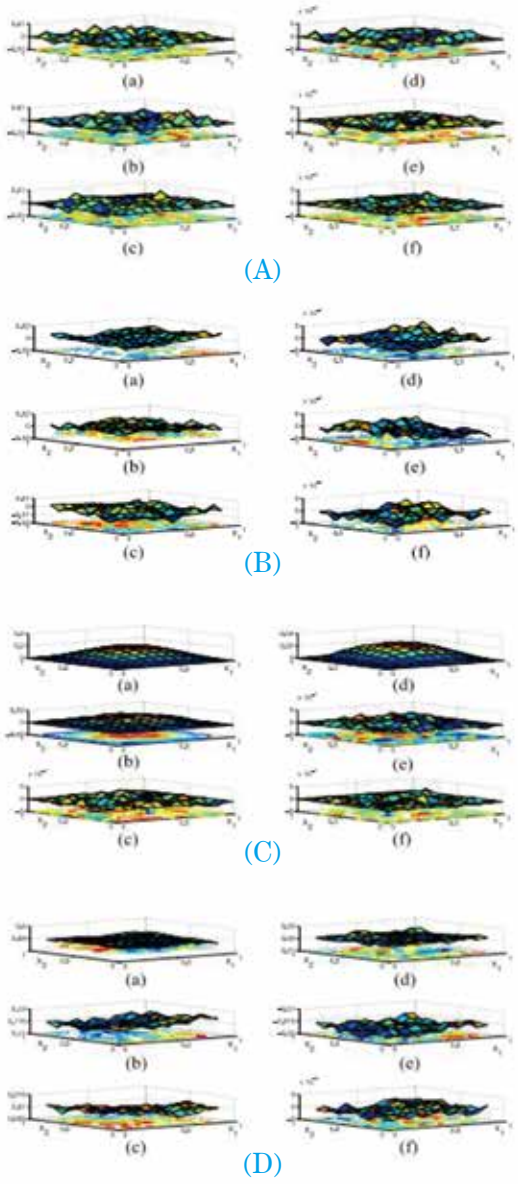

Figures (A), (B), (C) and (D) illustrate the estimation error and system state profiles e1(x,t), e2(x,t), y1(x,t) and y2(x,t) of BZ reaction system at boundary condition (D) and boundary condition (N) under the proposed fuzzy estimator-based controller at times t=3,6,10, respectively.

Authors

Shih-Ju Ho and Bor-Sen Chen (陳博現)

http://ieeexplore.ieee.org/stamp/stamp.jsp?tp=&arnumber=7147811

In-Line Three-Dimensional Holography of Nanocrystalline Objects at Atomic Resolution

Prof. F.-R. Chen
Department of Engineering and System Science

Nature Communications 7, 10603 (2016)

In the late 1950th Richard Feynman pointed out[1] that, "It would be very easy to make an analysis of any complicated chemical substance; all one would have to do would be to look at it and see where the atoms are." In principle, the latest generation aberration-corrected Transmission Electron Mocroscopes can achieve this goal but for a variety of reasons one is still far away from a reliable method that would meet Feynman's challenge of extracting the 3D position of all the atoms in an object in order to understand its physical and chemical properties. A most noticeable bottleneck is the large accumulated electron dose that is required to produce tilt series of atomic resolution images because electron dose rates are commonly chosen large (10^4 - 10^5eÅ^{-2}s^{-1}) to achieve a needed resolution around one Ångstrom and single atom sensitivity. Any such single image can exhibit uncontrolled electron beam-induced surfaces alterations or even bulk modifications particularly if particles are small.

In this paper we present a self consistent approach to recover the 3D atomic structure of nanocrystalline particles from single projections by exploiting the dynamic nature of electron scattering and pursuing a quantitative interpretation of the electron exit wave, which is reconstructed from focal series of high-resolution images. The exit wave contains not just the usual intensity, but entire field information, amplitude and phase, which is the same as " holography". In particular, this reconstruction method allows capturing images with choosable dose rates that can be adjusted to maintain structural integrity during the imaging process without compromising spatial atomic resolution and single atom sensitivity. Currently, exit wave can be reconstructed from images captured with dose rates reduced to a level of roughly one atto-Ampere Å^{-2} (6e Å^{-2}s^{-1}). Moreover, it is pointed out that the reconstructed electron wave in an image plane is not identical to the wave at the exit surface of the crystal because crystals exhibit a shape and surfaces are often not flat at the atomic scale but exhibit roughness. Therefore, focus values with respect to a common image plane change locally.

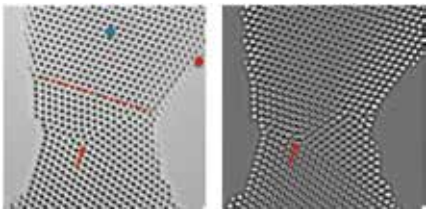

modulus Phase

Fig. 1
In-line hologram of Au [110] : Acceleration voltage = 300 kV. The hologram were reconstructed from focal series of 35 images with a focus step of 2 nm and Cs = 0 mm.

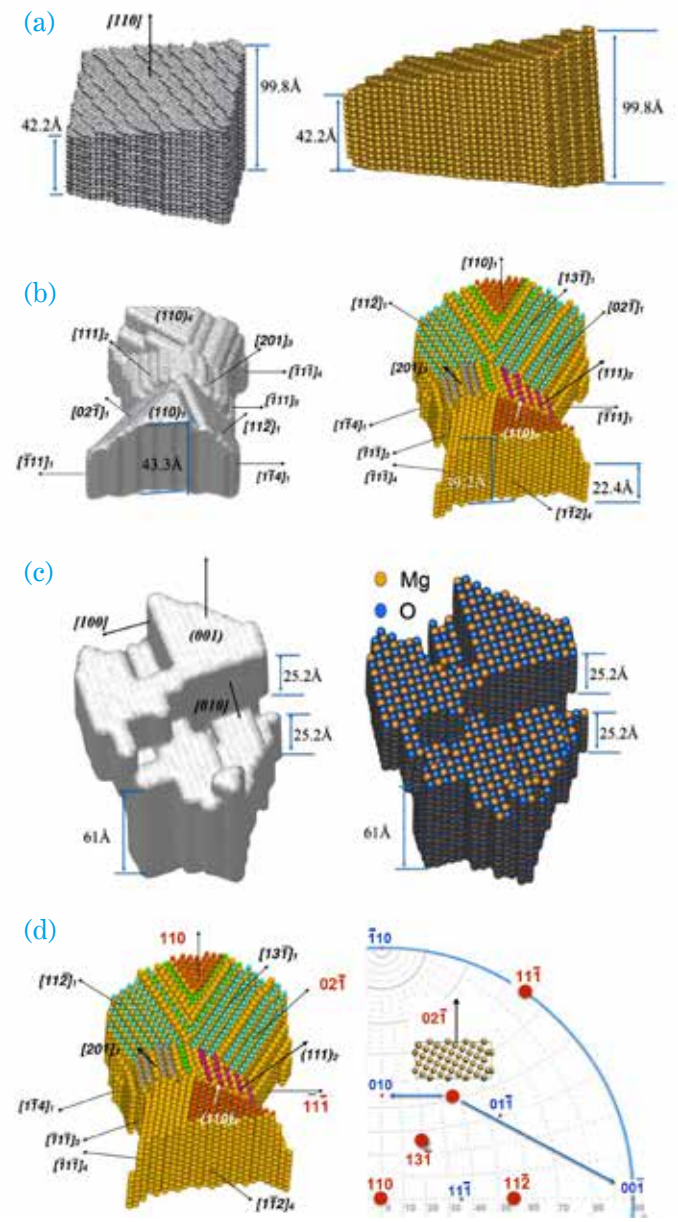

Fig. 2 Atomic resolution tomograms
(a) Surface shape and atomic structure views of the Ge [110] sample. (b) Surface shape and atomic structure views of the Au[110] sample. The facets are highlighted with different colours. (c) Surface shape and atomic structure views of the MgO [100] sample. Orange atoms: Mg, blue atoms: O (the size of the atoms is intentionally enlarged to render the shape of the particle). (d) The Wulf net shows the relationship of the high-energy facets (red dots) with low indexed facets for four grains indexed with i=1... 4. In grain 1, a [02] surface facet can be formed by low energetic [010] and [00] (red symbols) surfaces as shown by the insets and observed in the tomogram.

Authors

F.-R. Chen (陳福榮), D. Van Dyck & C. Kisielowski
http://www.nature.com/articles/ncomms10603

Making an Impact on Technology

Semiconductor Plasmonic Nanolasers: Current Status and Perspectives

Prof. Shangjr Gwo
Department of Physics

Reports on Progress in Physics vol. 79, 086501 (2016)

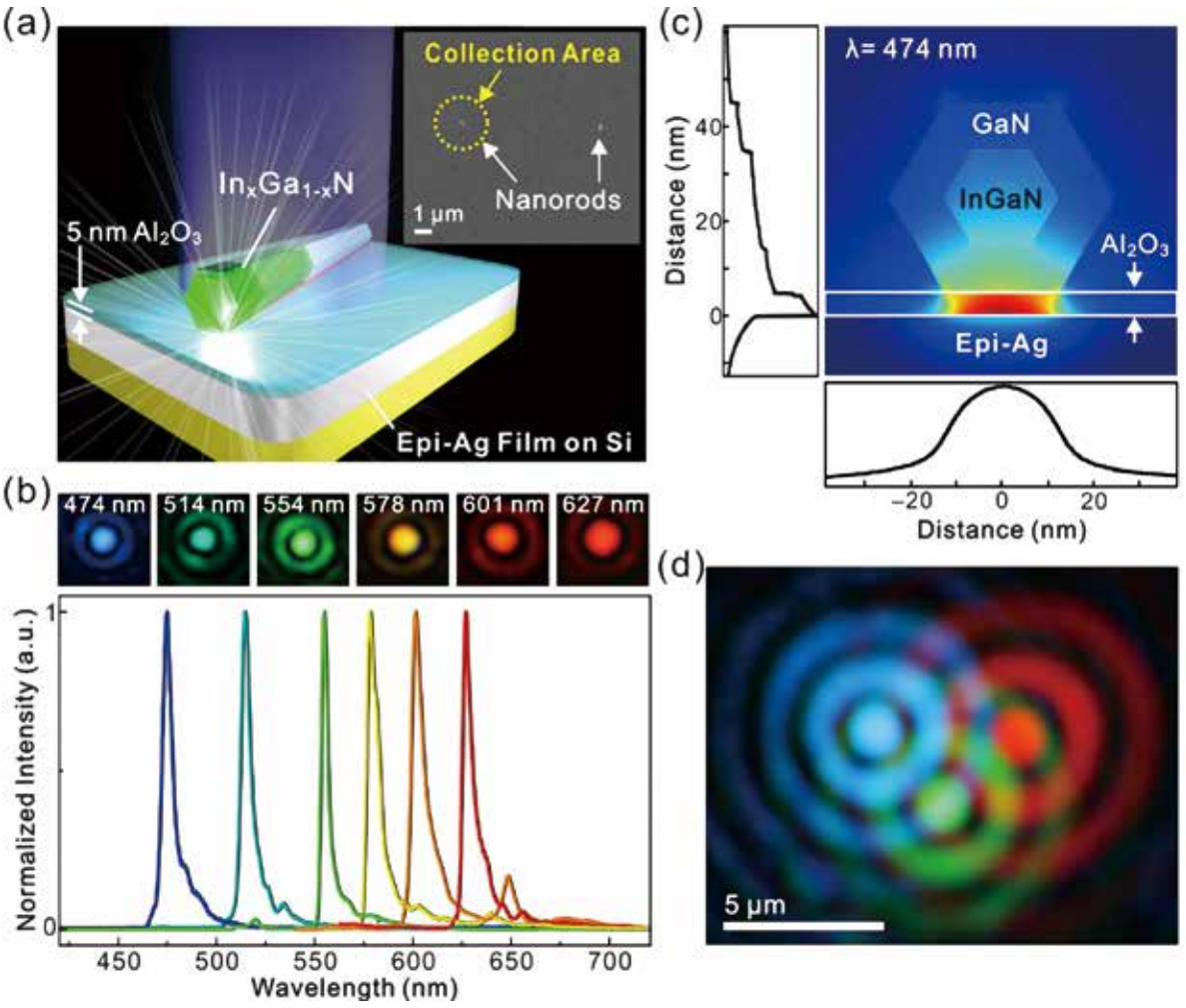

Fig. 1
Continuously tunable, all-color operation of III-nitride semiconductor plasmonic nanolasers using single InGaN@GaN core–shell nanorods with varied In compositions as the nanolaser gain media.

Scaling down semiconductor lasers in all three dimensions holds the key to the development of compact, low-threshold, and ultrafast coherent light sources, as well as integrated optoelectronic and plasmonic circuits. However, the minimum size of conventional semiconductor lasers utilizing dielectric cavity resonators (photonic cavities) is limited by the diffraction limit. To date, surface plasmon amplification stimulated emission of radiation (spaser)-based plasmonic nanolaser is the only photon and plasmon-emitting device capable of this remarkable feat. Specifically, it has been experimentally demonstrated that the use of plasmonic cavities based on metal-insulator-semiconductor (MIS) nanostructures can indeed break the diffraction limit in all three dimensions. In this review article, we present an updated overview of semiconductor plasmonic nanolasers. In particular, by using composition-varied indium gallium nitride/gallium nitride core–shell nanorods, it is possible to realize all-color, single-mode nanolasers in the full visible wavelength range with ultralow continuous-wave (CW) lasing thresholds. The lasing action in these subdiffraction plasmonic cavities is achieved via a unique autotuning mechanism based on the property of weak size dependence inherent in plasmonic nanolasers. As for the choice of metals in the plasmonic structures, epitaxial silver (Ag) crystals have been shown to be the superior constituent materials for plasmonic cavities due to their low plasmonic losses in the visible and near-infrared spectral regions. This review is based on our previous works published in 2012 (Yu-Jung Lu et al., Science vol. 337, pp. 450–453) and in 2014 (Yu-Jung Lu et al., Nano Lett. vol. 14, pp. 4381–4388).

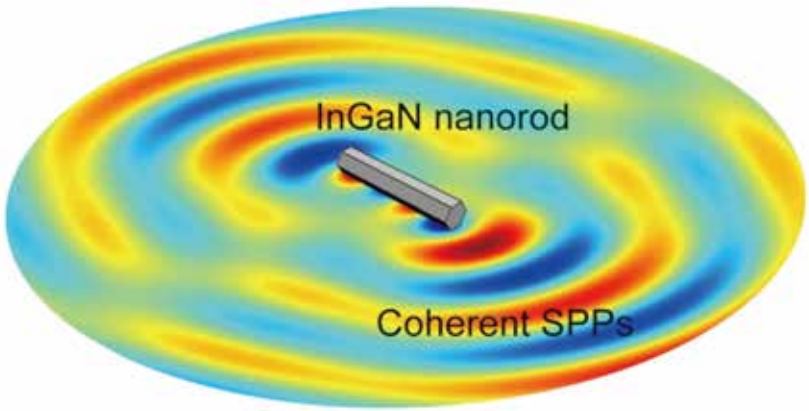

Fig. 2
Simulated radiation pattern of coherent surface plasmon polariton (SPP) emission from a spasing InGaN nanorod on an atomically smooth Ag surface.

Authors

Shangjr Gwo (果尚志) and Chih-Kang Shih
http://iopscience.iop.org/article/10.1088/0034-4885/79/8/086501

Elucidating the DNA – Histone Interaction in Nucleosome from the DNA – Dendrimer Complex

Prof. Hsin-Lung Chen
Department of Chemical Engineering and Frontier Research Center on Fundamental and Applied Sciences of Matters

Macromolecules, 49 (11), 4277–4285 (2016)

The longest DNA in chromosome can be as long as two meters in fully-stretched length. Since the cell nucleus in which the chromosomal DNA is accommodated is about 10 μm in dimension, the long DNA chains are believed to be compacted hierarchically with several levels to fit into the limited space of the nucleus. This problem, known as the"chromatin folding", is still under intensive study, as the detailed hierarchical structure associated with the DNA compaction has not been resolved completely.

Chromatin is composed of the basic building block called "nucleosome core particle" (NCP) which is interconnected by the linker DNA with different lengths. NCP contains a histone octamer (HO) and the nucleosomal DNA (~147 bp) that wraps around the HO with left-handed 1.75 turn superhelix. Through the utilization of synchrotron small angle X-ray scattering (SAXS), this study has taken a step in the direction of identifying the role of the interaction between hisone octamer (HO) and DNA in forming nucleosomes by using a simplified model system: the electrostatic complex of poly(amidoamine) (PAMAM G6) dendrimer with DNA. Our finding indicates that both dendrimer and HO have the ability to attract DNA chain to wrap around them with a comparable pitch length; however, the wrapping trajectory in dendriplex system is loose and fluctuating, while DNA wraps around HO through a sustained trajectory with very limited fluctuations. Furthermore, the dendrimers in the dendriplexes were gathered closely by DNA to achieve the free energy minimum by means of overcharging process, while the nucleosome core particles (NCPs) in the 12-mer nucleosome array were well separated by relatively long linker DNA. Our results indicate the existence of additional specific interactions beyond electrostatics between HO and DNA in nature to fix the DNA superhelix around HO and to select the favored DNA sequence to form the NCP. The present work attests that studies along the line of exploring the mechanism of sequence recognition by HO is one of the most crucial tasks for understanding the nucleosome and chromatin formation.

Fig. 1

Schematic illustrations of the supramolecular structures of the electrostatic complex of DNA with PAMAM G6 dendrimer (dendeiplex) and nucleosome array. In the dendriplex, DNA wraps around dendrimer loosely with essentially no linker DNA between successive dendriplex particles, while the superhelical trajectory in the nucleosome array is tight and rigid with the nucleosome core particles separated by relatively long linker DNA.

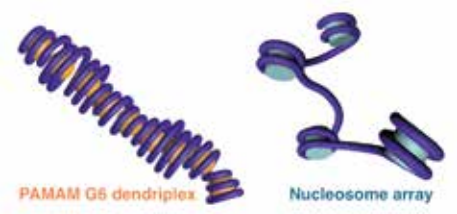

Fig. 2

(a) A comparison between the experimentally observed small angle SAXS profile and the calculated SAXS profiles using tight and loose wrapping model for the dp/0.5 dendriplex. (b) The chromatin-like fiber model with the DNA wrapping around dendrimers tightly. (c) The chromatin-like fiber model with the DNA wrapping around dendrimers loosely. The calculated SAXS curve based on the loose wrapping model closely resembles the experimental profile, attesting that DNA wraps around dendrimer loosely with very short DNA.

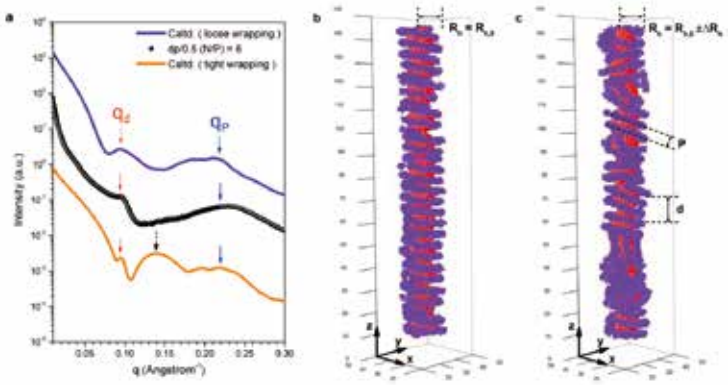

Fig. 3

(a) The observed SAXS profile (i), the fitted result using the atomic structure (ii), and the calculated profile from the coarse-grained NCP (iii). (b) The model of the coarse-grained NCP used for calculating the SAXS profile displayed by curve (iii) in (a). The fact that the observed SAXS profile of NCP was consistent with that calculated from its crystallographic structure attests that the internal structure of NCP in the solution was rigid, where the wrapping state of DNA in the NCP not only exhibited a significantly longer lifetime than the unwrapping state, but also showed very limited fluctuations in its superhelical trajectory.

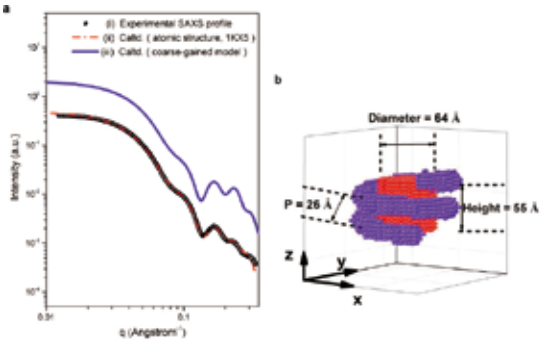

Authors

Yen-Chih Huang, Chun-Jen Su, Chun-Yu Chen, Hsin-Lung Chen (陳信龍), U-Ser Jeng, Nikolay V. Berezhnoy, Lars Nordenskiöld, and Viktor A. Ivanov

http://pubs.acs.org/doi/pdf/10.1021/acs.macromol.6b00311

Improving the Efficiency and Efficacy of Stochastic Trust-Region Response-Surface Method for Simulation Optimization

Prof. Kuo-Hao Chang
Department of Industrial Engineering and Engineering Management

IEEE Transactions on Automatic Control, 60(5), 1235-1243 (2015)

Stochastic Trust-Region Response-Surface method (STRONG) is a new response-surface-based framework for simulation optimization. The appeal of STRONG lies in that it preserves the advantages, yet eliminates the disadvantages, of traditional response surface methodology (RSM) that has been used for more than 50 years. Specifically, STRONG does not require human involvement in the search process and can guarantee to converge to the true optimum with probability one (w.p.1). In this paper, we propose an improved framework, called STRONG-X, that enhances the efficiency and efficacy of STRONG to widen its applicability to more practical problems. For efficiency improvement, STRONG-X includes a newly-developed experimental scheme that consists of construction of optimal simulation designs and an assignment strategy for random number streams to obtain computational gains. For efficacy improvement, a new variant, called STRONG-XG, is developed to achieve convergence under generally-distributed responses, as opposed to STRONG and STRONG-X where convergence is guaranteed only when the response is normal. An extensive numerical study is conducted to evaluate the efficiency and efficacy of STRONG-X and STRONG-XG. Moreover, two illustrative examples are provided to show the viability of STRONG-X and STRONG-XG in practical settings.

One application of the above-mentioned RSM-based simulation optimization methods is Vehicle fleet sizing for Automated Material Handling System (AMHS), which is an important but challenging problem due to complexity of AMHS design and uncertainty involved in the production process, e.g., random processing time. For a complex manufacturing system such as semiconductor manufacturing, the problem is even exacerbated. In this paper, we study the vehicle fleet sizing problem in semiconductor manufacturing and propose a formulation and a solution method, called simulation sequential metamodeling (SSM), to facilitate the determination of the optimal vehicle fleet size that minimizes the vehicle cost, while satisfying the time constraints. Our approach is to sequentially construct a series of metamodels, solve the approximate problem and evaluate the quality of the resulting solution. Once the resulting solution is satisfactory, the algorithm is terminated. Compared to the existing metamodeling approaches that employ enormous observations for one time, the sequential nature of SSM allows it to achieve much better computational efficiency. Furthermore, a newly-developed

estimation method enables SSM to quantify the quality of the resulting solution. Extensive numerical experiments show that SSM outperforms the existing methods and the computational advantage of SSM is increasing with the problem size and the level of the variance of response variables. An empirical study based on real data is conducted at the end to validate the viability of SSM in practical settings.

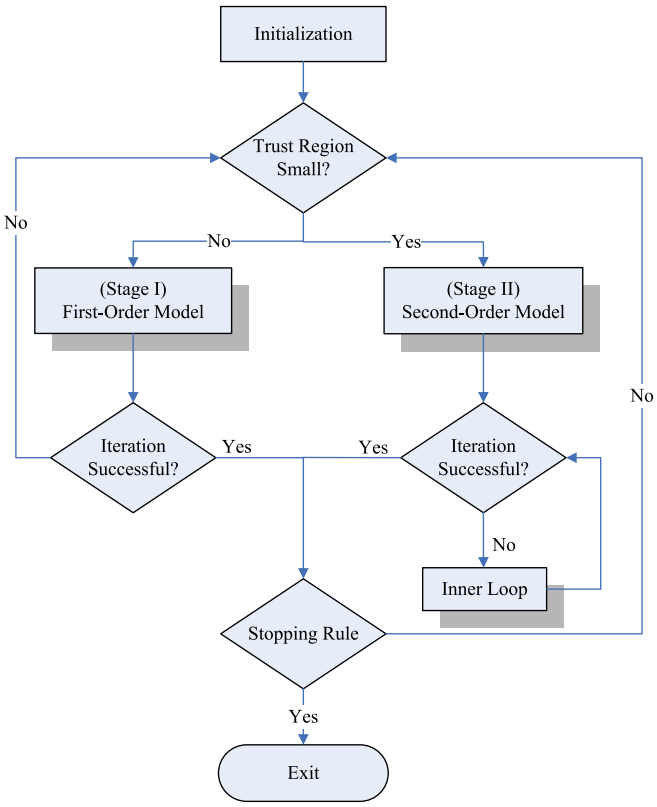

Fig. 1 Main framework of STRONG

The main framework of STRONG is shown in Figure 1. According to the size of the trust region, there are two stages, which we refer to as the outer loop and the inner loop. In Stage I, which is employed when the trust region is large, STRONG builds and optimizes a first-order model. If the solution found in Stage I is not satisfactory, the trust region shrinks. When the trust region shrinks to some point due to a number of unsuccessful iterations in Stage I, the algorithm transits to Stage II where a second-order model is built and optimized. If the algorithm still cannot find a satisfactory solution in Stage II, the inner loop is initiated where more simulation efforts are allocated to improve the quality of second-order models.

Fig. 2 Prof. Kuo-Hao Chang received 2015 IIE Transactions Best Paper Award

IIE Transactions is a prestigious journal in the areas of Industrial Engineering and Operations Research. IIE Transactions Best Paper Award is set up to recognize the best paper published in each of the focused issues of IIE Transactions.

Authors

Kuo-Hao Chang (張國浩)
http://ieeexplore.ieee.org/stamp/stamp.jsp?arnumber=6967732

Hierarchical Structure and Mechanical Properties of Snake and Turtle Eggshells

Prof. Po-Yu Chen
Department of Materials Science and Engineering

Acta Biomaterialia 31, 33–49 (2016)

After hundreds of million years of evolution, natural armors have evolved in various organisms, and has manifested in diverse forms such as eggshells, abalone shells, alligator osteoderms, turtle shells, and fish scales. Eggshells serve as multifunctional shields for successful embryogenesis, such as protection, moisture control and thermal regulation. Unlike calcareous avian eggshells which are brittle and hard, reptilians have leathery eggshells that are tough and flexible. Reptilian eggshells can withstand collision damages when laid in holes and dropped onto each other, and reduce abrasion caused by buried sand. In this study, we investigate structure and mechanical properties of eggshells of Taiwan cobra snake (Naja atra) and Chinese striped-neck turtle (Ocadia sinensis). From Acid Fuchsin Orange G (AFOG) staining and ATR-FTIR examination, we found that both eggshells are mainly composed of keratin. The mechanical properties of demineralized snake and turtle eggshells were evaluated by tensile and fracture tests and show distinctly difference. Turtle eggshells are relatively stiff and rigid, while snake eggshells behave as elastomers, which are highly extensible and reversible. The exceptional deformability (110–230% tensile strain) and toughness of snake eggshells are contributed by the wavy and random arrangement of keratin fibers as well as collagen layers. Multi-scale toughening mechanisms of snake eggshells were observed and elucidated, including crack deflection and twisting, fibers reorientation, sliding and bridging, inter-laminar shear effect, as well as the α–β phase transition of keratin. Inspirations from the structural and mechanical designs of reptilian eggshells may lead to the synthesis of tough, extensible, lightweight composites which could be further applied in the flexible devices, packaging and bio-medical fields.

Amniotic eggshells serve as multifunctional shields for successful embryogenesis. The avian eggshells have been extensively studied while there are very few studies on reptilian eggshells and most of them focused on mineralization and embryotic development. For the first time, the hierarchical structure and mechanical properties of snake and turtle eggshells are comprehensively and comparatively studied. Both snake and turtle eggshells are multilayer, hierarchically-structured composites consisting mainly of keratin yet their mechanical behaviors are distinctly different. Turtle eggshells are stiff and rigid, while snake eggshells are highly extensible (>200%) and reversible due to multiple deformation stages, phase transition of keratin and various toughening mechanisms. We believe that this study will make positive scientific impact and interest the broad and multidisciplinary readership.

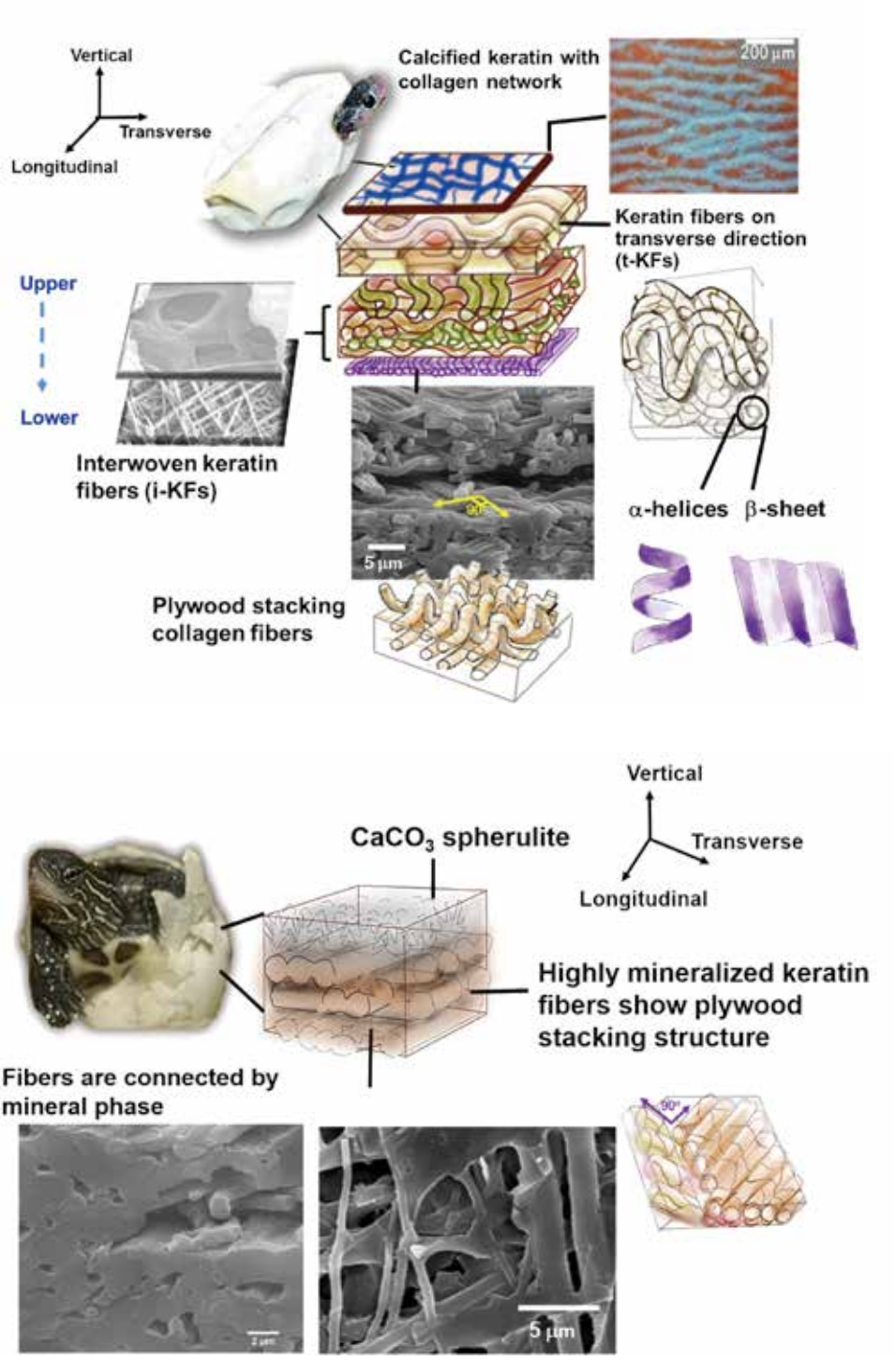

The hierarchical structures and representative tensile mechanical properties of snake and turtle eggshells: Snake eggshells are soft, ductile with exceptional toughness while turtle eggshells are relative stiff and brittle.

Authors

Yin Chang, Po-Yu Chen (陳柏宇)

http://www.sciencedirect.com/science/article/pii/S1742706115302166

Point-of-Care Diagnostic Devices for Monitoring Diseases and Food Safety

Prof. Chao-Min Cheng
Institute of Biomedical Engineering

A. Monitoring VEGF levels with low-volume sampling in major vision-threatening diseases: age-related macular degeneration and diabetic retinopathy

B. Development of a sampling collection device with diagnostic procedures

After completing his Ph.D. at Carnegie Mellon University and conducting postdoctoral research at Harvard University, Cheng Chao-Min returned to Taiwan as an independent P.I. at NTHU. His research focuses on cell biomechanics and the development of low-cost diagnostic devices. Cheng has already successfully developed paper-based diagnostic devices, and is currently working on developing similar devices but made of materials which are inexpensive and easy to obtain, such as cotton and wood fiber. Working together with clinical research units, Cheng has successfully developed different types of clinically relevant diagnostic devices for testing sperm vitality, female ovulation cycle, dengue fever, bullous pemphigus, proliferative diabetic retinopathy, age-related macular degeneration, and retinal vein occlusion. In addition, he has developed a new platform for exploring the process of cell growth and cell mechanics, and successfully fabricated chitosan-based nanostructures for understanding the biochemical reaction of normal and cancer cells as well.

During Cheng's four years at NTHU nearly 60 of his research articles have been published in leading journals in the fields of biomedical engineering, analytical chemistry, and biomaterials; eight of his reports have appeared as the cover articles. He has also served as the editors or guest editors of several decent journals. Moreover, Cheng is striving to find ways to mass produce some of the devices he has invented, and nearly 30 of his inventions have received patents or are under pending. Furthermore, he serves as a consultant to a number of domestic and foreign biotech companies.

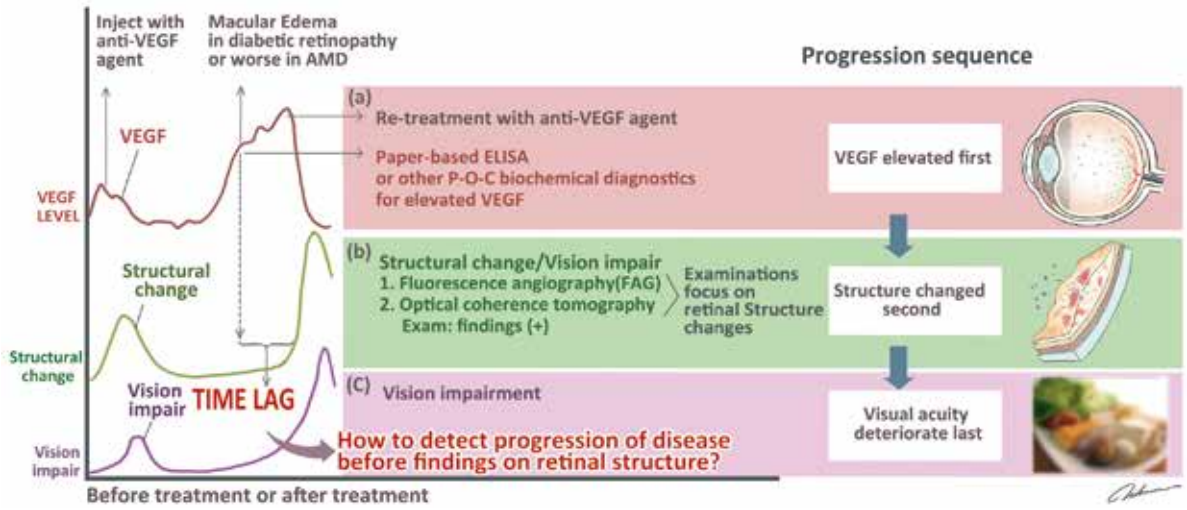

Cervicovaginal fluid plays an important role in the detection of many female genital diseases, but the lack of suitable collection devices in the market severely challenges test success rate. Appropriate clinical sampling devices for cervicovaginal fluid collection would help physicians detect diseases and disease states more rapidly, efficiently, and accurately. The objective of this study was to develop a readily usable sampling collection device that would eliminate macromolecular interference and accurately provide specimens for further studies. This study was designed to develop an effective device to collect cervicovaginal fluid from women with symptoms of endometrial lesions, women appearing in the clinic for a routine Papanicolaou smear, and/or women seeking a routine gynecologic checkup. Paper-based assay, ELISA, and qNano were used to provide accurate diagnoses. A total of 103 patients successfully used the developed device to collect cervicovaginal fluid. Some of the collected specimens were used to detect glycogen, lactate, and pH for determining pathogen infection. Other specimen samples were tested for the presence of female genital cancer by comparing interleukin 6 concentration and microvesicle concentration. We proposed a noninvasive screening test for the diagnosis of female genital diseases using a dual-material collection device. The outer, nonwoven fabric portion of this device was designed to filter macromolecules, and the inner cotton portion was designed to absorb cervicovaginal fluid.

Authors

Jhih-Yan Cheng, Mow-Jung Feng, Chia-Chi Wu, Jane Wang, Ting-Chang Chang, and Chao-Min Cheng (鄭兆珉)

http://pubs.rsc.org/en/Content/ArticleLanding/2015/LC/C4LC01052C#!divAbstract
http://pubs.acs.org/doi/abs/10.1021/acs.analchem.6b01269

Connectomics-Based Analysis of Information Flow in the *Drosophila* Brain

Prof. Ann-Shyn Chiang
Institute of Biotechnology

A Drosophila connectome was reconstructed by 12,995 neuron images in FlyCircuit 1.1

Hierarchical organization, small word, and rich club were observed in the brain

Pathways of information flow during behavior were predicted from network structure

Organization schemes of fly and mammalian brains showed fundamental similarities

Understanding the overall patterns of information flow within the brain has become a major goal of neuroscience. In the current study, we produced a first draft of the *Drosophila* connectome at the mesoscopic scale, reconstructed from 12,995 images of neuron projections collected in FlyCircuit (version 1.1). Neuron polarities were predicted according to morphological criteria, with nodes of the network corresponding to brain regions designated as local processing units (LPUs). The weight of each directed edge linking a pair of LPUs was determined by the number of neuron terminals that connected one LPU to the other. The resulting network showed hierarchical structure and small-world characteristics and consisted of five functional modules that corresponded to sensory modalities (olfactory, mechanoauditory, and two visual) and the pre-motor center. Rich-club organization was present in this network and involved LPUs in all sensory centers, and rich-club members formed a putative motor center of the brain. Major intra- and inter-modular loops were also identified that could play important roles for recurrent and reverberant information flow. The present analysis revealed whole-brain patterns of network structure and information flow. Additionally, we propose that the overall organizational scheme showed fundamental similarities to the network structure of the mammalian brain.

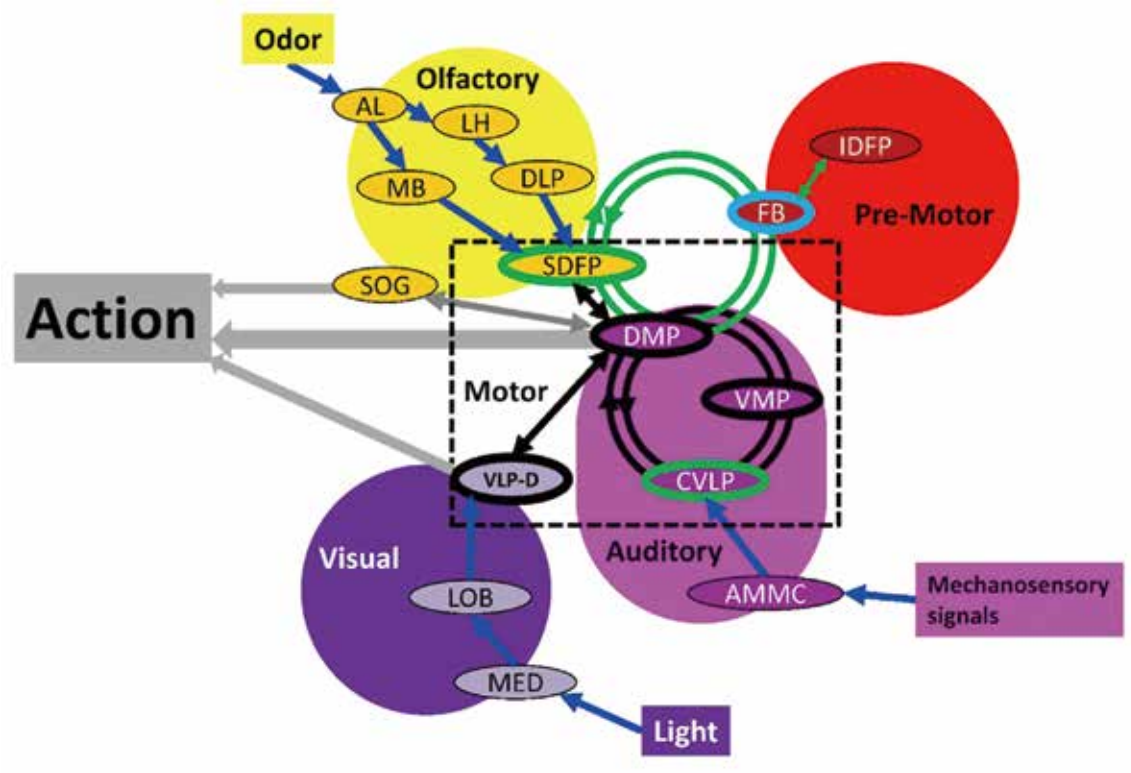

Through the analysis of connectivity among brain regions within the fly brain, we found a hierarchical structure for information flow from sensory input to behavioral output. The olfactory, auditory and visual signals are sent to AL, AMMC and MED, respectively. Signals were then processed in their corresponding sensory modules (yellow, magenta and purple regions) along the pathways indicated by the blue arrows, and converged on the possible motor center regions SDFP, CVLP, and VLP-D for olfaction, audition, and vision, respectively. After processing (black arrows) in the motor center, output commands were sent mainly through DMP and VLP-D, or alternatively, via SOG. The motor center communicated with the pre-motor center, and was involved in the strongest three-loop circuit (indicated by green circles) among SDFP, FB and DMP. Taken together, these data suggest that decision-making is produced through reiterated signal processing in a specialized pathway between the pre-motor and motor centers. The motor center finally launches a command of action according to the decision.

Authors

Chi-Tin Shih, Olaf Sporns, Shou-Li Yuan, Ta-Shun Su, Yen-Jen Lin, Chao-Chun Chuang, Ting-Yuan Wang, Chung-Chuang Lo, Ralph J. Greenspan, Ann-Shyn Chiang (江安世)
http://www.sciencedirect.com/science/article/pii/S096098221500336X
http://www.sciencedirect.com/science/article/pii/S0960982215003929

The Historical-Structural Discrimination Faced by Taiwanese Indigenous Austronesian Peoples can be Fully Disclosed in Their Contorted Modernization Process, Distinct Disease Prevalence Pattern and Shortened Life Expectancy

Prof. Shu-Min Huang
Institute of Anthropology

Asian Ethnicity, Vol. 17, No. 2, 294-312

Recipient of Taiwan's Presidential Science Award, November, 2015.

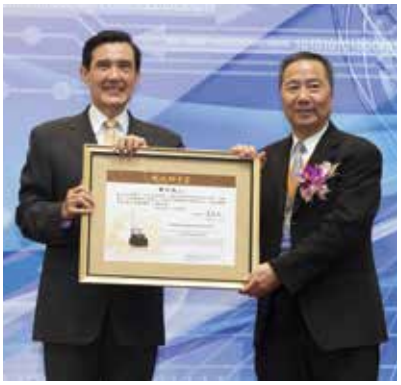

In collaboration with Dr. Shao-hua Liu, Associate Research Fellow at the Institute of Ethnology, Academia Sinica, we published one journal article and one book chapter in 2016.

Dr. Liu and I are co-PIs of a thematic research project titled, "Sustainable Development in Anthropocene: Changing Urban Life in Taiwan," under the Center of Sustainable Sciences in Academia Sinica. This is a continuation of our previous research on Taiwan's rural Austronesians who have migrated to cities in Taiwan. This year we published two articles. In "Discrimination and incorporation of Taiwanese indigenous Austronesian peoples," published in *Asian Ethnicity*, we analyzed the historical-structural discriminations the indigenes encountered, and the consequential unique disease prevalence patterns, shortened life expectancy, and dilemmas for future development.

In the book chapter, "Waterscape and Social Transformations in Southern Taiwan: The Damming of Mudan Creek," edited by T'sui-jung Liu and James Beattie, we use the Paiwan tribe in southern Taiwan as an example to examine how they were swirled into the modernization drive since the late 19th century, and the compulsory cultural adaptations, such as the conversion to rice paddy farming during the Japanese occupation period, and the construction of the Mudan Reservoir under the current regime.

Authors

Shu-min Huang (黃樹民) and Shao-hua Liu
http://dx.doi.org/10.1080/14631369.2015.1112726

Waterscape and Social Transformations in Southern Taiwan: The Damming of Mudan Creek

Prof. Shu-Min Huang
Institute of Anthropology

Ondon: Palgrave. Pps. 111-135

This paper uses the Paiwan tribe in southern Taiwan as an example to examine how they were swirled into the modernization drive since the late 19th century, and the compulsory cultural adaptations, such as the conversion to rice paddy farming during the Japanese occupation period, and the construction of the Mudan Reservoir under the current regime.

Authors

Shao-hua Liu and Shu-min Huang (黃樹民)
http://link.springer.com/chapter/10.1007%2F978-1-137-57231-8_5

Research Highlights

60 **Unravelling the Mystery of Vacuolar Phosphate Transporter**
Prof. Tzu-Yin Liu

61 **PICH Promotes Sister Chromatid Disjunction and Co-Operates with Topoisomerase II in Mitosis**
Prof. Lily Hui-Ching Wang

62 **MAK^{5} KƐ^{4} セ个 AND MAN^{3} ȵIN^{2} 瞞人 IN HAKKA: A HISTORICAL AND TYPOLOGICAL PERSPECTIVE in Hakka**
Interpreting 都 *to*^{1} TO in earlier Southern Min texts
Prof. Lien, Chinfa

63 **Formation of the Experiential Aspect Marker Pat^{4} 識 :Contact-induced Grammatical Change in Southern Min**
Prof. Lien, Chinfa

64 **Nietzsche and Husserl on the constitution of Ideas—Intersection between Genealogy and Phenomenology**
Prof. Chon-IP Ng

Diastereoselective [3+2] Annulation of Aromatic/ Vinylic Amides with Bicyclic Alkenes through Cobalt-Catalyzed C-H Activation and Intramolecular Nucleophilic Addition

Prof. Chien-Hong Cheng
Department of Chemistry

Angew. Chem. Int. Ed. 55, 4308-4311 (2016)

A highly diastereoselective method for the synthesis of dihydroepoxybenzofluorenone derivatives from aromatic/vinylic amides and bicyclic alkenes via cobalt-catalyzed C-H activation reaction is reported by the group of Prof. Chien-Hong Cheng in National Tsing Hua University. This new transformation is the first time that a [3+2] cycloaddition of secondary amides with alkenes, and it works well under mild reaction conditions and features a broad substrate scope. This reaction proceeds through cobalt-catalyzed C-H activation and intramolecular nucleophilic addition to the amide functional group.

Transition-metal-catalyzed C-H bond functionalization reactions have become an essential method for the synthesis of functionalized organic compounds. Instead of well-studied C-H activation reactions using Pd, Rh, Ru, Ir as catalysts, cobalt-catalyzed C-H activation reactions have also received much interest because of its earth-abundance and low-cost. Recently, many groups have shown that Co^{II}/Co^{III} salts can be used to functionalize aromatic/vinylic C(sp^2)-H bonds with alkynes/ alkenes. In the cobalt-catalyzed C-H activation reactions of amides with alkenes, most of them afforded the [4+2] or [4+1] annulation products. To challenge the favorable C-N bond-forming [4+2]/[4+1] cyclization reactions in annulation of secondary amides and alkynes/ alkenes, we disclose the first [3+2] annulation of aromatic/vinylic amides with bicyclic alkenes by cobalt-catalyzed C-H activation.

The Co-catalyzed amide C(sp^2)-H bond activation/[3+2] annulation reaction was optimized with 4-methyl-*N*-(quinolin-8-yl) benzamide (**1a**) and 7-oxabenzonorbornadiene (**2a**) as the substrates. After significant screening efforts, we can get the desired product **3aa** in 91% yield after isolation with the reaction condition shown in the **Scheme 2**. In the substrate scope of the reactions, a variety of amides with substituents at the *para, meta*, or *ortho* position of the aryl ring were tolerated, and gave them in good yields. The reaction also proceeded well with different bicyclic alkene including norbornene, norbornadiene, and benzonorbornadienes (**Scheme 2**). Based on our experimental studies and previous reports, a plausible catalytic cycle is proposed in **Scheme 3**. The catalytic reaction is likely initiated by the oxidation of Co^{II} to Co^{III} by Ag^{+}. Then, coordination of the amide substrate to the Co^{III} complex and subsequent cyclometalation by C-H bond cleavage provide intermediate **I**, followed by insertion to generate intermediate **II**. Intramolecular nucleophilic addition of the C-Co bond to the amide carbonyl group followed by protodemetalation and elimination of AQ provides the final ketone product and regenerates the catalytically active Co^{III} species. This study is published in 2016 at *Angew. Chem. Int. Ed.*

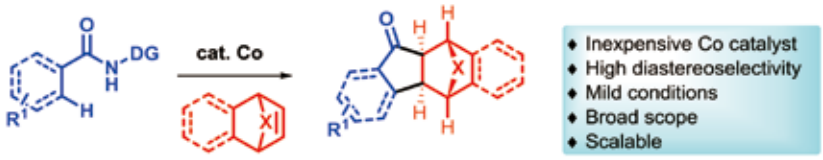

Scheme 1. Cobalt-catalyzed C-H activation and [3+2] annulation reactions of amides with alkenes.

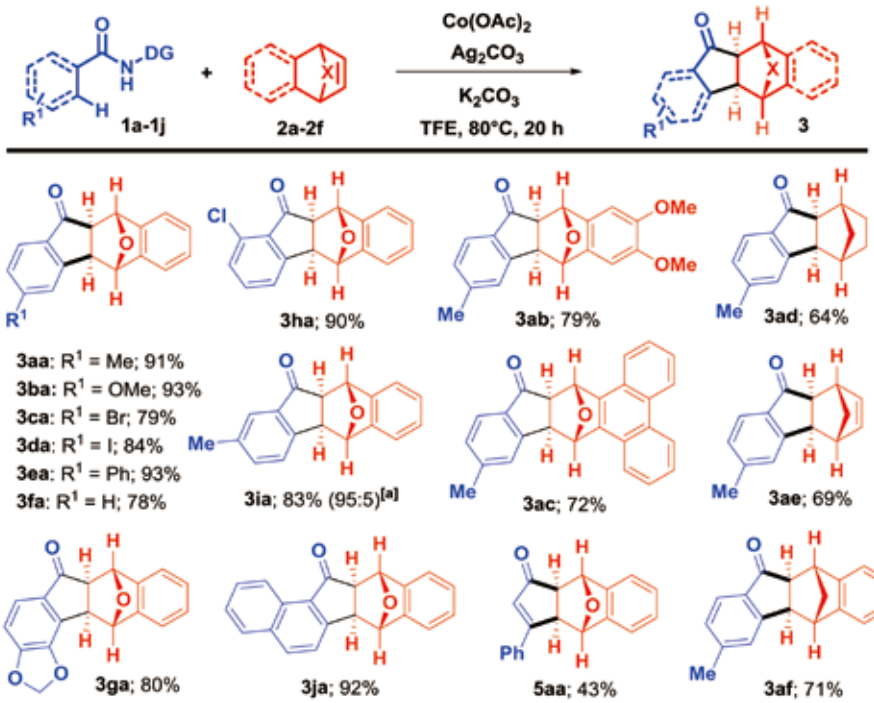

Scheme 2. Scope of the reaction. Reaction conditions: **1** (0.3 mmol), **2** (0.33 mmol), $Co(OAc)_2$ (0.12 mmol), Ag_2CO_3 (0.6 mmol), and K_2CO_3 (0.6 mmol) in TFE at 80° C for 20 h. Yields of isolated products are given. [a] The regioisomeric ratio was determined by ^1H NMR analysis and is given in parentheses; the major isomer is shown.

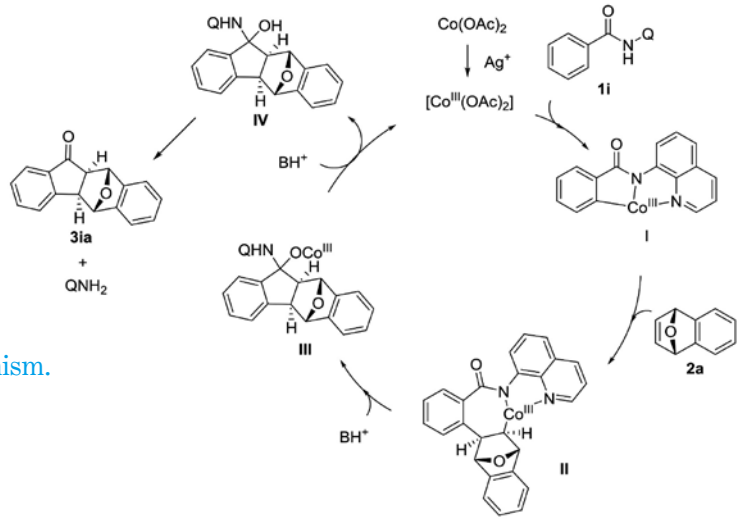

Scheme 3. Proposed reaction mechanism.

Authors

Parthasarathy Gandeepan, Pachaiyappan Rajamalli, and Chien-Hong Cheng (鄭建鴻)
http://dx.doi.org/10.1002/anie.201512018

Integrated Microfluidic Device Using a Single Universal Aptamer to Detect Multiple Types of Influenza Viruses

Prof. Gwo-Bin Lee
Department of Power Mechanical Engineering
Institute of Biomedical Engineering, Institute of NanoEngineering and Microsystems

Biosensors and Bioelectronics, vol. 86, pp. 247-254 (2016)

DNA aptamers that can bind specific molecular targets have great potential as probes for microbial diagnostic applications. However, aptamers may change their conformation under different operating conditions, thus affecting their affinity and specificity towards the target molecules. In this study, a new integrated microfluidic system was developed that exploited the predictable change in conformation of a single universal influenza aptamer exposed to differing ion concentrations in order to detect multiple types of the influenza virus. Furthermore, the fluorescent-labeled universal aptamer used in this system could distinguish and detect three different influenza viruses (influenza A H1N1, H3N2, and influenza B) at the same time in 20min and therefore has great potential for point-of-care applications requiring rapid diagnosis of influenza viruses.

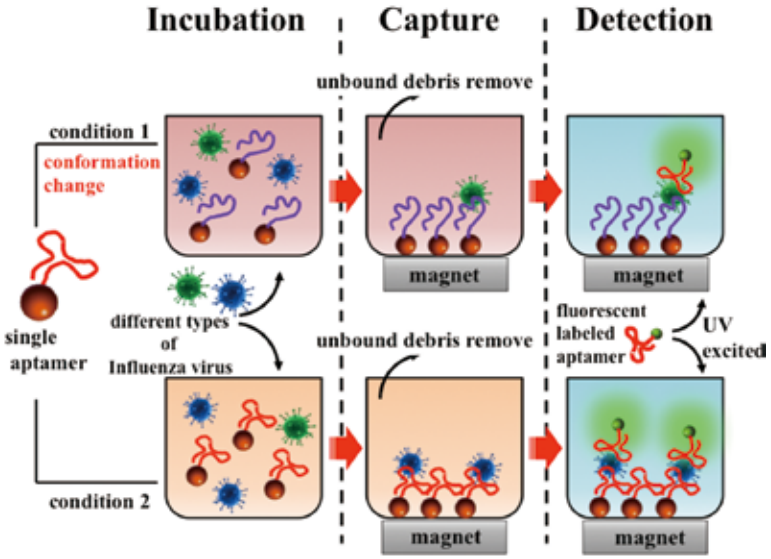

Fig. 1
Schematic illustration of the working principle for the single universal aptamer detection of different kinds of influenza viruses under two different reaction conditions.

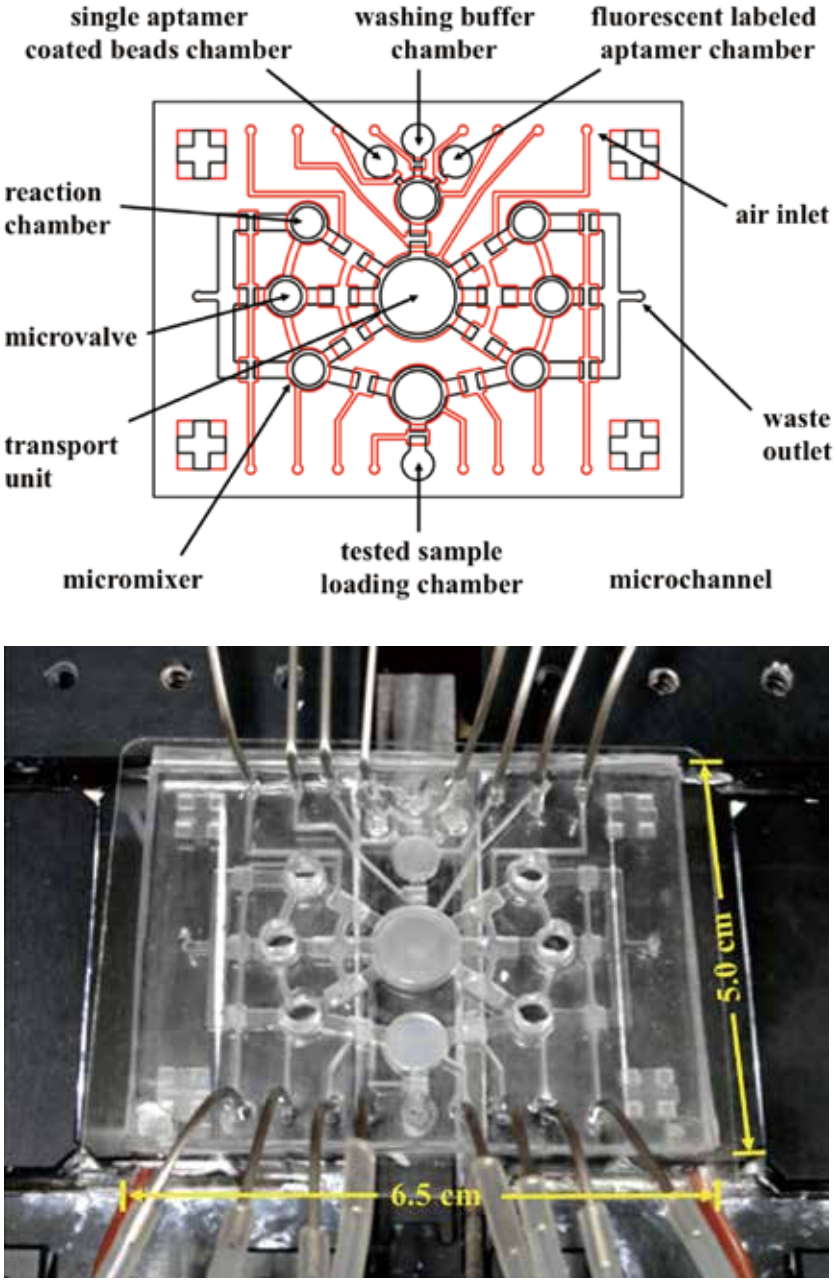

Fig. 2
(A) Schematic illustration of the integrated microfluidic chip for performing rapid diagnosis of three types of influenza viruses. (B) A photograph of the integrated microfluidic chip.

Authors

Chih-Hung Wang, Chih-Peng Chang, Gwo-Bin Lee (李國賓)
http://www.sciencedirect.com/science/article/pii/S095656631630611X

Ping-Pong Mesh: A New Resonant Clock Design for Surge Current and Area Overhead Reduction

Skew Minimization with Low Power for Wide-Voltage-Range Multi-Power-Mode Designs

Prof. S.C. Chang
Department of Computer Science, Institute of Communications Engineering, Institute of Information Systems and Applications

Accepted in IEEE Transactions Very Large Scale Integration Systems (TVLSI), Vol.24, Issue 4, pp.1189-1192, Feb. (2015)

Through his long-term cooperation with industry Chang has gained extensive understanding of the key issues in chip design. His team has proposed efficient algorithm, circuit architecture and EDA software to tackle environmental and process variation so as to significantly reduce leakage power of an IC chip and therefore, increase the standby time of mobile devices for volume production.

Ping-Pong Mesh: A New Resonant Clock Design for Surge Current and Area Overhead Reduction

In advanced technologies, on-chip-variation (OCV) has accounted for a large proportion of clock skew, which limits the performance of a circuit. To mitigate the OCV problem, a mesh structure has been widely used in high-performance designs. Unfortunately, clock mesh structure also causes large power consumption and large power-ground surge current. Therefore, recently, several approaches have been proposed to apply resonant clock to reduce power consumption. However, previous works often suffer from area overhead because of the need to insert large decoupling capacitors. In this paper, we propose a novel resonant clock mesh structure, called Ping-Pong mesh, to overcome these drawbacks. Our Ping-Pong mesh contains two sub-meshes, each of which plays the role of the decoupling capacitor of the other, and the clocks in two sub-meshes operate in completely opposite phases. Our Ping-Pong mesh has the following two advantages: (1) a Ping-Pong mesh does not need additional decoupling capacitors as in previous works; (2) a Ping-Pong mesh can reduce the power-ground surge current about half of previous works. Benchmark data consistently show that our Ping-Pong mesh does work well in practice.

Skew Minimization with Low Power for Wide-Voltage-Range Multi-Power-Mode Designs

In a multi-power-mode design, as the range of the supply voltage becomes wide, a large clock skew may occur among different power domains. To remove this clock skew, conventional power-mode-aware buffers (PMABs) require a large overhead on power consumption. In this paper, we propose a new PMAB architecture for wide-voltage-range multi-power-mode designs. The proposed PMAB architecture is composed of two serially- connected sub-PMABs at two different voltage levels, respectively: in the front sub-PMAB, the low voltage level is used for coarse- grained clock skew minimization; in the back sub-PMAB, the high voltage level is used for fine-grained clock skew minimization. Benchmark data show that the proposed approach can effectively eliminate the clock skew with small power consumption.

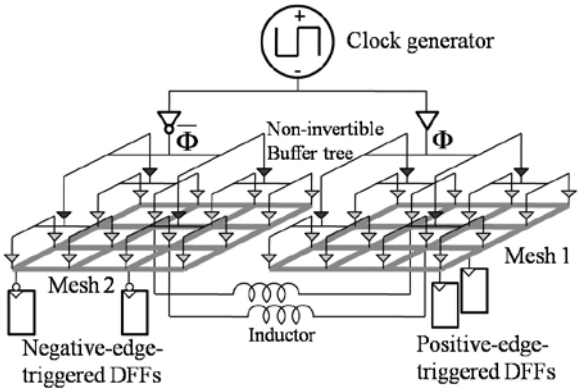

Fig. 1 A complete structure of Ping-Pong mesh.

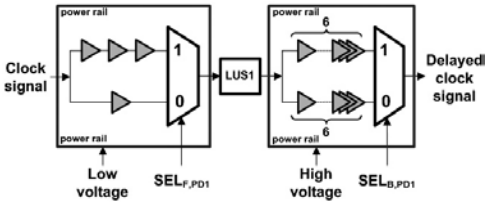

Fig. 2 A two-voltage-stage power-mode-aware buffer

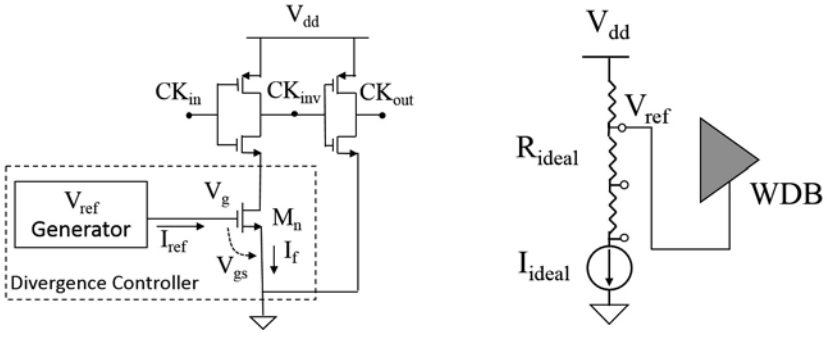

Fig. 3 (a) A wide-divergence buffer (b) Reference voltage generator with voltage biasing circuit

Authors

1.C.H. Chou, H.H. Yeh, S.H. Huang, Y.T. Nieh, S.C. Chang (張世杰), and Y.T. Chang
http://ieeexplore.ieee.org/document/7122932/?arnumber=7122932&tag=1
2.C.H. Chou, Y.T. Lai, Y.C. Chang, C.Y. Wang, L.C. Cheng, S.H. Huang and S.C. Chang (張世杰)
http://ieeexplore.ieee.org/document/7466841

Noninvasive, Targeted, and Non-Viral Ultrasound-Mediated GDNF Plasmid Delivery for Treatment of Parkinson's Disease

Prof. Chih-Kuang Yeh
Department of Biomedical Engineering and Environmental Sciences,
Institute of Nuclear Engineering and Science

Scientific Reports 6, Article number: 19579 (2016)

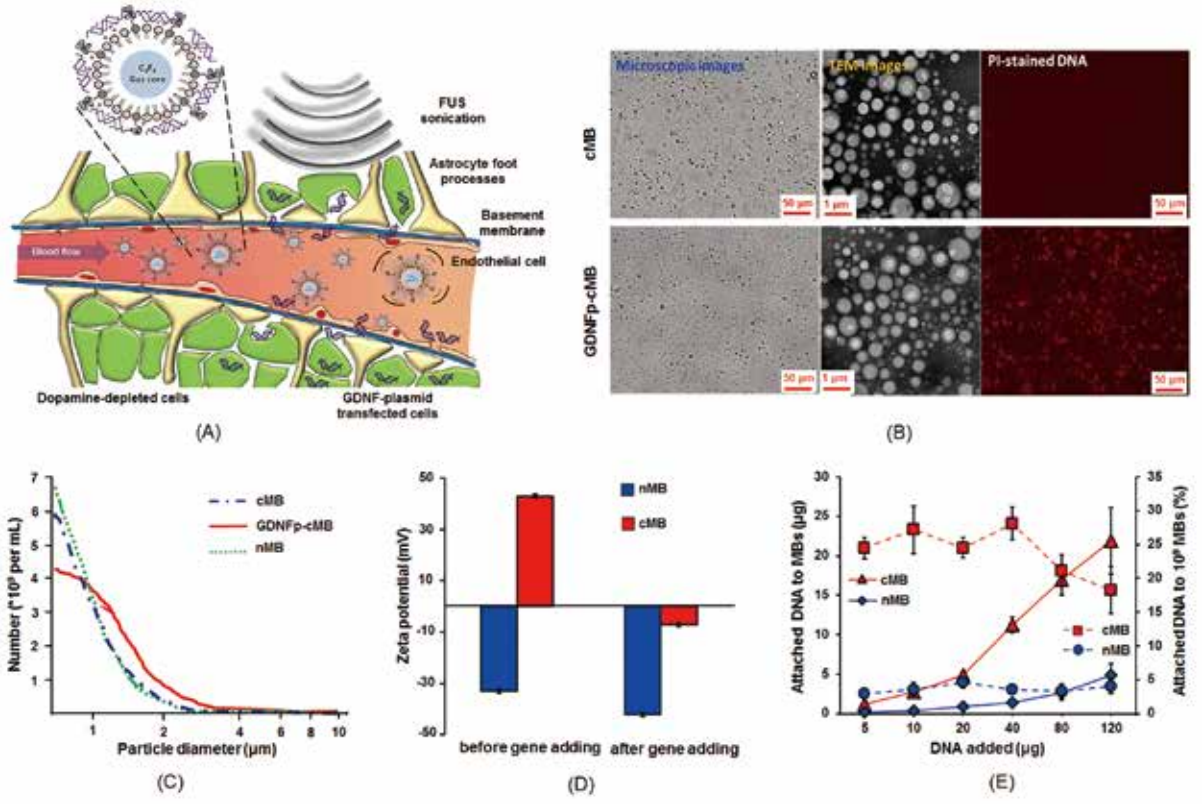

Concept and properties of GDNF-cMBs.
(A) Schematic of GDNFp-cMBs and mechanism for controlled gene transfection of GDNFp-cMBs into brain triggered by FUS. (B) Left: Microscope bright-field images; middle: TEM images; right: PI staining image of cMBs and GDNFp-cMBs. (C) Size distributions of cMBs, GDNFp-cMBs and nMBs. (D) Zeta potential of nMB and cMB before and after adding GDNFp. (E) DNA loading efficiency of GDNFp onto nMB and cMB. The left axis was the amount of GDNFp bound onto MBs (solid line). The right axis was the GDNFp loaded efficiency onto MBs (dotted line). Single asterisk, $p < 0.05$, versus nMBs. Data were analyzes by Student's paired t-test presented as mean ± SEM (n = 6 per group).

Parkinson's disease (PD) is a neurodegenerative disease associated with depleted dopamine production. Development of an endogenous dopamine generative mechanism is an urgent consideration for PD, and the gene techniques has currently been proposed, which replaces missing or dysfunction of the gene to achieve re-synthesis of dopamine. Glial cell line-derived neurotrophic factor (GDNF) supports the growth and survival of dopaminergic neurons. CNS gene delivery currently relies on invasive intracerebral injection to transit the blood-brain barrier. Non-viral gene delivery via systematic transvascular route is an attractive alternative because it is non-invasive, but a high-yield and targeted gene-expressed method is still lacking. In this study, we propose a novel non-viral gene delivery approach to achieve targeted gene transfection. Cationic microbubbles as gene carriers were developed to allow the stable formation of a bubble-GDNF gene complex, and transcranial focused ultrasound (FUS) exposure concurrently interacting with the bubble-gene complex allowed transient gene permeation and induced local GDNF expression. We demonstrate that the focused ultrasound-triggered GDNFp-loaded cationic microbubbles platform can achieve nonviral targeted gene delivery via a noninvasive administration route, outperform intracerebral injection in terms of targeted GDNF delivery of high-titer GDNF genes, and has a neuroprotection effect in Parkinson's disease (PD) animal models to successfully block PD syndrome progression and to restore behavioral function. This study explores the potential of using FUS and bubble-gene complexes to achieve noninvasive and targeted gene delivery for the treatment of neurodegenerative disease.

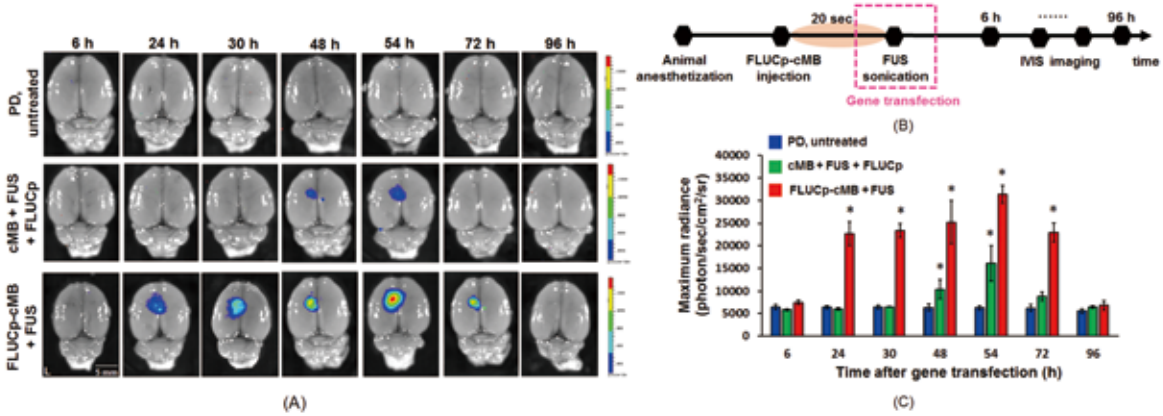

Ex vivo bioluminescent imaging after treatment.
(A) Ex vivo bioluminescent imaging acquired 6, 24, 30, 48, 54, 72 and 96 h after treatment. Upper: control rat without gene transfection; middle: cMB+FUS+FLUCp group; bottom: FLUCp-cMB+FUS. (B) Timeline of bioluminescent imaging after gene transfection. (C) Time course of bioluminescent intensity. Single asterisk, $p < 0.05$, versus PD untreated rat. Data were analyzes by one-way ANOVA (post hoc test: Dunnett; degrees of freedom: 6; F value: 9.7) and presented as mean ± SEM (n = 3 per group).

Authors

Fan CH, Ting CY, Lin CY, Chan HL, Chang YC, Chen YY, Liu HL, Yeh CK (葉秩光)
http://www.ncbi.nlm.nih.gov/pubmed/?term=Noninvasive%2C+Targeted%2C+and+Non-+Viral+Ultrasound-Mediated+GDNFPlasmid+Delivery+for+Treatment+of+Parkinson%E2%80%99s+Disease

A Tree-Based Approach for Addressing Self-Selection in Impact Studies with Big Data

Prof. Galit Shmueli
Institute of Service Science, College of Technology Management

MIS Quarterly, Vol 40, No. 2., pp. 819-848

Performance or impact assessment is an important component of empirical research in management and policy. The gold standard for assessing the impact of an intervention is a randomized controlled experiment (RCT). RCTs are rare due to costs and ethical and other considerations. Without randomization, an important challenge in impact assessment is that the intervention and control groups are often self-selected. Hence, comparing the intervention and control groups provides a biased estimate of the intervention effect. Two popular statistical methods for estimating intervention effects while addressing self-selection bias are the propensity score (PS) approach (Rosenbaum and Rubin 1983) and the Heckman approach (Heckman 1979). Both methods attempt to match the self-selected intervention group with a control group that has the same propensity to select the intervention. However, these methods have some practical limitations.

Yahav et al. (2016) introduce a tree-based approach adjusting for observable self-selection bias in intervention studies. The tree-based approach provides a standalone, automated, data-driven methodology that allows for (1) the examination of nascent interventions whose selection is difficult and costly to theoretically specify a priori, (2) detection of heterogeneous intervention effects for different pre-intervention profiles, (3) identification of pre-intervention variables that correlate with the self-selected intervention, and (4) visual presentation of intervention effects that is easy to discern and understand. As such, the tree-based approach is a useful tool for analyzing observational impact studies as well as for post-analysis of experimental data. The tree-based approach is particularly advantageous in the analyses of big data, or data with large sample sizes and a large number of variables. It outperforms PS in terms of computational time, data loss, and automatic capture of nonlinear relationships and heterogeneous interventions. It also requires less user specification and choices than PS, reducing potential data dredging.

The authors illustrate the method and the insights it yields in the context of three impact studies with different study designs: reanalysis of a field study on the effect of training on earnings, analysis of the impact of an electronic governance service in India based on a quasi-experiment, and performance comparison of contract pricing mechanisms and durations in IT outsourcing using observational data.

Assessing the effect of training on earnings (a reanalysis of a famous study by LaLonde (1986) and others), the new method was not only able to correctly estimate the overall effect, but it also detected a previously undetected pre-

training variable associated with different training effects for high school dropouts vs. completers.

Assessing the impact of a new online passport service in India by analyzing the results of a large survey of users of the online and offline systems, the tree approach identified a perception variable that is hard to hypothesize a-priori but that leads to different impacts of the online system: the citizen's awareness of electronic services provided by the Government of India (Figure 1). Assessing impact separately for the aware and unaware groups indeed uncovers different effects (Figure 2). In all examples, the insights are automatically generated by the tree and easily conveyed through a graphic.

The authors discuss the tree-based approach's performance in the context of big data, showing its suitability both in terms of technical scalability as well as in terms of statistical performance.

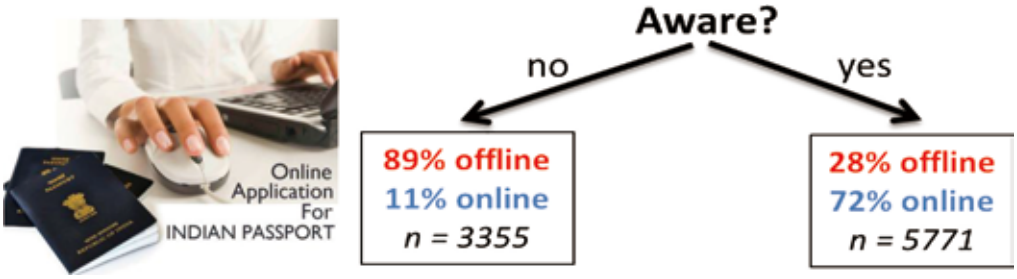

Fig. 1: Applying the tree approach for assessing the impact of a new online passport service in India. The tree identifies Awareness as a factor correlated with self-selection, where unaware citizens are less likely to use the online system. This means that impact should be assessed separately for the aware and unaware samples.

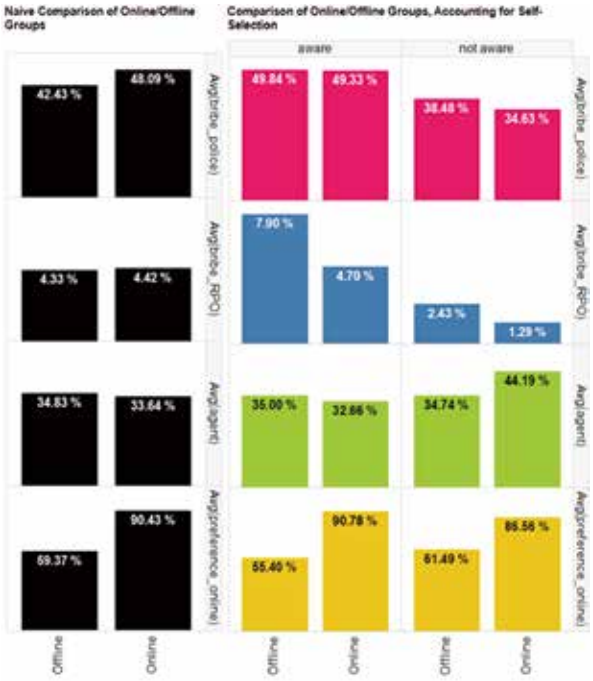

Fig. 2: Assessing impact for different outcomes (eg, police bribing, use of agent) using the overall samples (left, black) compared to separately for aware and unaware groups (right, colorful). The tree-based comparison reveals different and even reversed effects for each group (see third row).

Authors

Yahav, I., Shmueli, G. (徐茉莉) and Mani, D.
http://www.misq.org/contents-40-4

Unravelling the Mystery of Vacuolar Phosphate Transporter

Prof. Tzu-Yin Liu
Institute of Bioinformatics and Structural

Nature communications 7, 11095 (2016)

Inorganic phosphate (P_i) is an essential nutrient to plant growth, and thus is one of the main ingredients of fertilizer. Scientists know that more than 70% of total P_i in plants is stored in the cell vacuole, but for about half a century, no one has discovered how it actually gets there. By using MRI, our research team were able to observe the P_i content in the vacuoles of *Arabidopsis* seedlings and found the "door" by which P_i enters the vacuole, that is, the plant P_i transporter type 5 (PHT5). The Arabidopsis mutants lacking the plant PHT5 transporters accumulated more P_i in the cytoplasm. Conversely, overexpression of the PHT5 transporters increases the P_i content in the vacuole and decreases the P_i content in the cytoplasm, leading to the impaired cytoplasmic P_i homeostasis. In other words, a large amount of the PHT5 protein in Arabidopsis facilitates entry of P_i into the vacuole and the storage therein. However, even when the external environment provides an adequate supply of P_i, the Arabidopsis plants overexpressing the plant PHT5 transporters accumulate P_i in the vacuole, where it cannot be effectively utilized, so that the plant cell senses the shortage of cytoplasmic P_i, thereby activating the P_i deficiency-responsive genes that retarded plant growth. Taken together, our research team showed that P_i enters into the vacuole through the plant PHT5 transporters. As for the practical future benefits of this discovery, we think that it can be used to improve agricultural practices by enhancing the efficient usage of the internal P_i required for plant growth, thereby making it possible to reduce the use of P_i fertilizers in agriculture—one of the major sources of soil pollution. The research findings also break in a new territory in the study of vacuolar P_i transporters.

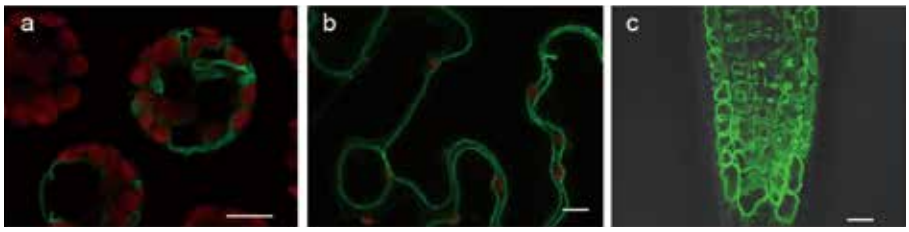

Expression and localization of PHT5;1-GFP in Arabidopsis mesophyll protoplasts (a), tobacco (*N. benthamiana*) leaves (b) and roots of *Arabidopsis* transgenic plants (c).

Authors

Liu TY (劉姿吟), Huang TK, Yang SY, Hong YT, Huang SM, Wang FN, Chiang SF, Tsai SY, Lu WC, Chiou TJ

http://www.nature.com/articles/ncomms11095
http://www.cell.com/trends/plant-science/fulltext/S1360-1385(16)30028-0
http://www.nthu.edu.tw/newsphoto/105news/hotnews-1050604.php
http://nthu-en.web.nthu.edu.tw/files/13-1902-106010.php

PICH Promotes Sister Chromatid Disjunction and Co-Operates with Topoisomerase II in Mitosis

Prof. Lily Hui-Ching Wang
Institute of Molecular and Cellular Biology

Nat Commun. Dec 8;6:8962. (2015)

PICH is a SNF2 family DNA translocase that binds to ultra-fine DNA bridges (UFBs) in mitosis. Numerous roles for PICH have been proposed from protein depletion experiments, but a consensus has failed to emerge. In this study, we report that deletion of PICH in avian cells causes chromosome structural abnormalities, and hypersensitivity to an inhibitor of Topoisomerase II (Topo II), ICRF-193. ICRF-193-treated PICH − / − cells undergo sister chromatid non-disjunction in anaphase, and frequently abort cytokinesis. PICH co-localizes with Topo IIα on UFBs and at the ribosomal DNA locus, and the timely resolution of both structures depends on the ATPase activity of PICH. Purified PICH protein strongly stimulates the catalytic activity of Topo II in vitro. Consistent with this, a human PICH − / − cell line exhibits chromosome instability and chromosome condensation and decatenation defects similar to those of ICRF-193-treated cells. We propose that PICH and Topo II cooperate to prevent chromosome missegregation events in mitosis.

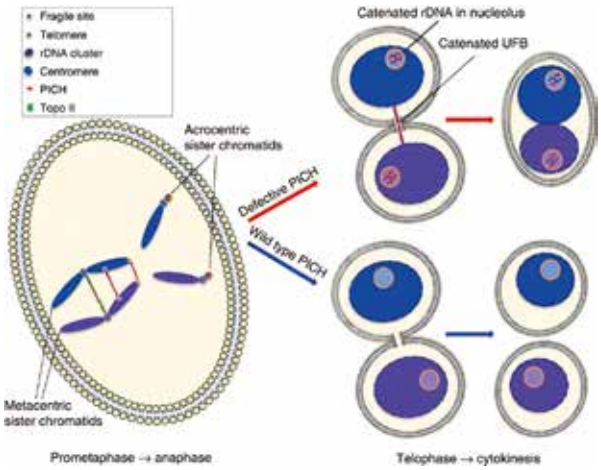

In prometaphase, sister chromatids are held together by cohesin (not shown) only at the centromeric region. Centromeres are still linked by interchromatid catenanes because cohesin blocks the access of Topo IIα to these. PICH and Topo IIα co-localize at rDNA. At the onset of anaphase, centromeric cohesin is removed and sister chromatids begin to separate. Tension is applied to interchromatid DNA links and PICH binds strongly to these DNA bridges. PICH stimulates decatenation of catenated centromeric DNA bridges by Topo IIα. At the rDNA loci, anaphase onset permits condensation to occur in the rDNA, which allows decatenation by Topo IIα. In telophase and during cytokinesis, cells with defective PICH can have persistent DNA bridging at the midzone. This prevents cytokinesis, leading to binucleation. In cells expressing wild-type PICH, DNA bridge decatenation is completed through the action of Topo II to permit cell division. ATPase-dead/defective PICH localizes to nucleoli in telophase and early G1-phase cells. In these cells, ATPase-dead PICH fails to stimulate rDNA decatenation by Topo IIα efficiently. The rDNA in these cells have persistent catenations. In cells expressing wild-type PICH, the rDNA is sufficiently decatenated by the action of Topo IIα during anaphase and telophase.

Authors

Christian F. Nielsen, Diana Huttner, Anna H. Bizard, Seiki Hirano, Tian-Neng Li, Timea Palmai-Pallag, Victoria A. Bjerregaard, Ying Liu, Erich A. Nigg, Lily Hui-Ching Wang (王慧菁), and Ian D. Hickson
http://www.nature.com/articles/ncomms9962

MAK^{5} KƐ^{4} 乜个 AND MAN^{3} ȵIN^{2} 瞞人 IN HAKKA: A HISTORICAL AND TYPOLOGICAL PERSPECTIVE in Hakka

Prof. Lien, Chinfa
Graduate Institute of Linguistics

Journal of Chinese Linguistics 44.1: 86-108. January., (2016)

In this paper I will first explore the issues centering around the evolution of the interrogative word 物 as a common source into its modern descendants mak^{7} and other forms in Hakka. In contrast to the more uniform form in Southern Min, varieties of Hakka boast more variants such as mak^{7}, ma?^{7} and man3. Such a variation can be accounted for in terms of minor regional difference as well as types of phonological process. The retention of the bilabial nasal initial of the word 物 as a reflex of the Middle Chinese 微 phonological category in Hakka lends support to the thesis of lexical diffusion that sound change is not phonologically independent but rather bears the result of interaction with lexicon. Second, on the basis of earlier Hakka texts I will examine the patterns in the distribution of the modern reflex of 物 often written as a demotic word 乜 in its capacity of a variable as a component of the complex interrogative words 'what', 'who' (=what person) and 'why' (=do what kind) or universal quantifiers in Hakka. The finding of the patterns of the Hakka interrogative word will be brought to bear on the patterns of its precursor in Early Modern Chinese colloquial texts. Close attention will be paid to the interaction of inherent lexical properties of the interrogative word and the grammatical constructions in which it occurs. Last of all, an attempt is made to survey the distribution and evolution of the Hakka-related 物 -based interrogative word in other dialectal areas.

Interpreting 都 *to*^{1} TO in earlier Southern Min texts

Prof. Lien, Chinfa
Graduate Institute of Linguistics

Lingua Sinica 1: 9. 1 – 18. December. (2015)

The paper explores the polyfunctional word 都 *to*^{1} TO in early Southern Min texts dating back to the sixteenth century or even earlier. Unlike 都 *dou*^{1} in Mandarin, which mainly functions as a maximality operator, 都 *to*^{1} in Southern Min is chiefly used as a modal particle

expressing a concessive meaning or meaning of unexpectedness as a type of conventional implicature rather than pragmatic inference. However, it can be identified as expressing maximality and exhaustivity in construction with wh-words and negation. In a nutshell, the concessive sense is taken as the default sense unless it is overridden by the interpretation of 都 *to*[1] as a maximality operator. I will examine the syntactic and semantic properties of 都 *to*[1] based on these texts. Its interpretation hinges on the structural position it occupies and the collocates it interacts with.

Formation of the Experiential Aspect Marker Pat[4] 識 :Contact-induced Grammatical Change in Southern Min

Prof. Lien, Chinfa
Graduate Institute of Linguistics

International Journal of Chinese Linguistics. 2.2. 273-299. December. (2015)

This paper first examines the distribution of *tseng*[5] 曾 as an experiential aspect marker, and then the distribution of *pat*[4] 識 both as a cognition verb and as an experiential aspect in five earlier Southern Min texts. (Wu 2001abcd and Quanzhou 2010) Almost three quarters of all instances of *tseng*[5] 曾 occur in non-positive contexts. The same percentage of occurrence is also true of *pat*[4] 識 , be it a cognition verb or an experiential aspect. A comparison of the use of *pat*[4] 識 as a verb and as an experiential aspect marker indicates that 16 (sixteen) tokens occur in non-positive context. Only one suspicious instance occurs in a positive context. Crucially, robust cases of reinforcement of juxtaposed negatives and experiential aspects, 未曾 , show that the emergence of the experiential aspect marker *pat*[4] ('ever') from its cognitive source may have been induced by the weakening of the early experiential aspect marker *tseng*[5] 曾 in the sequence *ber*[7]*-tseng*[5] 未曾 'have not yet; never', of which the-*tseng*[5] in *tseng*[5] was deleted to result a lacuna.

Authors

Lien, Chinfa (連金發)
http://www.cuhk.edu.hk/journal/jcl/jcl/chin_lin/44/44_1_4.html
http://link.springer.com/article/10.1186/s40655-015-0009-1
https://benjamins.com/#catalog/journals/ijchl.2.2.04lie/details

Nietzsche and Husserl on the constitution of Ideas—Intersection between Genealogy and Phenomenology

Prof. Chon-IP Ng
Institute of Philosophy

Dr. Wong Kwok-Kui (ed.), Perspectives on Nietzsche, Hong Kong: Chung Hwa, pp.123-148. (2016)

Both Nietzsche and Husserl presented themselves as radical critics of the Western metaphysics and even as the thinkers who break with this tradition. At first glance, however, they are in exact opposition to each other in their philosophical concerns and approaches. Husserl's phenomenology presented itself as the genuine successor of the Cartesian project of absolute grounding of philosophy and science, and its vocabularies and methodologies overlapped extensively with those of the Descartes and Kant. On the contrary, Nietzsche seems to represent a complete revolt against the Western philosophical tradition. He wrote on those topics that are peripheral, suppressed and neglected in the academic philosophy, and in a style which is strange, eccentric and full of literary devices which are far from being clear and rigorous.

Against the prevailing impression, my research aims to demonstrate an unexpected affinity between Nietzsche's genealogy and Husserl's genetic phenomenology, and map the intersection of them in the problem of the historical constitution and institution of Ideals. Despite the opposition of their philosophical approaches, both Nietzsche and Husserl attempt to trace the foundation of Western rationalism and civilization back to a sort "Idealization". Rationalism consists in the validity of a series of pure and absolute Ideals in the fields of knowledge and praxis. The establishment and spreading of those Ideals in a culture are however anything but a natural process. Thus, a radical understanding of their significance and their foundation should involves an analysis of the mental and corporeal operation, an exposition of the pre-given cultural condition and a revelation of the original intentionality and its successive transfigurations that enable their constitution. These are exactly what Nietzsche and Husserl regarded as the central tasks for philosophical genealogy and genetic phenomenology respectively.

With this affinity as common ground, my research strives to mark precisely where the paths of Nietzsche and Husserl converge and diverge. It shows that both Nietzsche and Husserl were motivated by a deep concern of the present crisis of the Western culture when they reflected on the problem of "Idealization", and their diagnoses on this cultural crisis are strikingly alike: The contemporary culture suffers from the illness of "nihilism" – the

devastation of our values system –, and this crisis of the contemporary culture arose from the deviation of the Western rationality from its basis in the concrete, sensible life.

According to Husserl, a blind faith in objectivism leads the modern scientists to mistake the outcomes of the methodic procedures and conceptual construction in scientific research as self-sustainable reality. Hence, they overlook the sensible, subjective life-world and misunderstand the value-freed theoretical model as the only proper representation of the reality. Likewise, Nietzsche traces the pathology of nihilism of the modern man to the distortion of the value of sensible life. Nihilism broke out as the metaphysical basis of our value system collapsed, and latter has its origin in turn in the fictitious projection of the value Ideals which transcend and overcast our concrete, sensible life. Value is supposed to strength our life and bring it to flourish, but the metaphysically projected value Ideals impels us to ignore our earthy need and desire.

What distinguish Nietzsche and Husserl from each other fundamentally is their different evaluation of the "Idealization". For Nietzsche, "Idealization" was nothing but a fiction. It leads inevitably to nihilism in the modern world and to asceticism in modern life. Husserl, on the contrary, regarded "Idealization" as a legitimate sublimation of certain natural tendencies already inherent in our pre-scientific cognitions and practices. The oblivion of the "Life-world" is the result of a distortion of the "Idealization", rather than its original intentionality.

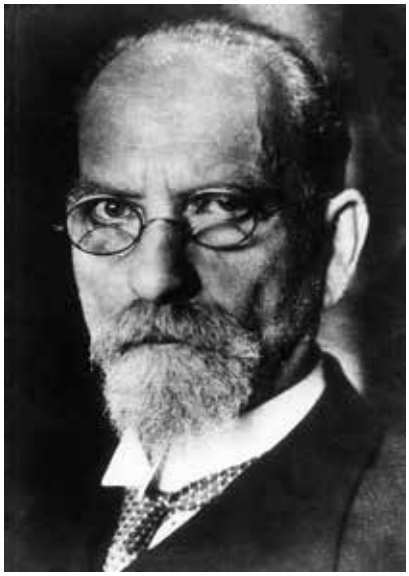

Between the thoughts of Nietzsche and Husserl, there are unexpected intersection

Authors

Chon Ip Ng (吳俊業)

Joint R & D Center of Important Results

HIWIN-NTHU Joint Research & Development Center Focuses on Precision Machine Technologies

"HIWIN – National Tsing Hua University (NTHU) Joint Research & Development Center," was established in 2014 at NTHU in Hsinchu, Taiwan. This joint research and development center is the largest- and longest-invested efforts in Taiwan by industry in university. It is not an exaggeration to refer it as the "Apollo moon landing program" among industry-university collaborative programs in Taiwan, as commented by Professor Hong Hocheng, the President of NTHU. Since the inauguration of the center, at least 11 Professors and more than 60 students from different departments have participated in proprietary R&D projects with budget exceeding NTD 20 Million in 2016. The center plays a unique role in developing and transforming basic science and engineering research through state-of-the-art creative engineering pathways into value-added precision components and systems that definitely can position Taiwan and HIWIN Company as the world leaders in precision intelligent machine industry. Currently, a few joint research programs are undertaking, all of which involve in-depth cross-disciplinary knowledge contents on top with solid practical experiences.

The present major R&D topics undertaken in the Center include hydrostatic bearing development, absolute magnetic encoder development and magnetic sensor technology. As an example, the R&D on precision magnetic encoders is briefly introduced herein. Magnetic encoders are mainly used in machines to detect the position of a motion stage to which they are installed. Motivated by the drawbacks of optical encoders such as high cost, unfriendly to harsh environment, etc., this research is dedicated and aimed for developing magnetic encoders to compete with optical encoders in the future marketplace. The scope ranges from design and validation of magnetic materials for realization of high-density recording, for precision magnetization for either incremental or absolute coding, for characterization of self-made magneto-resistance sensors and Hall-effect sensors as signal detection devices, which are further integrated with signal processing IC design, mechanical assembly calibration and system verification. Under the demands of machine tools manufacturers, we have designed and fabricated a linear- and a rotary-magnetic scales, which feasibility and performance have been validated through integration with linear guideways and servomotors, respectively. For example, the project led by Prof. Cheng-Kuo Sung on systemic integration has successfully

demonstrated effectiveness of a direct drive motor with high resolution of rotary-magnetic encoder. The project "magnetic encoder for absolute position" led by Prof. Jen-Yuan Chang has developed a unique read head with novel algorithm for absolute positon feedback, as illustrated in Figure 1 and Figure 2, respectively. Utilizing the aforementioned precision magnetic encoders, according to the ambitious demand goal from HIWIN to build a world-leading ultra-precision machine tool, in-depth know-how for precision components such as hydrostatic tool spindles, hydrostatic workpiece spindles, rotary hydrostatic bearing stages, linear hydrostatic bearing stages and a patented spindle mounting device enabled by magneto-rheological fluid as exampled in Figure 3 have been carefully developed and validated in the Center.

It is anticipated that with the seamless integration of the high precision components and systems, the HIWIN–NTHU Joint Research & Development Center will continue to serve as the pioneer to strengthen in-depth and in-width R&D for Taiwan and HIWIN as key player on the world stage of precision machine technologies.

Fig. 1: Integration of rotary-magnetic encoder on direct drive motor.

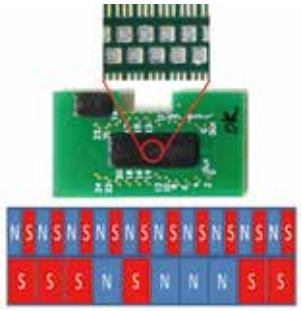

Fig. 2: Schematic patterns of absolute magnetic coding and corresponding sensors on PCB.

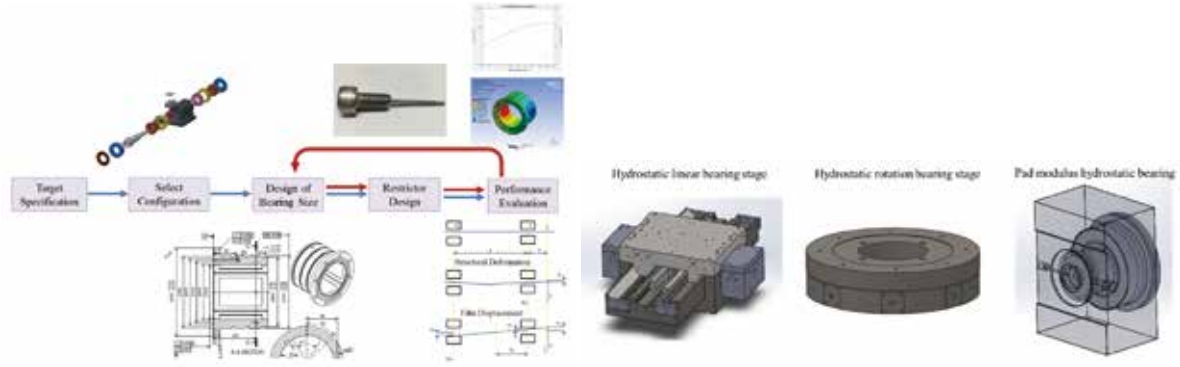

Fig. 3: Examples of precision machine components and systems developed from the Center.

TSMC-NTHU Joint Research Center Focuses on Future Generation Semiconductor Devices Development

Collaborative research between TSMC and NTHU has been in the form of individual research projects (JDPs) between interested faculty members and business units of TSMC for many years. In order to integrate all JDPs with focuses on front-end integrated circuits technology development as well as attracting young talents into the semiconductor field, the Center was established in January, 2014 with a pledged annual financial support of at least NTD 15 Million from TSMC. A unique design is that 30% of the total Center budget is allocated to educate talented students in semiconductor field in the form of scholarships.

Since then, at least 30 Professors and more than 200 students from different departments have participated in the TSMC-NTHU Joint Research Center with the annual budget exceeding NTD 22 Million in 2016. The current major research focuses of the Center include advanced memory (flash, ReRAM, MRAM, etc) development, investigation of FinFET beyond 16 nm, process reliability improvement, 2D material exploration, as well as CMOS/MEMS sensors development for IoT applications. For example, the project led by Prof. Ya-Chin King and Chrong-Jung Lin on '1Kbit FINFET Dielectric (FIND) RRAM in Pure 16nm FinFET CMOS Logic Process' is firstly proposed and demonstrated by 1kbit RRAM macro on 16nm standard FinFET CMOS logic platform (See Fig.1). The structure of the RRAM, which consists of one FinFET transistor and an HfO2-based resistive film for a storage node of the cell, is shrink to an aggressive cell size of $0.07632\mu m^2$ without additional mask or process step. Prof. Chen-Fu Chien and his associates developed a novel genetic algorithm of multi-subpopulation parameters with hybrid estimation of distribution to effectively and efficiently support intelligent manufacturing and validated this approach in advanced wafer fab. The project 'Integrated Fan-Out Wafer-Level Chip-Scale Packaging (InFO WLCSP)' led by Prof. Chen-Wen Wu, proposes a cost model for analyzing the cost with respect to N_{TD}(the number of touchdown), N_P(the polish count), and NS(the number of sits concurrently tested by a probe card), in order to achieve small chip form factor with low manufacturing cost (See Fig.2, 3).

1Kbit FINFET Dielectric (FIND) RRAM in Pure 16nm FinFET CMOS Logic Process

Prof. Ya-Chin King and Chrong-Jung Lin

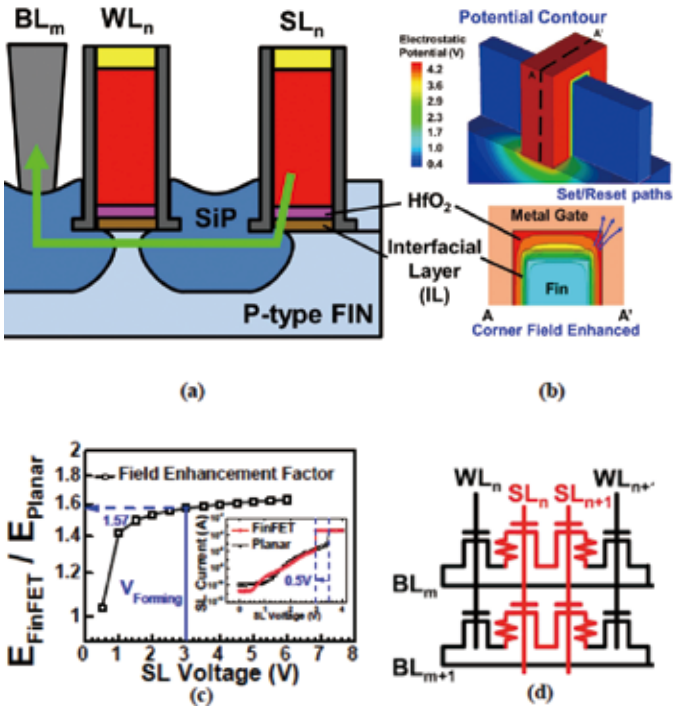

Fig. 1: (a) Cell structure of FIND RRAM with HfO_2-Based resistive film (b) Electric field enhanced in the FinFET corner and the set and reset paths are concentrated (c) Fin curvature cause 1.57 times of field enhancement and 0.5V forming voltage lower (d) NOR array arrangement of the 1kbit FIND RRAM

Integrated Fan-Out Wafer-Level Chip-Scale Packaging (InFO WLCSP)

Prof. Chen-Wen Wu

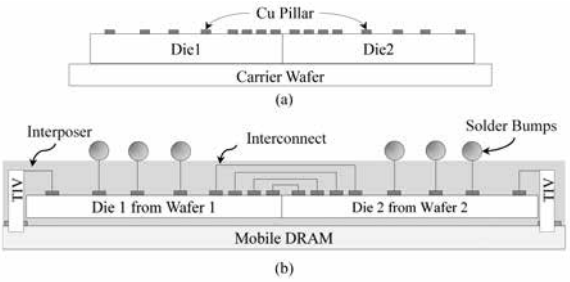

Fig. 2: The architecture of a simplified InFO WLCSP (a) after KGD test and (b) at wafer-level final test.

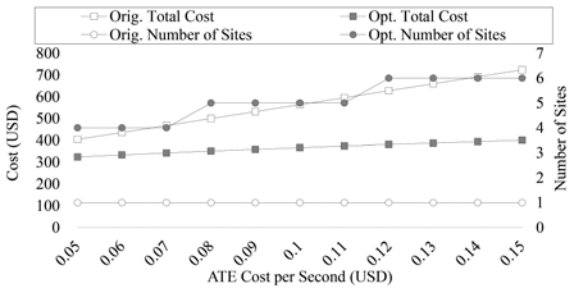

Fig. 3: The probe cost, test cost, and test time under different number of sites in a probe card.

Besides research activities, the TSMC-NTHU Joint Research Center offers many scholastic activities to attract students of all grades into semiconductor related fields for advanced studies. For example, a number of sophomore and junior students are invited to join the summer Elite Camp with the opportunity to interact directly with center professors so as to inspire their interests in semiconductor research. The Center Research Project Competition offers an opportunity for students to learn semiconductors through competition among NTHU students as well as their peers at NTU, NCTU and NCKU. Above all, a sizable portion of the Center budget, over NTD 3 Million, is allocated for center students in the form of scholarships to retain excellent students to study semiconductors.

MediaTek-NTHU Research Center Advancing the Frontier of Future Generation Smart Mobile Devices

The MediaTek-NTHU Research Center was established in 2014 with a mission of developing the most advanced technologies for future generation smart mobile devices. The tight cooperation between MediaTek and NTHU through the center has developed many innovative, forward-looking technologies and trained many high quality students.

The project, "OpenCL 2.0 Runtime on HSA Platform" led by Prof. Jenq-Kuen Lee, aims to expand OpenCL for integrating CPU, GPU, and DSP to do heterogeneous multi-core computing, and plans OpenCL 3.0 expansion DSP Profile. A preliminary OpenCL Runtime has been developed, which was contributed to the HSA official website. The code has already been integrated to POCL, which is the most popular open source OpenCL framework. The project has also submitted three proposals in Khronos f2f meeting for C, C++, and modem DSP features for the upcoming OpenCL 3.0. Once accepted, they will become part of the OpenCL 3.0 standard.

In view of the importance of the quasi-cyclic low density parity check (QC-LDPC) code for new radio in the next generation 5G cellular system, Prof. Jen-Ming Wu leads the project "Double QC-LDPC Code" and develops an

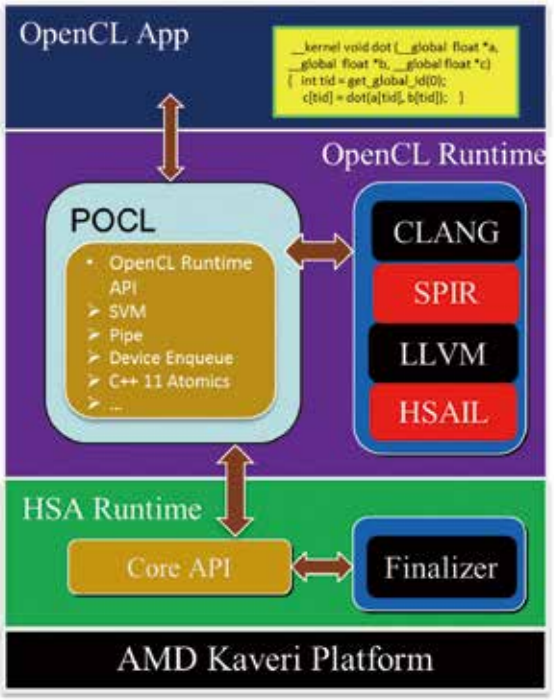

Fig. 1: The OpenCL 2.0 Runtime on HSA platform.

innovative Double QC-LDPC (DQC-LDPC) code design with parity-check matrices. The proposed DQC-LDPC code is compatible to the classical QC-LDPC codes and has the added advantages of (1) flexibility in supporting low to high code rates from 1/3 to 8/9, and (2) very low complexity in the encoding structure. The work has been awarded the Taiwan and US patent in 2016.

The project, "Layout-Oriented Defect Set Reduction for Fast Circuit Simulation in Cell-Aware Test", led by Prof. Cheng-Wen Wu, considers the most advanced cell-aware test (CAT) methodology for cell-internal faults. CAT requires the help of detailed defect injected transistor-level circuit simulation and defect-enhanced SAF ATPG. However, the defect set to be considered is huge and thus this step is very time consuming. This project takes layout into consideration when we construct the defect set for each cell, effectively removing the redundant or unnecessary defects and therefore reducing the circuit simulation time dramatically. We propose a generalized approach that can be used to build the fault models based on the cell layout, where the generated faults are closer to the realistic physical defects on the layout, so the number of faults is significantly reduced. The proposed method is verified by commercial 180nm and 350nm CMOS standard cell library, and the circuit simulation time is reduced to only 19% as compared to the original CAT methodology.

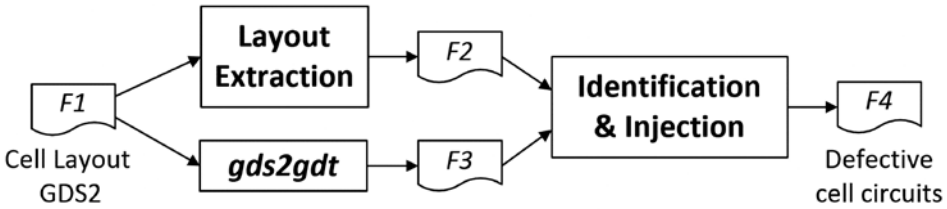

Fig. 2: Flow of the proposed methodology.

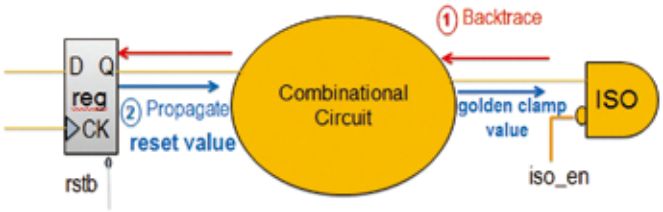

Fig. 3: Backtracing from an ISO input to the corresponding register.

In the project, "A Static Approach to Verifying Isolation Clamp Values", Prof. Chun-Yao Wang studies Isolation (ISO) cells, which are used to prevent an unknown (X) propagation when there are signals going from an OFF power-domain to an ON power-domain. The problem is that incorrect ISO clamp values of control signals could easily cause catastrophic system failure, while simulation-based approaches cannot completely deal with this issue. In this work, we propose a static verification solution to verify the correctness of ISO clamp value. With our tracing algorithm, we can check if ISO clamp values are consistent with the reset values of source registers. This is done by backtracing from an ISO input to the corresponding register to get the reset value. Then we propagate the reset value through the combinational circuit between the corresponding register and the ISO to have the golden clamp value, which is used to check if the ISO clamp value is correct or not. If the golden clamp value does not match the ISO clamp value, we will give users an error report of this mismatch.

Unimicron-NTHU Joint Research & Development Surface Roughness Effect on Signal Integrity

We study Huray's surface roughness model and use it to predict high frequency roughness effect in PCBs or microwave components. To apply Huray model, the establishment of theoretical calculation is our first step before we get to the actual measurements. Here we study the functional characteristics of the Huray model and compare the calculated results with the traditional Grossie model.

First, by the comparison of different pyramid base size and nodule size, we found that the calculated surface ratio variation with base size is very small under the same roughness (height) condition, as showed in fig.1. The other is that the surface ratio drops as the nodule size increases under the same roughness condition, this can be easily understood since the larger the nodule size in each pyramid, the fewer nodule number can be filled, also lower the surface ratio.

Second, we compare rough surface power loss under different condition between Huray model and Grossie model. In fig.2, it's obvious that the power loss of the Grossie model saturated near 1 um at 10 GHz. For Huray's model, the power loss increases as roughness and nodule radius increase.

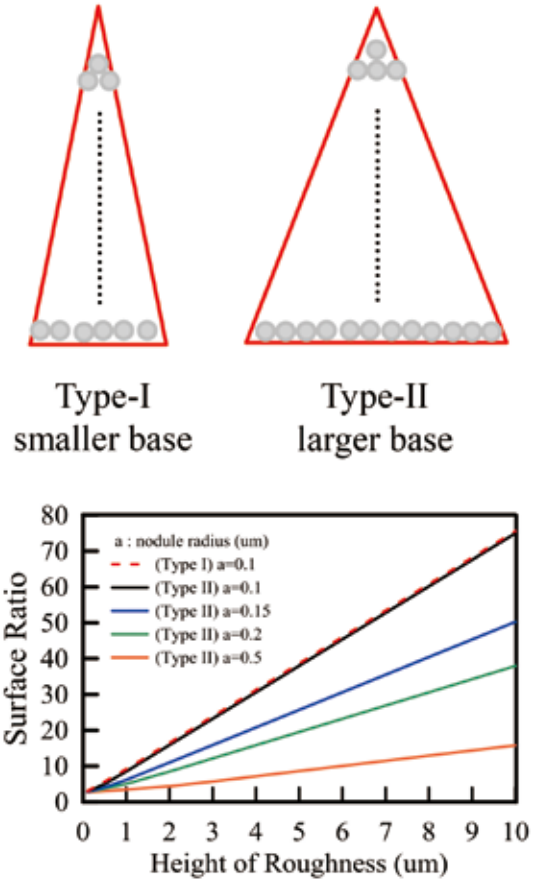

Fig. 1

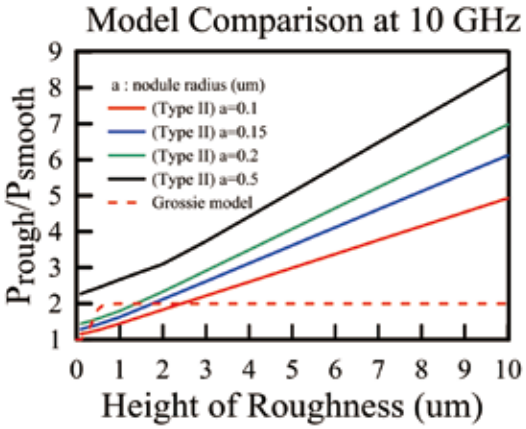

Fig. 2

At last we do some simulations with HFSS 16.2 and a single-trace, 50 mm long microstrip with 50 um trace thickness, 345 um trace width, 200 um thick FR4 substrate is used. In time domain, a 1 V voltage square wave pulse is applied, as in fig.3, the saturation happens in Grossie model but not in Huray's.

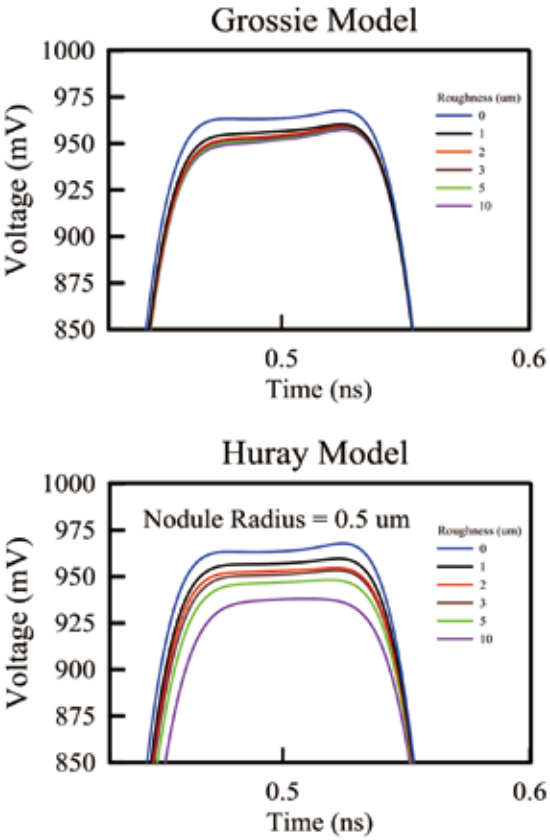

Fig. 3

By careful comparison in fig.4, we found that the larger the roughness, the larger the voltage drop by the same variation of nodule size, same behavior can be found for the nodule size comparison. From these we can say that the roughness and the nodule size magnifies each other's effect on conduction loss. Both parameters increments can deteriorate signal integrity by eating away fast rising (a.k.a. high frequency) components in the square wave and thus increase the signal rise time.

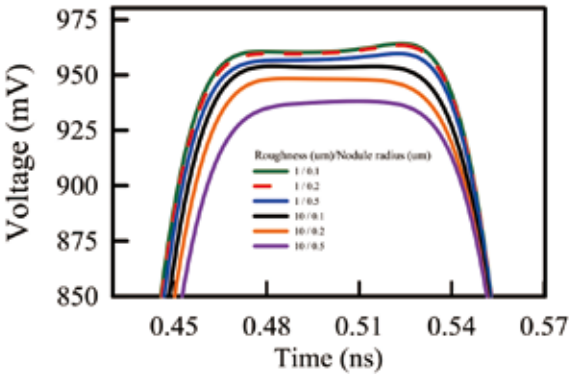

Fig. 4

Authors

http://www.oldfriend.url.tw/article/IEEE_paper/roughness/5_TA2_Paul_Huray.pdf

LiteOn-NTHU Joint Research Center Aims at Spurring the Collaborative Research on the Cutting Edge Technologies

On October 1, 2015, Lite-On Technology Co., Ltd. and National Tsing Hua University joined hand to establish the “Liteon-NTHU Joint Research Center". With a total investment of at least NTD 85 million from Lite-On within five years, the Center aims at spurring the collaborative research on the cutting edge technologies for cross-domain applications through integrating the resources of the two parties. The areas of particular interest include big data, IoT, advanced materials, robotics, and innovative management models.

Over the past year, the Center has identified 22 potential subjects for bilateral collaboration. Through 46 discussion meetings, 10 subjects have been transformed into research proposals, from which four projects have been funded thus far. Four business units, including Leotek, Enclosure, HIS and IMG, of the NMEG Business Group of Lite-On are actively participating in the collaboration. The Center also devotes its effort to organizing the forums centering on the crucial themes for the current development and future direction of Lite-On. The themes of the forums having been organized are: lean manufacturing and management, IP strategy, and application of big data. The Center is currently assisting the NMEG Business Group in integrating the core competencies of its eight business units to explore the key technologies associated with the smart mobility with the NTHU faculty in the coming years.

In the project, "Development of Supplier Information e-System and Risk Assessment ", Prof. Chien-Chi Chang and his students have developed a computerized supplier information e-system to help the managers of Lite-On subjectively perform the risk assessment analysis of each supplier. The prediction model was built based on the advanced data analysis technique with the inputs from the historical auditing data and other relevant information. The risk factors identified by the system can provide a useful reference for the managers to make optimum resource arrangements for auditing or even as a warning tool in identifying the high potential risk suppliers.

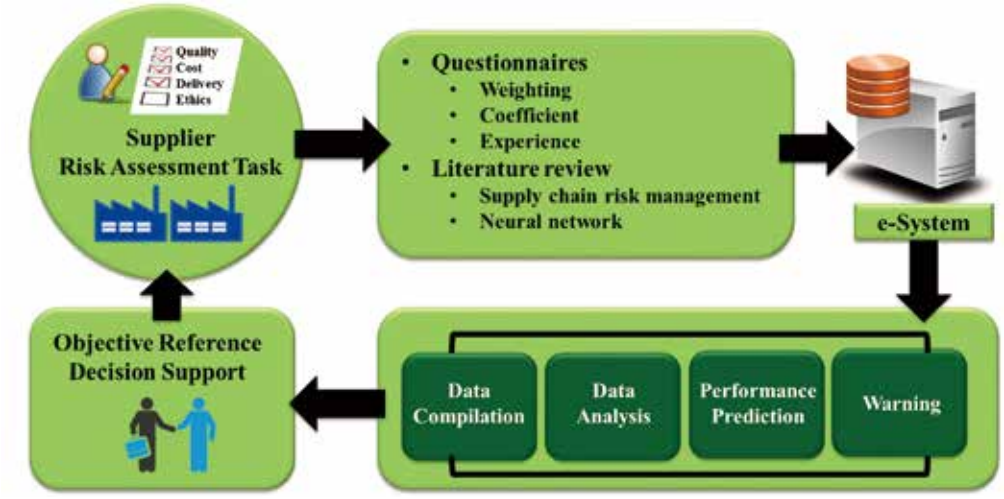

In collaboration with Lite-On, the project, "Yield Improvement on Plastic Process Through Data Analytics", led by Prof. Kuo-Hao Chang collects extensive manufacturing data using design-of-experiment techniques and analyzes them based on powerful statistical tools, which together enables the identification of the most important parameters among many, and the determination of the optimal parameter settings. Several rounds of verification experiments are conducted to ensure that the yields have been significantly enhanced. An insightful training program is provided with Lite-On to facilitate the use of these useful data analytics techniques.

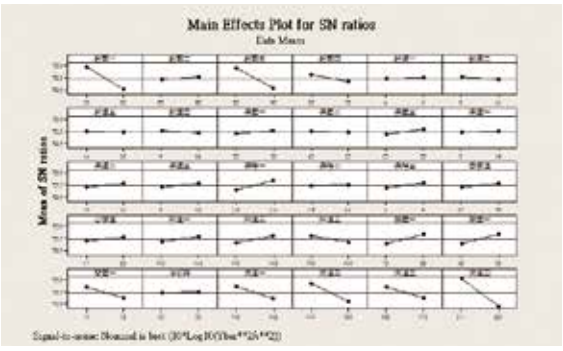

Fig. 1
Identifying the most important parameters through data analytics

Fig. 2
Providing a training program for future reference

Research Highlights

Natural Sciences

▼ Multiple Zeta Values in Positive Characteristic

Prof. Chieh-Yu Chang
Department of Mathematics

We establish an effective criterion to determine whether a give multizeta zeta value in positive characteristic is Eulerian or not. Its characteristic zero counterpart is still an open question.
https://www.ems-ph.org/journals/forthcoming.php?jrn=jems

▼ The Effect of Excessive Dioxide in the Atmosphere on the Growth of Phytoplankton Species

Prof. Sze-Bi Hsu
Department of Mathematics

This work deals with a resource competition model of two algal species in a water column with excessive dioxide in the atmosphere. The model takes the form of system of reaction diffusion equations describing two species compete for two substitutable resources CO2 and CARB which CARB and CO2 exchanges at the surface of ocean. We first consider the growth of single species by maximum principle and degree theory. Then we consider the competition of two algal species showing that coexistence is possible by using uniform persistence theory and global bifurcation theory.
http://www.math.nthu.edu.tw/~sbhsu

▼ Wave Propagation in Reaction-Diffusion Systems

Prof. Chao-Nien Chen
Department of Mathematics

Reaction-diffusion systems serve as models for studying pattern formation in various fields of science. Many patterns emerge from homogeneous media that are destabilized by a spatial modulation. For instance, stripe and spot patterns frequently appear in chemical reactions. These patterns are robust in the sense that they exist in a wide range of parameters being close to neighborhoods of Turing's instability. Near such a bifurcation, the Turing patterns necessarily are of small amplitude and more or less uniformly distributed. Besides these regular patterns, localized structures often result from the balance between dissipation and nonlinearity. Localized patterns in structure are usually located far away from the homogeneous equilibrium. Fronts are generic structures connecting two different states of a system having a bi-stable nonlinearity, while the profile of a pulse is in close proximity to a trivial background state except for one or several localized spatial regions where changes are substantial.
Depending on the system parameters and initial conditions, localized waves may stay at rest or propagate with a dynamically stabilized velocity. The transition from a stationary object to a traveling wave breaks the symmetry of the structures. Such localized structures are commonly observed and referred to as dissipative solitons; for instance the nerve pulses in biological systems, concentration drops in chemical systems and current filaments in physical systems. Employing variational arguments, we established the existence of traveling wave solutions. Moreover estimates of wave speed together with asymptotical profile have also been obtained.

▼ Strictly Convex Central Configurations of the Planar Five-Body Problem

Prof. Kuo-Chang Chen
Department of Mathematics

Classification for central configurations is an important and challenging problem in celestial mechanics.
In this paper we investigate strictly convex central configurations of the planar five-body problem, and prove some necessary conditions for such configurations. In particular, given such a central configuration with multiplier λ and total mass M, we show that all exterior edges are less than $r_0=(M/\lambda)^{1/3}$, at most two interior edges are less than or equal to r_0, and its subsystem with four masses cannot be a central configuration. Our work develops some formulae in a classic work by W.L.Williams in 1938, in the meanwhile we rectify some unsupported assumption in there.

▼ The Geometry of the Universe

Prof. Wun-Yi Shu
Institute of Statistics

In the late 1990s, observations of type Ia supernovae led to the astounding discovery that the universe is expanding at an accelerating rate. The explanation of this anomalous acceleration has been one of the great problems in physics since that discovery. We propose cosmological models that can simply and elegantly explain the cosmic acceleration via the geometric structure of the spacetime continuum, without introducing a cosmological constant into the standard Einstein field equation, negating the necessity for the existence of dark energy. In this geometry, the three fundamental physical dimensions length, time, and mass are related in new kind of relativity. There are four conspicuous features of these models: 1) the speed of light and the "gravitational constant" are not constant, but vary with the evolution of the universe, 2) time has no beginning and no end; i.e., there is neither a big bang nor big crunch singularity, 3) the spatial section of the universe is a 3-sphere, and 4) in the process of evolution, the universe experiences phases of both acceleration and deceleration. One of these models is selected and tested against current cosmological observations, and is found to fit the redshift- luminosity distance data quite well.
https://arxiv.org/abs/1007.1750
http://www.technologyreview.com/blog/arxiv/26170/
http://www.physorg.com/news199591806.html

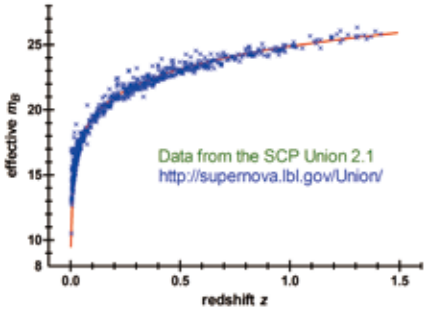

▼ Revealed Dust-Hidden Cosmic Star Formation History at 0<z<2.2 More Reliably than Before by Taking Advantage of the AKARI Space Telescope's Continuous Mid-IR Filters

Prof. Tomo Goto
Institute of Astronomy

Revealing cosmic star formation history is one of the major goals of observational astronomy. However, due to the extinction by dust, the traditional method of observing in redshifted ultraviolet/optical light cannot detect star formation (SF) hidden by dust.

Infrared light can see through the dust. Together with team members, I launched the AKARI infrared space telescope. Using the mid-IR data of the AKARI space telescope, combined with the new CFHT optical/near-infrared data I obtained, we revealed the cosmic star formation history at $0<z<2.2$ (Fig.1). This measurement is more accurate than previous work, because the AKARI satellite has continuous filters in mid-infrared wavelengths (2-24μm). Previous satellites (Spitzer, ISO, and WISE) suffered from gaps between filters, resulting in a large uncertainty.
http://mnras.oxfordjournals.org/content/452/2/1684

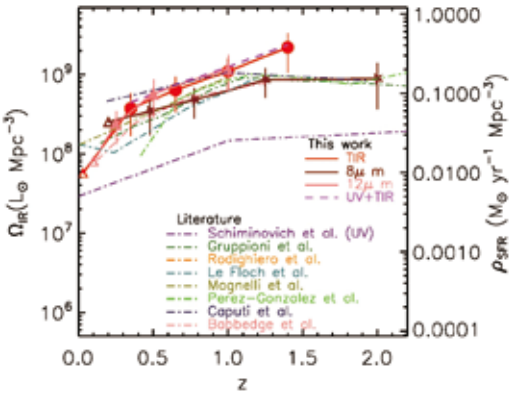

Fig.1. Cosmic star-formation history revealed by the AKARI. The solid lines are our results. The dashed lines are from literature. Thanks to AKARI space telescope's continuous mid-IR filters, our measurements are more reliable than previous work.

▼ Symplectic Geometry, Lie Groups, Lie Algebras

Prof. Meng-Kiat Chuah
Department of Mathematics

1. The complex semisimple Lie algebras are uniquely determined by their Dynkin diagrams, so structures on the Lie algebras are revealed by additional information on these diagrams. In a joint work with Fioresi, this idea is used to study the root systems of Kac-Moody Lie algebras. It initiates academic interaction with the Italian mathematics community for future cooperation.
2. The automorphism group of a complex semisimple Lie algebra is a Lie group. The quotient by its identity component is called the outer automorphism group, and a classical result says that it is isomorphic to the group of diagram symmetries on the Dynkin diagram. A recent work with postdoctoral fellow Zhang generalizes this result to the real semisimple Lie algebra, where the outer automorphism group is shown to be isomorphic to the group of symmetries on a painted diagram.

▼ Development of the Next-Generation Compton Telescope

Prof. Hsiang-Kuang Chang
Institute of Astronomy

The Compton Spectrometer and Imager (COSI) project is a collaboration of UCB/SSL and LBNL in the US, NTHU, NCU, AS/Phys and NARL/NDL in Taiwan, and IRAP in France. NTHU is the PI institution of the COSI-Taiwan team. The heart of COSI is an array consisting of 3 layers of 2x2 high-purity germanium detectors (HPGeD). Each GeD volume is 8cm x 8cm x 1.5cm. It has 37 strip anodes on each side in orthogonal directions. Such a cross-strip detector array provides high-resolution 3-dimentional tracking of Compton scattering events in the detector volume, and therefore significantly increases sensitivity of detecting photons in the energy range from 0.2 MeV to 10 MeV.

In the COSI 2016 balloon flight, COSI was launched on May 16, 2016, from Wanaka, New Zealand, by NASA/CSBF. It flew around the earth at an altitude of 33.5 km and landed in Peru on July 2, 2016. This flight has demonstrated COSI's performance. A bright Gamma Ray Burst (GRB 20160530A) was discovered by COSI during the flight. More scientific results on MeV gamma-ray emissions from the galactic center, the Crab and some other sources of X-ray binaries (XRB), Active Galactic Nuclei (AGN) and gamma-ray pulsars will come after accumulated data are fully processed and analyzed. Another similar flight for COSI is scheduled in 2018. The COSI collaboration is also working on proposing a satellite mission to NASA. The technology developed in the COSI project can be applied to medical imaging, in particular for cancer diagnostics and ion therapy range verification, and to environment radiation monitoring, such as in airports and nuclear power plants.

▼ Helical Magnetic Fields in the NGC 1333 IRAS 4A Protostellar Outflows

Prof. Shih-Ping Lai
Institute of Astronomy

We present Submillimeter Array polarization observations of the CO J = 3–2 line toward NGC 1333 IRAS 4A. The CO Stokes I maps at an angular resolution of ~1" reveal two bipolar outflows from the binary sources of NGC 1333 IRAS 4A. The kinematic features of the CO emission can be modeled by wind-driven outflows at ~20° inclined from the plane of the sky. Close to the protostars the CO polarization, at an angular resolution of ~2.″3, has a position angle approximately parallel to the magnetic field direction inferred from the dust polarizations. The CO polarization direction appears to vary smoothly from an hourglass field around the core to an arc-like morphology wrapping around the outflow, suggesting a helical structure of magnetic fields that inherits the poloidal fields at the launching point and consists of toroidal fields at a farther distance of outflow. The helical magnetic field is consistent with the theoretical expectations for launching and collimating outflows from a magnetized rotating disk. Considering that the CO polarized emission is mainly contributed from the low-velocity and low-resolution data, the helical magnetic field is likely a product of the wind–envelope interaction in the wind-driven outflows. The CO data reveal a PA of ~30° deflection in the outflows. The variation in the CO polarization angle seems to correlate with the deflections. We speculate that the helical magnetic field contributes to ~10° deflection of the outflows by means of Lorentz force.

http://iopscience.iop.org/article/10.3847/0004-637X/819/2/159/meta;jsessionid=29AA276F986D0104E4F85B6CA57CB2F6.c3.iopscience.cld.iop.org

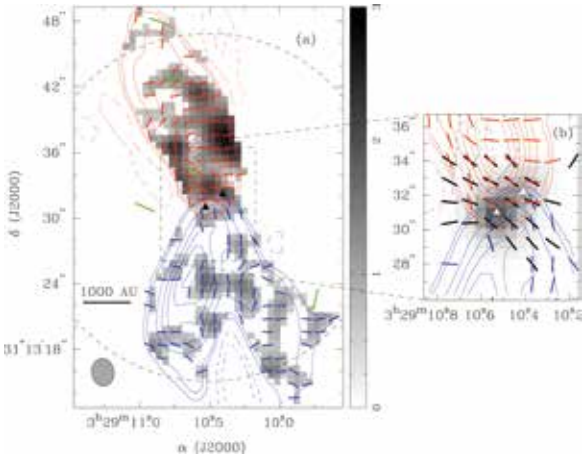

Engineering and Applied Sciences

▼ Development of 3D Printed Knotted Reactor for Online Differentiating Silver Nanoparticles and Ions in Municipal Wastewater Samples

Prof. Yuh-chang Sun
Department of Biomedical Engineering and Environmental Sciences

As discarded into our environment, whether silver nanoparticles (AgNPs) persisted and released silver ions (Ag^+) has remained an unresolved issue. To evaluate the species of environmental AgNPs, we employed a three-dimensional (3D) printed knotted reactor (KR) coupled with an inductively coupled plasma mass spectrometry (ICP-MS) to construct a differentiation scheme for quantitative assessment of AgNPs and Ag^+ in complicated wastewater sample through adjusting the operating parameters of the presence/absence of a rinse solution and the sample acidity. Furthermore, xanthane was chosen as a dispersion medium to stabilize and extract AgNPs from complicated wastewater samples. After method's optimization, the detection limits were 0.52 and 0.86 ng L^{-1} for determination of the total AgNPs and Ag^+ (sample run at pH 12 without rinse solution) and 0.86 ng L^{-1} for determination of the Ag^+ ions alone (sample run at pH 11 with 1500-μL rinse solution); our proposed differentiation system was shown to be tolerant to wastewater sample matrix and provide superior reliability of differentiating AgNPs/Ag^+ than the conventional centrifugal filtration method. Based on our analytical results, the major species in the acquired wastewater was confirmed to be nanoparticulate silver rather than ionic Ag^+ species (Ag^+/Ag_{total}: 1.1%), which also highlighted that the full-scale chemical fate of AgNPs should be integrated into future assessments of the environmental health effects and utilization of AgNP-containing products.

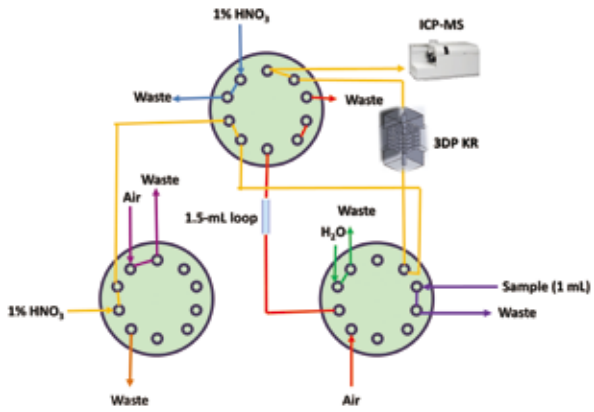

▼ Continuous Microfluidic Assortment of Interactive Ligands (CMAIL)

Prof. Chihchen Chen
Institute of NanoEngineering and MicroSystems

Department of Power Mechanical Engineering

Finding an interactive ligand-receptor pair is crucial to many applications, including the development of monoclonal antibodies. Biopanning, a commonly used technique for affinity screening, involves a series of washing steps and is lengthy and tedious. Here we present an approach termed continuous microfluidic assortment of interactive ligands, or CMAIL, for the screening and sorting of antigen-binding single-chain variable antibody fragments (scFv) displayed on bacteriophages (phages). Phages carrying native negative charges on their coat proteins were electrophoresed through a hydrogel matrix functionalized with target antigens under two alternating orthogonal electric fields. During the weak horizontal electric field phase, phages were differentially swept laterally depending on their affinity for the antigen, and all phages were electrophoresed down to be collected during the strong vertical electric field phase. Phages of different affinity were spatially separated, allowing the continuous operation. More than 10^5 CFU (colony forming unit) antigen-interacting phages were isolated with ~100% specificity from a phage library containing 3×10^9 individual members within 40 minutes of sorting using CMAIL. CMAIL is rapid, sensitive, specific, and does not employ washing, elution or magnetic beads. In conclusion, we have developed an efficient and cost-effective method for isolating and sorting affinity reagents involving phage display.

http://www.nature.com/articles/srep32454

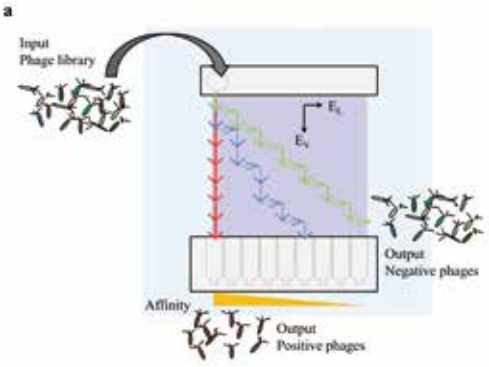

▼ Blue-Light Hazard Free Candlelight OLED

Prof. Jwo-Huei Jou
Department of Materials Science and Engineering

The medical community has been sounding the alarm with increasing frequency regarding the health hazards of blue light. An International Energy Agency report highlighted that blue and cool-white light emitting diodes (LEDs) could damage the light sensitive tissues of the eyes and cause blindness. Numerous medical studies have also reported that intense blue or white light may cause irreversible retinal damage, discoloring the famous paintings of Van Gogh and others, physiological disorders, and increasing risk of various cancers resulting from the suppression of melatonin secretion, circadian disruption and sleep disorders.

Notably, candles emit low blue emission with a low color temperature that can minimize all kinds of blue-hazards. Candle light is able to create a romantic atmosphere, and the pleasant sensation may originate from the naturally occurring melatonin secretion, which helps people relax. In cases where lighting is needed, this secretion is less suppressed when dim light with a low color temperature is applied. In contrast, melatonin generation would be markedly suppressed in the presence of a bright light with a high color temperature importantly; the lack of melatonin due to frequent exposure to intense light at night can increase cancer risk. Suppression of melatonin secretion has been reported upon exposure of 3000 or 5000 K fluorescent lights at 200 lx, which is dimmer than the typical 500 lx office lighting, but brighter than the 100 lx lighting used at home. Much milder suppression can only be observed as the color temperature is further reduced. The notorious effect of blue light on melatonin suppression has also been identified. These studies support calls from medical experts for the development of a new light source for use at night that shows lo color temperature or is free of blue emission to safeguard human health. The healthy candlelight OLED is expected to replace most of the current blue light-enriched lighting measures, including CFLs and LEDs, as well as the traditional candles invented by Egyptian 5,000 years ago. 'Lighting Renaissance" is also expected to trigger on this basis.

To encounter these issues, Prof. Jou's OLED research group invented a blue-light hazard free candlelight OLED with a low color temperature of 2,279 K, an external quantum efficiency of 27.4% and an efficacy of 85.4 lm W^{-1} which is at least 800 times that of candles and over five times of incandescent bulbs. The group has also developed a high light quality candle light OLED with a low color temperature of 1,914 K and a high color rendering index (CRI) of 93. The emissive spectrum of the device shows more than 80% similarity with that of the candle. The indigenously developed OLED is non-obtrusive in nature and also free from flickering, glare, UV, IR and mercury-discharge. Apart from the candle light OLED, Prof. Jou research group also invented high efficiency and natural light style lighting devices including *sunlight-style OLED, pseudo-natural light-style OLED, dusk-hue light-style OLED and better OLED light sources for plant factory.*

http://pubs.rsc.org/en/Content/ArticleLanding/2016/TC/C6TC01968D#!divAbstract

▼ White-Light-Induced Collective Heating of Gold Nanocomposite/*Bombyx mori* Silk Thin Films with Ultrahigh Broadband Absorbance

Prof. Dehui Wan
Institute of Biomedical Engineering

This paper describes a systematic investigation of the phenomenon of white-light-induced heating in silk fibroin films embedded with gold nanoparticles (Au NPs). The Au NPs functioned to develop an ultrahigh broadband absorber, allowing white light to be used as a source for photothermal generation. With an increase of the Au content in the composite films, the absorbance was enhanced significantly around the localized surface plasmon resonance (LSPR) wavelength, while non-LSPR wavelengths were also increased dramatically. The greater amount of absorbed light increased the rate of photoheating. The optimized composite film exhibited ultrahigh absorbances of approximately 95% over the spectral range from 350 to 750 nm, with moderate absorbances (>60%) at longer wavelengths (750-1000 nm). As a result, the composite film absorbed almost all of the incident light and, accordingly, converted this optical energy to local heat. Therefore, significant temperature increases (ca. 100°C) were readily obtained when we irradiated the composite film under a light-emitting diode or halogen lamp. Moreover, such composite films displayed linear light-to-heat responses with respect to the light intensity, as well as great photothermal stability. A broadband absorptive film coated on a simple Al/Si Schottky diode displayed a linear, significant, stable photo-thermo-electronic effect in response to varying the light intensity.

http://pubs.acs.org/doi/full/10.1021/acsnano.5b04913

▼ Characterization of the Near-Field and Convectional Transport Behavior of Micro and Nanoparticles in Nanoscale Plasmonic Optical Lattices

Prof. Ya-Tang Yang
Institute of Electronics Engineering

Photothermal effect has been a major obstacle in the field of plasmonic optical tweeer. In this work, we report the characterization of the transport of micro- and nanospheres in a simple square nanoscale plasmonic optical lattice. The optical potential was created by exciting plasmon resonance by illuminating an array of gold nanodiscs with a focused Gaussian beam. This optical potential produced both in-lattice particle transport behavior, which was due to near-field optical gradient forces, and high-velocity (micron per second) out-of-lattice particle transport due to evanescent field. As a comparison, the natural convection velocity field from a delocalized temperature profile produced by the photothermal heating of the nanoplasmonic array was computed in numerical simulations. This work elucidates the role of photothermal effects on micro- and nanoparticle transport in plasmonic optical lattices. This research is joint collaboration between Prof. Ya-Tang Yang in National Tsing Hua University and Prof. Gilad Yossifon in Technion-Israel Institute of Technology.
http://scitation.aip.org/content/aip/journal/bmf/10/3/10.1063/1.4948775

▼ An Electrostatically-Driven 2D Micro-Scanning Mirror With Capacitive Sensing for Projection Display

Prof. Michael S.-C. Lu
Institute of Electronics Engineering

Bi-axial or two-dimensional MEMS micro-scanning mirrors are considered the key component for laser scanning projectors. Many studies have shown the mechanical characterization of fabricated devices driven by various mechanisms. This work presents an electrostatically-driven bi-axial micro-scanner with capacitive position sensing for Lissajous scanning projection. With the added sensing capability, a PLL (phase-locked loop)-based oscillator loop is developed to sustain mechanical resonance and to provide mirror position information, which are equally important for practical applications. The micro-scanner and the required circuits are implemented using bulk micromachining SOI (silicon on insulator) and 0.35-μm CMOS (complementary metal oxide semiconductor) technologies, respectively. The measured resonant frequencies of the bi-axial micro-scanner for the slow and fast-axis scans are 1.4 and 21.9 kHz, and the associated optical scan angles are 22.5° and 40° , respectively, under pulse modulation of 48 and 115 V_{pp}. The fabricated micro-scanner is adopted in a laser beam scanning projection system to achieve WVGA (852 x 480) display resolution.
http://www.sciencedirect.com/science/article/pii/S0924424714004427

▼ D-Σ(Division-Summation) Digital Control

Prof. Tsai-Fu Wu
Department of Electrical Engineering

High-power components of converters usually play an important role in power-electronic applications. Due to their non-linear characteristics and grid-voltage distortion, the Park transformation, abc to dq frame transformation, having been adopted for near 30 years, cannot be used for deriving valid duty-ratio control laws, which results in current fluctuation and increases core size to limit filter-inductance variation. Based on the considerations of the wide inductance variation and the grid-voltage distortion, our team develops a D-Σ digital control including the advantages of deadbeat control and current feed-forward control to increase dynamic response. The proposed D-Σ digital control can cover wide inductance variation and reduce core size significantly. For example, if filter inductance has nine-time variation, it can reduce core size about five times. With the proposed D-Σ digital control, the inverter can be operated in current-controll modes, such as grid connection, rectification with power factor correction (PFC), active power filter (APF) and static synchronous compensator (STATCOM). Moreover, with our proposed impedance estimation approach, the D-Σ digital control can also cover voltage-controll inverter applications, *i.e.* UPS. The proposed D-Σ digital control has breakthrough innovation and can be applied to many converter applications, which can cover wide inductance variation and grid-voltage distortion, reducing the cost of power converters about 15 %. Thus, the proposed D-Σ digital control is a very important key-technique innovation.
http://ieeexplore.ieee.org/xpls/icp.jsp?arnumber=6579076

▼Advanced Memory Circuitry Design

Prof. Meng-Fan Chang
Department of Electrical Engineering

1. For PCM to be a true contender, a multi-level-cell (MLC) topology with at least a moderate data retention time is required. However, the resistance-drift (R-drift) effect causes cell resistance (RCELL) to increase with time, exceeding the ECC correction ability within hours of being programmed. Conventional R-drift mitigation approaches using reference-cell-based resistance tracking (RCRT) and DRAM-like refresh (DR) are feasible, but at the cost of compromising distinguished PCM traits: random write, low latency, and low power. This paper proposes a resistance drift compensation (RDC) scheme to mitigate against R-drift without such compromises, while minimizing the speed and power consumption penalties. The MLC-PCM fixed-threshold retention (FTR) raw-bit-error-rate (RBER) has been suppressed by over two orders of magnitude, reducing it below practical ECC capability limits.

2. By Using high density and high performance ReRAM combined with CMOS process, this project propose one macro solution of nonvolatile SRAM (nvSRAM) and nonvolatile Flip-Flop (nvFF). 7T1R nvSRAM containing servel assisting backup/wackup scheme, Self-Write-Termination (SWT), Adaptive Parallel Decoder and Space Domain Controller circuits for reducing backup/wakeup power consumption. Also, a novel of Self-Write-Termination nvFF comply the smallest area overhead compare with other nvFF, and greatly reduce backup power consumption.

3. Nonvolatile TCAM (nvTCAM) was developed to reduce cell area (A), search energy (ES), and standby power. nvTCAMs were previously designed using diode-4T2R (D4T2R) with STT-MTJ, 2T2R with phase-change memory, 4T2R and 3T1R with ReRAM. However, these NV devices suffer from the following issues: 1) High ES requirements due to cell-DC-current (IDC-CELL) as well as large match-line (ML) parasitic load (CML), particularly when word-length (WDL) is long; 2) Large A due to the use of two NVM (2R) devices or in-cell control logic; 3) Limited WDL caused by small ML current-ratio (IML-ratio IML-MIS/N*IML-M) between mismatch current (IML-MIS) and the leakage-current (IML-M) from cells on a ML, particularly when NVM resistance (R)-ratio (=RHRS /RLRS) between high-R (HRS, RHRS) and low-R (LRS, RLRS) states is small due to process variation; 4) Long search delays (TSD) due to large CML and small IML-ratio. A 2.5T1R cell to reduce Area (reduce 4.2x area overhead), CML(512 bits R-ratio 50x ; 1024 bits R-ratio 100x), and ES(reduce 48% energy overhead) as well as increase IML-ratio
http://ieeexplore.ieee.org/document/7417943/

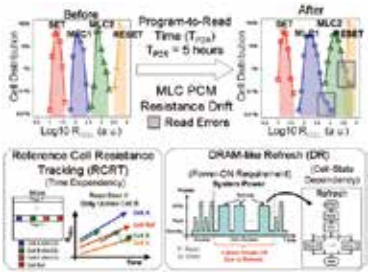

Fig.1. Measured MLC PCM resistance drift and challenges of conventional approaches.

▼Temperature-Aware Online Testing of Power-Delivery TSVs in 3D-ICs

Prof. Shi-Yu Huang
Department of Electrical Engineering

A latent defect in a power-delivery TSV in a 3D IC could cause power glitches under a heavy workload in the field and thereby leading to timing failure. In order to catch these defects before they actually strike, on-line ring-oscillator based VDD-drop monitoring schemes have been proposed previously. However, these methods have not taken into account the effect of the temperature, which could affect their accuracy in the final VDD prediction. In this thesis, we present a temperature-aware test method for power-delivery TSVs, with several features - including a process-calibration scheme and a temperature-aware worst-case VDD prediction scheme. Based on the these schemes, the pass-or-fail decision on the quality of a power-TSV can be made more accurately.

The result of actual experiment, the range from each monitor of predicted worst VDD-drop is [158.2mV, 187.5mV] at supply VDD is 1V and temperature is at room temperature 29.8 ° C. Then we warm up chip by hair dryer to simulate chip operating in high temperature. When the predicted temperature is 80.5° C, the range from each monitor of predicted worst VDD-drop is [162.9mV, 193.2mV]. The different of result is small because the data analysis with temperature-aware. If we analyze data with temperature-unaware, the range of predicted VDD-drop is [177.3mV, 204.6mV]. This experiment can verify our scheme can predict VDD-drop accurately with calibration process variation and temperature-aware.
http://ieeexplore.ieee.org/document/7334617/

▼ Fast Physically-Correct Refocusing for Sparse Light Fields Using Block-Based Multi-Rate View Interpolation

Prof. Chao-Tsung Huang
Department of Electrical Engineering

Conventional realistic refocusing applications are applied on dense light fields which require a large amount of storage space. In contrast, using sparse light fields can alleviate such requirement and therefore could enable massive consumer adoption. However, the induced computing resource for compensating the insufficient view sampling is very high. In this work, we propose a fast physically-correct refocusing algorithm to address this issue while maintaining realistic image quality. In particular, the run time can be as fast as the conventional single-image blurring which causes serious boundary artifacts.

http://www.ee.nthu.edu.tw/chaotsung/sparse_lf_refocus/index.html

▼ Interactive Videos: Plausible Video Editing using Sparse Structure Points

Prof. Hung-Kuo Chu
Department of Computer Science

Video remains the method of choice for capturing temporal events. However, without access to the underlying 3D scene models, it remains difficult to make object level edits in a single video or across multiple videos. While it may be possible to explicitly reconstruct the 3D geometries to facilitate these edits, such a workflow is cumbersome, expensive, and tedious. We present a much simpler workflow to create plausible editing and mixing of raw video footage using only sparse structure points (SSP) directly recovered from the raw sequences. First, we utilize user-scribbles to structure the point representations obtained using structure-from-motion on the input videos. The resultant structure points, even when noisy and sparse, are then used to enable various video edits in 3D, including view perturbation, keyframe animation, object duplication and transfer across videos, etc. Using the structure points, we then devised an image based rendering algorithm to synthesize the videos where the objects are manipulated.

http://cgv.cs.nthu.edu.tw/projects/Smart_Geometry/InteractiveVideos

▼ Enabling Adaptive Cloud Gaming in an Open-Source Cloud Gaming Platform

Prof. Cheng-Hsin Hsu
Department of Computer Science

Cloud gaming platforms run games on cloud servers and allow players to play games through the Internet without buying expensive desktops. However, delivering high-quality cloud gaming experience is challenging, mainly because gamers ask for both high-quality game scenes and low response delay. Moreover, the cloud systems and network resources change in small time scales, so that a finer-grained adaptation mechanism is required for each game session.

We study the problem of adapting cloud gaming to maximize the gamer experience in dynamic systems and networks. Without adaptations, cloud gaming platforms continuously deliver the cloud games to gamers at the highest possible quality even when the resources are insufficient, which may overload the network. Thus, the video bitrate of an ongoing cloud gaming session should be reduced if the end-to-end bandwidth is insufficient. Moreover, when the bandwidth is significantly reduced, the video frame rate may have to be reduced to maintain a satisfying graphics quality. Otherwise, gamers would suffer from degraded gaming experience due to late and lost frames, and may quit the games prematurely.

We study the following three challenges to solve the adaptation problem: (i) quantifying gamer experience via crowdsourcing to understand the impacts of different frame rate and bitrates, (ii) reconfiguring video codecs to allow an open-source cloud gaming platform, called GamingAnywhere, to change the video codec configuration on-the-fly, and (iii) quickly adapting videos in dynamic networks to dynamic networks using a proposed algorithm. We integrate the proposed algorithm with GamingAnywhere to demonstrate that our proposal is practical and efficient. Moreover, we conduct trace-driven simulations to evaluate our cloud gaming platform in large-scale setups.

http://ieeexplore.ieee.org/document/7137667/?arnumber=7137667

▼ Design Automation on Microfluidic Biochips

Prof. Tsung-Yi Ho

Department of Computer Science

Prof. Ho presents the first–ever solution for automated testing of flow-based microfluidic biochips (joint work from Duke University and Stanford University). Its contributions are deep and comprehensive, including fault modeling and test generation, as well as experimental demonstration on multiple fabricated chips in use for biochemistry. This paper represents a major advance over the current strategy of visual inspection under a microscope; This work has substantially reduced the time (days to seconds) and cost of testing and, more importantly, the fault coverage is significantly improved. This work has received the Best paper awards in IEEE VLSI Test Symposium 2013 and the annual Donald O. Pederson Best Paper Award of IEEE Transactions on Computer-Aided Design of Integrated Circuits and Systems 2015.

▼ Human-Computer Interaction Technology

Prof. Hao-Chuan Wang

Department of Computer Science

Effective communication between those who are not fluent in a non-native language can potentially be quite difficult. The common language selected to be used throughout an exchange can encumber those who might not speak it as proficiently as others. Remote communication further heightens the difficulty since less channels are available for communication. We introduce HandVis, a video conferencing interface that visualizes elements of hand gesture, such as trajectory and amount. Gesture is intended to be a communicative tool that can compensate for language deficits. The results of a user study indicate how HandVis can be utilized constructively by less-proficient speakers during cross-lingual communication.

http://www.haochuanwang.info

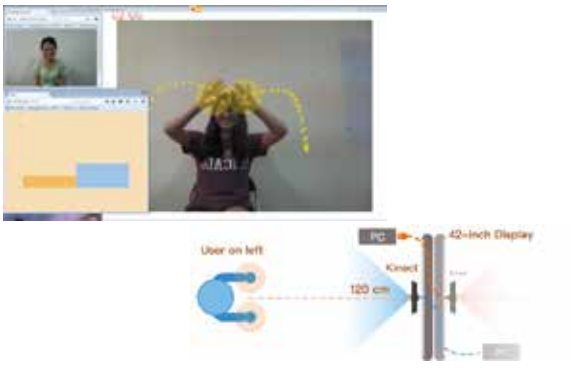

▼ Boron Neutron Capture Therapy (BNCT)

Prof. Yen-Wan Hsueh Liu

Institute of Nuclear Engineering and Science

To investigate the efficacy and safety of fractionated boron neutron capture therapy (BNCT) for recurrent head and neck (H&N) cancer after photon radiation therapy. In this prospective phase 1/2 trial, 2-fraction BNCT with intravenous L-boronophenylalanine (L-BPA, 400 mg/kg) was administered at a 28-day interval. Before each fraction, fluorine-18-labeled-BPA positron emission tomography was conducted to determine the tumor/normal tissue ratio of an individual tumor. The prescription dose (D80) of 20 Gy-Eq per fraction was selected to cover 80% of the gross tumor volume by using a dose volume histogram, while minimizing the volume of oral mucosa receiving >10 Gy-W. Tumor responses and adverse effects were assessed using the Response Evaluation Criteria in Solid Tumors v1.1 and the Common Terminology Criteria for Adverse Events v3.0, respectively.

Seventeen patients with a previous cumulative radiation dose of 63-165 Gy were enrolled. All but 2 participants received 2 fractions of BNCT. The median tumor/normal tissue ratio was 3.4 for the first fraction and 2.5 for the second, whereas the median D80 for the first and second fraction was 19.8 and 14.6Gy-W, respectively. After a median follow-up period of 19.7 months (range, 5.2-52 mo), 6 participants exhibited a complete response and 6 exhibited a partial response. Regarding acute toxicity, 5 participants showed grade 3 mucositis and 1 participant showed grade 4 laryngeal edema and carotid hemorrhage. Regarding late toxicity, 2 participants exhibited grade 3 cranial neuropathy. Four of six participants (67%) receiving total D80>40 Gy-W had a complete response. Two-year overall survival was 47%. Two-year locoregional control was 28%. Our results suggested that 2-fraction BNCT with adaptive dose prescription was effective and safe in locally recurrent H&N cancer. Modifications to our protocol may yield more satisfactory results in the future.

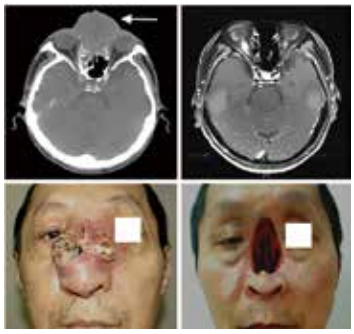

Before and after BNCT treatment

▼ Direct Synthesis and Practical Bandgap Estimation of Multilayer Arsenene Nanoribbons

Prof. Jenq-Horng Liang
Institute of Nuclear Engineering and Science

The multilayer arsenene nanoribbons uniformly distributed on InAs was synthesized by the plasma-assisted process that has been utilized for synthesis of multilayer graphene, germanene, and violet phosphorene. The formation mechanism could be interpreted by thermodynamics, in which the variations of Gibbs free energy (ΔG) of reactions result in the selectivity of reactions. The ~2.3 eV bandgap of multilayer arsenene nanoribbons was estimated by a photoluminescence (PL) measurement. The bandgap opening was caused by the quantum confinement effect of the nanoribbon structure and the turbostratic stacking of arsenene layers. The attractive two-dimensional (2D) material, whose band structure is proper for applications of switching and light-emitting devices, was first synthesized.

http://pubs.acs.org/doi/abs/10.1021/acs.chemmater.5b04949

▼ Translocation of Polyelectrolyte through a Nanopore

Prof. Pai-Yi Hsiao
Department of Engineering and System Science

Using molecular dynamics simulations, we study charged polymers threading through a nanopore, driven by a potential difference set between the membrane wall. We find that the translocation time displays a scaling behavior with the chain length N and the electric field strength E, as $\tau \sim N^{\alpha} E^{-\delta}$. The exponents are not universal, but depend on the field strength. We study the conformation change of chain, the ion distribution, and the ion condensation during a translocation process. We investigate the tension propagation on the chain backbone and the waiting time function. The drift-diffusion properties of translocation are discussed.

http://mx.nthu.edu.tw/~pyhsiao/

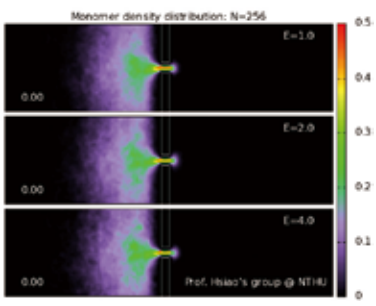

▼ Performance of Inversion, Accumulation and Junctionless mode N-Type and P-Type Bulk Silicon FinFETs with 3-nm Gate Length

Prof. Yung-Chun Wu
Department of Engineering and System Science

The main research results is prove the 3 nm gate channel length (L_G) Silicon FinFET is still workful. We start from the introduction of challenges facing the sub-10 nm technology node. The device performance will be detected by exploring 3 nm FinFETs based on three difference operating mechanisms **(Inversion mode (IM), accumulation (AC), and Junctionless (JL))**, and the device characteristics of these three modes at sub-5 nm technology node will also be investigated in details. In addition, the electron density and device operating performance of various mechanisms will also be investigated, such as DIBL, SS, and I_{on}/I_{off} ratio. This study can support the semiconductor Moore's law can extended to 3-nm node.

http://semiconductorlab.iwopop.com/

▼ A 10b Two-Stage Multi-Channel RDAC with Switch Resistance Compensation and Current Reuse for Low-Power and High-Color-Depth LCD Column Driver ICs

Prof. Chih-Wen Lu
Department of Engineering and System Science

This study proposes a 10-bit low-power high-color-depth LCD column driver IC with two-stage multi-channel RDACs and switch resistance compensation. The design removes intermediate buffers from two-stage RDACs and uses global reference buffers to isolate the global resistor string and output channels. Because the global resistor string is isolated from output channels, the global resistor string can use a larger resistance value to achieve lower power consumption. This study proposes a class-AB buffer for the global reference buffers to compensate for the errors caused by the voltage drop on switches connected in series with the channel resistor string. The channel resistor strings also reuse the output stage current of the global buffer to reduce power consumption. A prototype of a 200-channel column driver was fabricated using 0.18-μm CMOS technology with the worst DNL/INL being 1.2/1.1 LSB. The proposed 10-bit DAC occupies only 66 % of the area of a conventional 8-bit RDAC using the same technology. The 200-channel column driver consumes a total static current of only 0.38 mA.

▼ Inter-Strain Differences in Default Mode Network: A Resting State fMRI Study on Spontaneously Hypertensive Rat and Wistar Kyoto Rat

Prof. Fu-Nien Wang
Department of Biomedical Engineering and Environmental Sciences

Genetic divergences among mammalian strains are presented phenotypically in various aspects of physical appearance such as body shape and facial features. Yet how genetic diversity is expressed in brain function still remains unclear. Functional connectivity has been shown to be a valuable approach in characterizing the relationship between brain functions and behaviors. The default mode network (DMN) of the human brain, which can be detected by monitoring the intrinsic low-frequency fluctuations in neural circuitry, has been widely investigated since its discovery more than a decade ago. The DMN is postulated to support various self-referential functions like imagination, conceptual processing, and conscious awareness. Alterations in the brain DMN have been found in human neuropsychological disorders. In this study we selected the spontaneously hypertensive rat (SHR) and the Wistar Kyoto rat (WKY), two inbred rat strains with close genetic origins, to investigate variations in the DMN.

The spontaneously hypertensive rat (SHR) was initially developed as an animal model for studying hypertension. It is an inbred strain that was established by selecting for hypertension in the Wistar Kyoto rat (WKY) strain. Thus, WKY rats are regarded as the most suitable control group for studying SHR rats. Although these two inbred strains have enormously similar genes, the expressions on cardiovascular and neuropsychological functions are quite different. Therefore, our question is: Is it possible to find the inherent variances in brain activities and organizations on these two rat strains? Investigations of these genetically similar strains could be somewhat analogous to the ongoing Human Connectome Project that focuses on twins and their non-twin siblings. Homozygous rats of an inbred strain are like twins, while the two strains with similar genetic origins, SHR and WKY, are comparable to non-twin siblings. Therefore, we set out to investigate the DMN of SHR and WKY rats. In this study, DMN and functional connectivity networks were analyzed through resting state functional MRI (rs-fMRI) scans using seed-based correlation analysis.

Our results showed that the major DMN differences are the activities in hippocampal area and caudate putamen region. This may be correlated to the hyperactive behavior of the SHR strain. Advanced animal model studies on variations in the DMN may have potential to shed new light on translational medicine, especially with regard to neuropsychological disorders.

http://www.nature.com/articles/srep21697/figures/1

▼ Dual Targeted Photo-penetrated Delivery of Multiple Micelles/ Hydrophobic Drugs by a Nanopea for Enhanced Tumor Therapy

Prof. Shang-Hsiu Hu
Department of Biomedical Engineering and Environmental Sciences

A photo-responsive pea-like capsule (nanopea) that doubles as a photothermal agent constructed by wrapping multiple polymer micelles (polyvinyl alcohol, PVA) in reduced graphene oxide nanoshells (rGO) through double emulsion approach. Nanopeas can transport fully concealed hydrophobic drug, docetaxel (DTX), in the multiple PVA micelles to be later released by photo-actuation triggered by near-infrared irradiation. Through integrating the rod-shaped adhesion and lactoferrin (Lf) targeting, the nanopea enhances both cancer cell uptake *in vitro* and particles accumulation at tumor *in vivo*. A photo-penetrated delivery of micelles/DTX at tumor site was actuated by NIR irradiation which ruptures the nanopeas as well as releases nano-sized micelles/DTX. This trigger also results in thermal damage to the tumor and increases the micelles/DTX permeability, facilitating the drug penetration into the deep tumor far from blood vessel for thermal chemotherapy. This nanopea with the capability of imaging, enhanced tumor accumulation, NIR-triggered tumor penetration and hyperthermia ablation for photothermal chemotherapy boosts tumor treatment and potentially uses in other biological applications.

http://www.chemeurope.com/en/publications/938937/dual-targeted-photopenetrative-delivery-of-multiple-micelles-hydrophobic-drugs-by-a-nanopea-for-enhanced-tumor-therapy.html

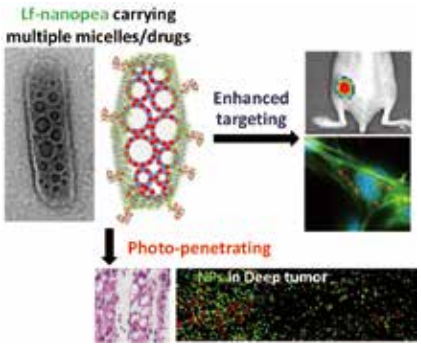

▼ Real-Time Monitoring of Inertial Cavitation Effects of Microbubbles by Using MRI:In VitroExperiments

Prof. Hsu-Hsia Peng
Department of Biomedical Engineering and Environmental Sciences

Theory and Methods: Strong turbulence produced in MB solution at the onset of IC results in the difficulty to refocus signal echoes and thus the decrease in signal intensity (SI). Fundamental investigations were conducted using an agar phantom containing MB dilutions exposed to 1.85-MHz FUS. The effects of various experimental conditions including MB concentrations, imaging slice thicknesses, chamber diameters, acoustic pressures, duty cycles, and pulse repetition frequencies (PRFs) were discussed.

Results: Continuous 2.8 MPa FUS exposure resulted in SI changed from 11% to 55% whenMBs concentrations increased from 0.025% to 0.1%. When slice thickness increased from 3 mm to 6 or 8 mm, smaller SI changes were observed (84%, 59%, and 46%). Images acquired with chamber diameter of 6 and 3 mm showed SI changes of 84% and 35%, respectively. In burst modes, higher duty cycles exhibited higher SI changes, and lower PRFs exhibited smaller and longer SI decrease.

Conclusion: Under various conditions, substantial signal changes were observable, suggesting the feasibility of applying HASTE to real-time monitor IC effect under FUS exposure.

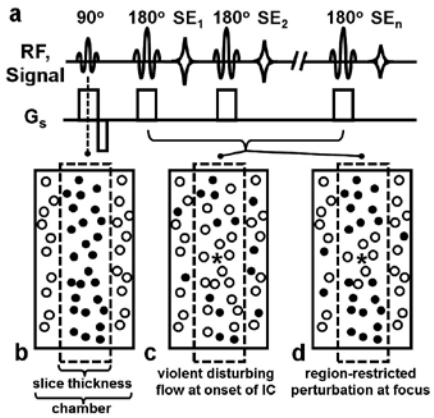

Fig. 1. (a) The pulse sequence of HASTE. (b) After applying the 90o RF excitation, only parts of protons, which were within the selected imaging slice, were excited (dark circle). Other protons within the chamber but outside the selected slice (hollow circle) were not perturbed by the 90o RF pulse. (c) On FUS transmission (star sign: focus), because the HASTE sequence acquires images with multiple 180o RF refocusing pulses during a TR, the violent disturbing flow with chaotic velocity may have been caused at the onset of IC of MBs. (d) A region-restricted perturbation around the focal point.

Renewable Energy

▼ Secondary Frequency and Voltage Droop Control in Isolated AC Micro-Grids

Prof. Chia-Chi Chu
Department of Electrical Engineering

As the penetration of renewable energy sources is increasing in the AC micro-grid, the stability of the closed-loop system has raised a major concern since conventional distributed interface converters (DICs) used in the AC micro-grid do not have a rotating mass, and hence low inertia. High penetration of DIC-based micro-grid may result in poor frequency and voltage response during large disturbance. In order to overcome this difficulty, the virtual synchronous generator (VSGs) was proposed recently in which the DIC mimics conventional synchronous generators (SGs) by designing proper parameters of the SG into each local droop control mechanism of the DIC. Meanwhile, due to the recent advances of distributed control, the concept of consensus-based control can be applied to study this droop control problem of VSGs. One important feature of this consensus-based control is that it can be implemented on each local DIC with communications among their neighboring DICs. In contrast to most existing secondary control schemes, no central controller is required. Under this framework, if DICs are redesigned as VSGs, the frequency and voltage of each DIC can be restored to their pre-specified values obtained from the steady-state analysis. In addition, the proper real and reactive power sharing still can be achieved according to the nominal rating of each DIC. The stability of the closed-loop system is ensured by the transient energy function under certain mild conditions.Numerical experiments of a 14-bus/6-DIC micro-grid system on real-time simulators are performed to validate the effectiveness of the proposed control mechanism.

http://ieeexplore.ieee.org/xpls/abs_all.jsp?arnumber=7182801

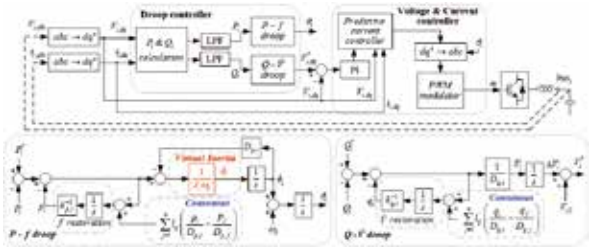

▼ Development of a Micro-Grid with Multiple Renewable Sources and Energy Storage Devices

Prof. Chang-Ming Liaw
Department of Electrical Engineering

Micro-grid can be operated independently from traditional grid to increase the energy utilization and reduce the carbon-oxide emission. However, the generating sources in micro-grid are generally unstable and unpredictable. In addition, the output conditions of energy storage devices are also varied. Hence, a suited interface converter is needed for interfacing each device to the common bus in micro-grid. This study is mainly concerned with the development of a DC micro-grid with multiple renewable sources and energy storage devices. And the proper operation control is explored. The developed micro-grid is equipped with: (i) wind permanent-magnet synchronous generator (PMSG) and photovoltaic (PV). Various other possible harvested AC/DC sources can be plugged in via the embedded interface converters; (ii) hybrid energy storage system consisting of battery, super-capacitor, and permanent-magnet synchronous motor (PMSM) driven flywheel; (iii) bidirectional single-phase three-wire (1P3W) load inverter providing 60Hz 220V/110V output voltages; and (iv) dump load. In addition, the EV can be incorporated as a movable storage device.

▼ High Efficiency Self-Generation Type Sterilization Device

Prof. Wei-Keng Lin
Department of Engineering and System Scienc

Use of water fluid dynamic for power generation, water-driven UV disinfection products. No additional power, easy to install a water purification product. Solve chlorine of swimming pool affect human health problems, prevention of air conditioners, water tower of Legionnaires bacteria, and spa, SPA beauty and breeding industry

http://www.ecs.ess.nthu.edu.tw

▼ Atomic Clusters Modification on Nanocatalyst Surface

Prof. Tsan-Yao Chen
Department of Engineering and System Science

Using Synchrotron based small-angle X-ray scattering, in-situ X-ray scattering, X-ray absorption spectroscopy and X-ray total scattering analysis to reconstruct the 3D atomic structure of nanocatalysts in atomic precision. The corresponding results are published in the inside front cover of CrystEngComm *(Core-Shell nano Crystallite Growth via Heterogeneous Interface Manipulation" CrystEngComm* **2015**, 17, 45, 8623-8631), and other high impact factor journals (e.g., ACS Applied Materials & Interfaces, PCCP, JPCC). The atomic cluster modification by Au atomic clusters substantially improves the CO tolerance of catalysts in methanol oxidation reaction by 4-fold or higher as compared to the control nanocatalysts (Rucore-Ptshell nanocrystal which have been considered as high CO tolerance materials in fuel cell reformer).

http://pubs.acs.org/doi/abs/10.1021/acs.jpcc.6b00801

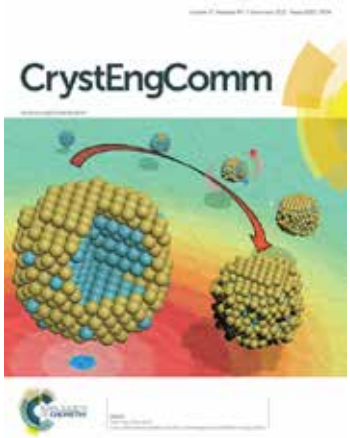

Humanities and Social Sciences

▼ Effectiveness of Feedback for Enhancing English Pronunciation in an ASR-Based CALL System

Prof. Shelley Shwu-Ching Young
Institute of Learning Sciences

This paper presents a study on implementing the ASR-based CALL (computer-assisted language learning based upon automatic speech recognition) system embedded with both formative and summative feedback approaches and using implicit and explicit strategies to enhance adult and young learners' English pronunciation. Two groups of learners including 18 adults and 16 seventh graders participated in the study. The results indicate that the formative feedback had a positive impact on improving the learners' speaking articulation, and the summative feedback aided the learners' self-reflection and helped them to track their speaking progress. Furthermore, the implicit information such as model pronunciation with full sentences and audio recast benefitted the adult learners, whereas the young learners preferred the explicit learning information such as textual information of individual words for self-correction. In addition, the results of this study also confirm that learners have different perceptions of the media modalities designed with implicit and explicit strategies in the feedback. Feedback with audio modality is more suitable for adults, whereas juxtaposed textual and audio modalities are better for young learners.

http://onlinelibrary.wiley.com.nthulib-oc.nthu.edu.tw/doi/10.1111/jcal.12079/abstract

▼ Taiwanese Writers and Left-Wing Corridor in East Asia

Prof. Shu-Chin Liu
College of Humanities and Social Sciences

In "Left-Wing Corridor and Non-Turn Narrative: Poetry and Drama Guerrilla of Wu Kun-huang, a Taiwanese Writer Writing in Japanese," I depict the traces of cross-border interchange between Taiwanese writers in Japan and the Chinese, Taiwanese, Korean, and Manchurian leftists in Japan in the 1930s. This paper has been released in Japan, Korea, and China. With the dual viewpoints of "left-wing corridor" and "non-turn narrative," I illustrate the role of communication played by Taiwanese writers with bilingual proficiency in the course of the development of "left-wing corridor" between Shanghai and Tokyo. This paper has been translated into English "Wu Kun-huang (1909-1989) and Communist Underground in East Asia: Minority Discourse and Writers in Colonial Taiwan" and will be released in an international conference in Europe and US.

▼ Environmental History in Ming China

Prof. Cho-Ying Li
Institute of History

Xia Yuanji (1366-1430) was appointed by the Yongle Emperor to take charge of water management in the Lower Yangzi Delta from 1403 to 1405. As is well known, the Yongle emperor ascended the throne by usurpation in 1402, and this article explores the relationship between Xia's water management and efforts to establish the legitimacy of the Yongle administration. It is contended here that Xia's appointment, his discourse on the sage-kings, and his choice of hydraulic strategies—as well as Yongle's attitude toward water management—were closely related and directed at bolstering Yongle's legitimacy. Taking inspiration from the theory of political ecology, I analyze the "Three Rivers" discourse formulated by Xia Yuanji from a political perspective. I argue that this discourse served to undergird Xia's approach to water management because it implied that Yongle was a sage-king in the mold of the Great Yu, who was of course highly admired for his benevolence toward the people. The "Three Rivers" discourse also provided a clear description of the waterway system in the Lower Yangzi and laid out an effective way of taking advantage of the work done by Xia's predecessors in the Yuan dynasty. Through an analysis of Xia's approach to water management, this article also intends to offer a reflection on current research methodology. While existing literature on water management mostly focuses on environmental changes and concrete hydraulic policy, this article proposes that it is also important to pay due attention to historical actors' political expectations and to the cultural implications of certain discourses in order to obtain a better understanding of the significance and consequences of a particular policy. Viewing hydraulic issues from this angle, this article maintains that water management is often more appropriately understood as an action directed at a political purpose, and not simply a response to a natural catastrophe.

2015-2016 R&D REPORT

Office of Research and Development
National Tsing Hua University

No. 101, Section 2, Kuang-Fu Road,
Hsinchu, Taiwan 30013, R.O.C.
Tel : +886-3-571-7470
http://rdweb.nthu.edu.tw/Default.aspx
http://rdweb.nthu.edu.tw/English/English.aspx

National Tsing Hua University
No. 101, Section 2, Kuang-Fu Road, Hsinchu, Taiwan 30013, R.O.C.
Tel : +886-3-571-5131
http://www.nthu.edu.tw